

**ROLE OF CATIONIC CHARGE IN PEPTIDE
AND PROTEIN INTERNALIZATION BY CELLS**

By

Stephen M. Fuchs

A dissertation submitted in partial fulfillment

Of the requirements for the degree of

Doctor of Philosophy

(Biochemistry)

at the

UNIVERSITY OF WISCONSIN-MADISON

2006

A dissertation entitled

ROLE OF CATIONIC CHARGE IN PEPTIDE
AND PROTEIN INTERNALIZATION BY CELLS

submitted to the Graduate School of the
University of Wisconsin-Madison
in partial fulfillment of the requirements for the
degree of Doctor of Philosophy

by

STEPHEN M. FUCHS

Date of Final Oral Examination:

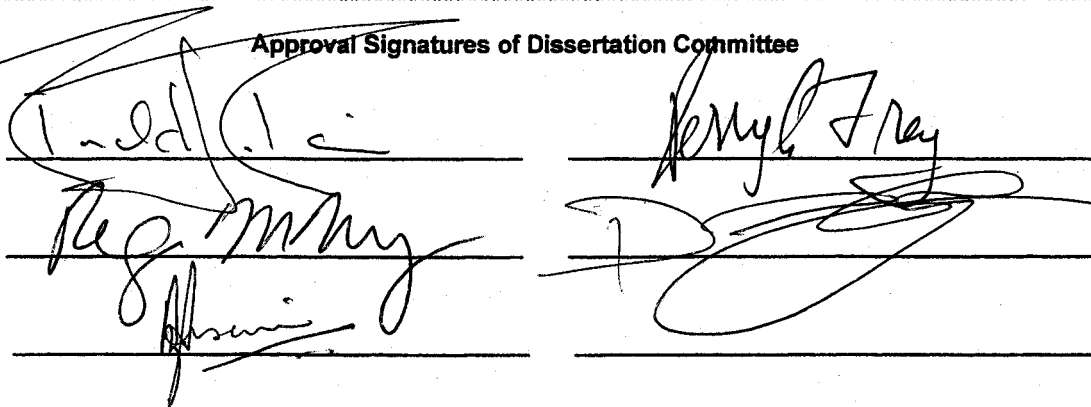
FEBRUARY 27, 2006

Month & Year Degree to be awarded: December

May 2006

August

Approval Signatures of Dissertation Committee



Signature, Dean of Graduate School



Role of Cationic Charge in Peptide and Protein Internalization By Cells

Stephen M. Fuchs

Under the supervision of Professor Ronald T. Raines

At the University of Wisconsin-Madison

Cells contain a number of biological barriers that function to sequester certain molecules within cells but also to exclude other macromolecules. These barriers, while essential, often prove to be a major obstacle in the development of new therapeutics. This dissertation describes the design of molecules that are capable of entering cells as well as insight into the mechanism of internalization.

Chapter Two describes work to uncover the mechanism of nonaarginine (R_9) entry into cells. R_9 entry is shown to differ in living and fixed cells grown in culture. In fixed cells, entry is energy independent and localizes to the nucleolus. In living cells, entry occurs through endocytosis, an energy-dependent process. Further, entry is mediated by the presence of sulfated glycosaminoglycans and not the lipid membrane.

Chapter Three furthers the practical applications of polycationic peptides such as R_9 . These peptides are shown to be useful as fusion tags for improved cellular uptake. Further, R_9 is demonstrated to make an effective tag for protein purification and protein immobilization on surfaces.

Chapter Four describes the design of a green fluorescent protein (GFP) capable of cellular entry that is independent of a cationic tag. Site-directed mutagenesis is used to endow a surface of a protein with greater cationic character. In so doing, a cationic GFP (cGFP) is created which

is capable of cellular entry. cGFP has the same fluorescence and biophysical properties as the wild-type protein. Chapter Five expands upon this initial work by using cGFP to assay HIV protease function in living cells. cGFP is tethered to a fluorescent FRET (Fluorescence Resonance Energy Transfer) partner via a linker that contains a sequence recognized by HIV protease. When this linker is cleaved by HIV protease in cells, the fluorescence properties of the substrate are changed, thus creating an *in vivo* marker for HIV infection.

Acknowledgements

My experience in the Raines lab has been not only educational but fulfilling and memorable. I have had the pleasure to work with some wonderful people over the years. Specifically, I would like to thank Dr. Tony Klink, Dr. Peter Leland, and Prof. Chiwook Park for mentoring me in my early years. My classmate Kimberly Dickson has also been a great help throughout my time in the Raines lab. I want to thank my mentor within the lab, Prof. Brian Miller, for teaching me the value of a good experiment and a good beer. Bryan Smith, Tom Rutkoski, Frank Kotch, Eugene Lee, Eric Benedict, and Jeet Kalia, have all been great colleagues and great friends.

My research could not have been conducted in solitude. I am indebted to Dr. Parit Plainkum for his tireless work on the zymogen project. My undergraduate researcher, Ryan Groeschl, and my many rotation students played a big part in the work described in Appendix I and elsewhere. My great collaborator, Chris Jewell, has been extremely helpful with our film experiments. Dr. Darrell McCaslin and Dr. Gary Case have provided much assistance as well.

Other friends have aided me in my graduate studies as well. Dr. Kurt Vogel and Dr. George Hanson were great mentors during and since my internship at Panvera. Nearly seven years of lunch on Tuesdays with Rich Gradman, Luke Moe, and Greg Zornetzer has been almost as important to me as their friendship. Bob White, Matthew Harris, and Nick Reiter have been great friends, colleagues, and band members for a very long time. Many other friends have been both helpful with work and also with helpful in forgetting about work. Thank you all for the last six and a half years.

Ron Raines has been a wonderful advisor. I have learned a lot about how to run a successful lab from you. I haven't always liked the way things were done, but I've learned why they were

done that way. I thank you also for allowing me the opportunity to explore my many scientific interests while at the same time steering me in a proper scientific direction.

I thank my family. Your undying love and support has always been evident but never more appreciated than over the last few years. I am truly lucky to have such wonderful parents and sister. Thank you.

Lastly, I thank Erin: my best friend, greatest supporter, and soon to be wife. You have made the past five years the best years of my life. I look forward to many, many more. Celebrating my prelim at the Stadium bar was the best decision I've ever made.

Table of Contents

Table of Contents

Abstract	i
Acknowledgements	iii
Table of Contents	v
List of Figures	viii
List of Tables.....	x
List of Abbreviations.....	xi

Chapter One

Introduction.....	1
1.1 Overview	2
1.2 Polycation-Mediated Transport	3
1.3 Physicochemical Properties of Cationic Peptides.....	7
1.4 Mechanism of Cation-Mediated Transport	9
1.5 Other Functions of Cationic Peptides	15
1.6 Prospectus.....	16
1.7 Conclusion.....	18

Chapter Two

Pathway for Polyarginine Entry into Cells	26
2.1 Abstract	27
2.2 Introduction	28
2.3 Materials and Methods.....	30

2.4 Results	33
2.5 Discussion.....	35
Chapter Three	
Polyarginine as a Multifunctional Tag	51
3.1 Abstract	52
3.2 Introduction	53
3.3 Materials and Methods.....	54
3.4 Results	59
3.5 Discussion.....	62
Chapter Four	
Cell-Permeable Green Fluorescent Protein.....	76
4.1 Abstract	77
4.2 Introduction	78
4.3 Materials and Methods.....	80
4.4 Results	84
4.5 Discussion.....	86
Chapter Five	
Detection of HIV-1 Protease Activity using a Cell-Permeable	
Variant of GFP substrate.....	101
5.1 Abstract	102
5.2 Introduction	103
5.3 Materials and Methods.....	105

5.4 Results	109
5.5 Discussion.....	111
 Appendix I	
Design of Toxic Ribonuclease A Variants with Increased Cellular Uptake.....	123
Introduction	124
Materials and Methods.....	125
Results.....	128
Discussion	130
 Appendix II	
Release of Cationic Peptides and Proteins from Multilayered Thin Films.....	139
Introduction.....	140
Materials and Methods.....	141
Preliminary Results.....	147
Discussion	148
References.....	163

List of Figures

Figure 1-1	Lipid translocation model of PTD internalization (Circa 2000)	20
Figure 1-2	Role of HS in PTD internalization into cells (Circa 2004)	22
Figure 1-3	Current model for PTD internalization	24
Figure 2-1	Localization of TAMRA-R ₉ in living and fixed cells	39
Figure 2-2	Co-localization of TAMRA-R ₉ in living cells	41
Figure 2-3	Dependence of TAMRA-R ₉ internalization on glycosaminoglycans	43
Figure 2-4	Affinity of TAMRA-R ₉ for heparin	45
Figure 2-5	R ₉ -induced leakage of egg PC liposomes	47
Figure 2-6	Pathway for transduction of R ₉ into cells	49
Figure 3-1	Effect of R ₉ tags on RNase A purification by cation-exchange chromatography	66
Figure 3-2	Effect of an R ₉ tag on conformational stability of RNase A	68
Figure 3-3	Effect of an R ₉ tag on RNase A uptake by CHO-K1 cells	70
Figure 3-4	Effect of R ₉ tag on the cytotoxicity of RNase A variants	72
Figure 3-5	Immobilization of R ₉ -tagged RNase A variants	74
Figure 4-1	Design scheme for the cell-permeable GFP variant (cGFP)	91
Figure 4-2	Characterization of the fluorescence properties of cGFP	93
Figure 4-3	Gdn-HCl-induced unfolding of eGFP and cGFP	95

Figure 4-4	Dose-dependence of the internalization of GFP variants in HeLa cells.....	97
Figure 4-5	cGFP internalization in glycosaminoglycan-deficient cell lines.....	99
Figure 5-1	Design of cell-permeable FRET substrate for HIV protease	115
Figure 5-2	<i>in vitro</i> cleavage of cGFP substrate by HIV protease.....	117
Figure 5-3	Cell lines for transient expression of HIV-PR.....	119
Figure 5-4	Live-cell visualization of HIV protease activity in 293T/17 cells	121
Figure AI-1	Electropotential model of RNase A.....	133
Figure AI-2	Cytotoxicity of RNase A and cationic variants in K-562 cells	135
Figure AI-3	Cytotoxicity of cationic variants and R ₉ -tagged RNases in K-562 cells	137
Figure AII-1	Schematic depicting the formation of a LBL multilayer polyelectrolyte film.....	151
Figure AII-2	Synthetic scheme for TMR-CR ₉ ester	153
Figure AII-3	Release of TMR-R ₉ and TMR-CR ₉ from multilayer films.....	155
Figure AII-4	Improved synthetic scheme for TMR-R ₉ amide and ester isosteres.....	157
Figure AII-5	Synthesis and erosion of RNase films	159
Figure AII-6	Release of RNase films into COS-7 cells	161

List of Tables

Table 1-1	Cationic peptides with translocation activity	19
Table 3-1	Biochemical parameters of RNase A variants.....	65
Table 4-1	Thermodynamic parameters for Gdn-HCl-induced unfolding of eGFP and cGFP	90
Table AI-1	Biochemical parameters of RNase A and cationic variants	132

List of Abbreviations

β -gal	β -galactosidase
5-IAF	5-iodoacetamidofluorescein
6-FAM	6-carboxyfluorescein
Ant	antennapedia homeodomain
ATCC	American Type Culture Collection
ATP	adenosine triphosphate
BRET	bioluminescence resonance energy transfer
cGFP	cationic green fluorescent protein
CHO	Chinese hamster ovary cell
CPB	carboxypeptidase B
DCC	Dicyclohexylcarbodiimide
DIEA	N,N-diisopropylethylamine
DMAP	4-dimethylaminopyridine
DNA	deoxyribonucleic acid
DTT	dithiothreitol

EDTA	ethylenediaminetetraacetic acid
eGFP	enhanced green fluorescent protein
EMMA	endoosmolysis by masking of a membrane active agent
FGF	fibroblast growth factor
FPLC	fast performance liquid chromatography
FR	folate receptor
FRET	fluorescence resonance energy transfer
GAG	glycosaminoglycan
Gdn	guanidine
GFP	green fluorescent protein
HEPES	N-[2-hydroxyethyl]piperazine-N'-[4-butanesulfonic acid]
HIV-1	human immunodeficiency virus type-1
HIV-PR	human immunodeficiency virus type-1 protease
HPLC	high pressure liquid chromatography
HS	heparan sulfate
HSPG	heparan sulfate proteoglycans
IgG	immunoglobulin G

IPTG	isopropyl-1-thio- β -D-galactopyranoside
K ⁺	potassium ion
MALDI-TOF	matrix-assisted laser desorption ionization–time-of-flight
MES	morpholinoethanesulfonic acid
M _r	relative molecular mass
Ni-NTA	nickel–nitrilotriacetic acid
NMR	nuclear magnetic resonance
<i>OD</i>	optical density
ONC	onconase
PBS	Dulbecco's phosphate-buffered saline
PBS+	Dulbecco's phosphate buffered saline + 500 mM NaCl
PC	egg phosphatidylcholine
PCR	polymerase chain reaction
PMSF	phenylmethanesulfonylfluoride
PTDs	protein transduction domains
PyBOP	(benzotriazol-1-yloxy)tripyrrolidinophosphonium hexafluorophosphate
R ₉	nonaarginine

rDNA	recombinant DNA
RI	ribonuclease inhibitor protein
RNA	ribonucleic acid
RNase A	ribonuclease A
SDS-PAGE	sodium dodecyl sulfate-polyacrylamide gel electrophoresis
TAMRA	5- (and 6-)carboxytetramethylrhodamine
TAR	TAT-responsive element
TB	terrific broth
TCEP	tris[2-carboxyethylphospine]hydrochloride
TFA	trifluoroacetic acid
T_m	temperature at the midpoint of the thermal denaturation curve
TR	transferrin receptor
Tris	tris(hydroxymethyl)aminomethane
TRITC	5- (and 6-)tetramethylrhodamine isothiocyanate

Chapter One

Introduction

Portions of this chapter will form a solicited review. Fuchs, S. M., and Raines, R. T. (2006)

‘Visions and Reflections’ The future of polyarginine, *Cellular and Molecular Life Sciences*, In Preparation.

Overview

The first documented use of a protein as a chemotherapeutic was the administration of insulin to treat diabetes in 1922 (Banting and Best, 1922). Insulin has since become one of the most influential pharmaceuticals in our society (Levinson, 2003). Today the use of protein drugs is on the rise accounting for 35% of new active substances (Tang *et al.*, 2004). As of 2003, there were 43 recombinant protein therapeutics approved for use by the US Food and Drug Administration and numerous others are in clinical trials (Marafino and Pugsley, 2003). Of these, insulin, interferon, and erythropoietin are all multibillion-dollar drugs.

Protein chemotherapies often suffer from many technical limitations. These include expense of production, immunogenicity, and general toxicity (Marafino and Pugsley, 2003; Chirino *et al.*, 2004). Many of these drawbacks are due to the high concentrations needed for effectiveness. Improving the uptake of these proteins by cells is one strategy to afford lower effective doses. Therefore, a great deal of recent effort has been made to better understand the mechanism of macromolecular uptake by cells. Success is of great importance, not only for protein therapeutics but also for gene delivery and other biological applications.

The promise of proteins as useful chemotherapeutics has presented scientists with new challenges. Specifically, how do we endow these molecules with the ability to enter cells? The answer, so far, mainly involves “hijacking” pre-existing cellular machineries. Fusing proteins, either genetically or chemically, to ligands with endogenous cell–surface receptors can increase the uptake of the macromolecule. For example, cells contain a protein called transferrin receptor (TR), which binds the major iron carrier, transferrin, and facilitates its uptake into cells. Fusing transferrin to many types of molecules has resulted in increased uptake and greater activity

(O'Keefe and Draper, 1985). Folate, an essential vitamin, binds to a cell-surface folate receptor (FR), which facilitates its utilization in cells as an essential enzymic cofactor (Stanger, 2002). Folate can be fused to toxic proteins or peptides, and thus increase the uptake of these molecules (Leamon and Low, 1991, 1993). This is of interest because it has been noted that many cancer cells overexpress FR to compensate for their higher metabolic needs (Lu and Low, 2002, 2003). Thus folate conjugates are particularly attractive new therapies for combating neoplasias (Lu and Low, 2002; Lu *et al.*, 2004).

More recently, both naturally derived and synthetic peptides, have been found to undergo cellular internalization (Prochiantz, 2000; Wadia and Dowdy, 2002; Fischer *et al.*, 2005). Further, these peptides can be fused to other molecules and facilitate their uptake. Many of these peptides are similar in that they are highly basic and between 8–20 residues in length. This class of cationic transport molecules is of particular interest to researchers due to their small size and the efficiency of internalization.

Here we shall describe the properties of cationic proteins and peptides as well as efforts to determine the mechanism of their cellular uptake. We shall also discuss applications for these peptides, as well as imperatives for the future of this rapidly emerging field.

1.1 Polycation-mediated transport

Cationic peptides have widespread use as tags for proteins and small molecules. This use is due to their versatility as molecular transporters as well as handles for other functions (see Section 1.6). The potential of cationic molecules to enhance the uptake of macromolecules,

however, has been well known for nearly fifty years. Here, we describe briefly the relevant history of polycation-mediated transport of macromolecules into cells.

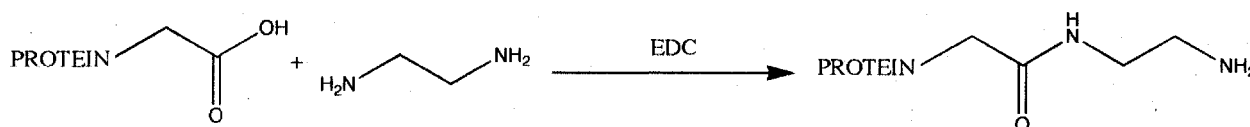
Origins of Cationic Uptake

Some of the earliest studies of cancer focused on physicochemical differences between normal and cancerous tissues. One notable observation was that cancer cells had a greater negative charge than normal cells as measured by the electrophoretic mobility of cells in suspension (James *et al.*, 1956). Thus, one of the earliest theories for the selective targeting of cancer cells involved the use of positively-charged polymers to deliver drugs (Kornguth *et al.*, 1961; Anghileri *et al.*, 1976; Shen and Ryser, 1979).

About forty years ago, Hugues Ryser began to explore the transport of proteins using radiolabeled albumin and a number of different cell types. He showed that the uptake of albumin by tumor cells was increased when the proteins were complexed with cationic proteins, specifically histones (Ryser and Hancock, 1965). Ryser also showed that cationic polyamino acids (polylysine, polyarginine, and polyhistidine) exhibited similar effects (Ryser and Hancock, 1965). Ryser attributed the ability of these proteins to increase albumin uptake to the cationic nature of their primary sequence (Ryser, 1968). Later work by Ryser and coworkers showed that polylysine was effective in increasing the uptake of small molecules as well. Specifically, the presence of polylysine increased the potency of methotrexate towards a resistant Chinese hamster ovary-derived cell line (Shen and Ryser, 1979). Thus, early work demonstrated that basic polypeptides enhanced uptake of many types of macromolecules by cells.

Chemical Cationization

The discovery that cationic character was related to cellular uptake gave birth to a new field of cationic drug delivery. Although the number of cationic proteins is rather small, Pardridge and coworkers recognized the potential of chemically modifying proteins to increase cationic character. Proteins could be made more basic by converting protein carboxyl groups to amines by condensation with diamines such as ethylenediamine (Scheme I) (Triguero *et al.*, 1989). The first descriptions of chemical cationization of proteins were reported for the modification of immunoglobulin antibodies (IgG) with ethylenediamine (Pardridge *et al.*, 1990). Pardridge and coworkers reported that modification of ^{125}I -labeled IgG with ethylenediamine resulted in greatly increased uptake of IgG in the 10 rat organs surveyed, including the brain (Triguero *et al.*, 1989). The increased uptake could be attributed to the increase in charge of the modified protein.



Scheme I: Chemical modification of proteins with diamines

Chemical cationization has been used to increase the efficacy of toxic molecules as well. Members of the bovine pancreatic ribonuclease (RNase A) superfamily can be toxic to mammalian cells. Yamada and coworkers were able to chemically modify RNase A to give a protein with greater toxicity, due to both increased internalization of RNase A, as well as lower affinity for the cytosolic ribonuclease inhibitor protein (RI) (Futami *et al.*, 2001). Interestingly, chemical modification of RNase A, while resulting in a more cytotoxic protein, decreased the

catalytic activity of the enzyme nearly 100-fold. This result highlights an important drawback to chemical modification: chemical cationization gives rise to a heterogeneous population of modified proteins. The most reactive carboxyl groups are often those most accessible to solvent. Unfortunately, these surface carboxyl groups are also often important for either protein–protein interactions or protein function, and thus modification can disrupt the natural function of these modified proteins.

Cationic Peptides – Protein Transduction Domains

In 1988, two research groups independently discovered that the Tat protein from HIV-1 virus was able to cross cell membranes and enter the cytosol (Frankel and Pabo, 1988; Green and Loewenstein, 1988). This activity is thought to be important in HIV infection, as the Tat protein is capable of leaving an infected cell and entering another infected cell and there turning on viral gene transcription (Brady and Kashanchi, 2005). Deletion studies determined that the domain of HIV-1 Tat responsible for cellular entry is the domain that also binds to the Tat-responsive element in RNA (TAR) (Cordingley *et al.*, 1990). This 11 amino acid sequence, KYRRRQRRRGN, corresponds to residues 48-58 of the HIV-1 protein and only the basic residues are required for cellular internalization (Vives *et al.*, 1997).

In 1999, Schwarze and Dowdy fused the HIV-1 Tat peptide sequence to β -galactosidase and showed that it successfully delivered the enzyme to multiple cell types within a mouse (Schwarze *et al.*, 1999). This study revitalized the field of cation-mediated delivery and brought focus to cationic peptides as potential vehicles for macromolecular delivery. They and others have since called these peptides “protein transduction domains” (PTDs). Although this name is

probably a misnomer (translocation is a more appropriate term for transversing a biological barrier), it is in common use today.

1.3 Physicochemical Properties of Cationic Peptides

The discovery of PTDs in the 1990s led to an explosion of studies on other cationic peptides and molecules capable of cellular entry. Numerous reviews have been written on the subject (Leifert and Whitton, 2003; Brooks *et al.*, 2005; Fittipaldi and Giacca, 2005; Futaki, 2005; Gupta *et al.*, 2005; Wadia and Dowdy, 2005; Zorko and Langel, 2005). The following section is focused on the chemical and biophysical properties of these remarkable peptides.

The earliest and best-characterized PTD is the sequence derived from the HIV-1 Tat protein. Suzuki and coworkers examined a number of cationic RNA- and DNA-binding peptides, finding that many of these sequences were capable of similar transport (Suzuki *et al.*, 2002). Apparently the cationic features of many RNA- and DNA-binding proteins contribute not only to their ability to bind nucleic acids but also to cellular internalization.

Mitchell *et al.* showed that cellular transport was not limited to just naturally occurring sequences, but that synthetic sequences of polyarginine, polylysine, or polyornithine were also capable of cellular entry (Mitchell *et al.*, 2000). Polyarginine was found to be superior to other homopolymeric amino acids. Rothbard and coworkers have expanded upon this initial study to show that, in addition to its positive charge, it is the ability of the guanidinium group of arginine residues to make multiple hydrogen bonds that enhances cellular transport activity (Rothbard *et al.*, 2004; Rothbard *et al.*, 2005).

The optimal HIV-1 Tat sequence for translocation is 11 amino acids (Vives *et al.*, 1997). Several studies revealed that the optimal length of polyarginine necessary for transport was between 5 and 11 residues, with octa- and nonaarginine (R₉) being the most efficiently transported (Mitchell *et al.*, 2000; Suzuki *et al.*, 2002). The authors suggest peptides that are too short (~ 5 residues) do not allow for strong enough interactions with cell-surface components, and peptides that are too long (~ 20 residues) could be limited by secondary structure formation. These limits have been confirmed for a number of other peptides (Ho *et al.*, 2001; Wadia and Dowdy, 2002; Brooks *et al.*, 2005; Rothbard *et al.*, 2005).

Early attempts to understand the internalization mechanism of PTDs focused on finding a cell-surface receptor protein. One set of experiments compared enantiomers of peptides. Peptides composed of all D-amino acids have physicochemical properties equivalent to naturally occurring L-peptides, but D-peptides would not bind to receptors that recognize L-peptides due to their inverted stereochemistry (Wade *et al.*, 1990). These studies indicated that D-amino acid peptides and L-amino acid peptides were internalized equally, suggesting there was no chiral receptor for PTDs (Derossi *et al.*, 1996). This implied that stereochemistry was not important for transport activity, and thus it was unlikely that PTDs were recognized by a protein receptor.

Other experiments aimed to determine if the peptide backbone was essential for internalization. Wender and coworkers made peptoid and oligocarbamate polymers displaying guanidinium-containing side chains (Wender *et al.*, 2000; Wender *et al.*, 2002). Gellman and coworkers made β -peptides displaying similar functionalities (Umezawa *et al.*, 2002; Potocky *et al.*, 2003, 2005). In all cases, these synthetic molecules were readily transported into cells. Thus, it seems that only the charge and not the backbone is important for PTD internalization.

Structure–function studies of PTDs have revealed that they are highly tolerant to mutation in their primary structure (Table 1-1). Although basic amino acids are needed for efficient entry, hydrophobic residues also appear to contribute to uptake by possibly inducing secondary structure in the presence of biological membranes (Ho *et al.*, 2001). In general, PTDs function with a diverse group of side chains as well as with modified backbones. From a number of different studies, we can conclude that there are certain features that seem to be optimal for efficient cellular entry: a linear polymer displaying 7–9 guanidinium groups.

1.4 Mechanism of cation-mediated internalization

The finding that small cationic peptides could cross cell membranes and enter the cytosol was of major interest to the field of protein therapeutics. Current protein therapeutics act primarily against extracellular targets (Stayton *et al.*, 2005), mainly because most proteins are not internalized by cells. Developing tools to ferry proteins across membranes would open up an entirely new spectrum of potential therapeutics. Essential to the development of better cationic tags, however, is an understanding of the mechanism by which these peptides enter cells. Toward that end, much work has been done to understand the interactions between these peptides and the cell surface. The next section will explore the mechanistic studies of PTDs somewhat chronologically, as the model has changed considerably over the past few years.

Initial studies of PTD internalization focused on HIV-Tat peptide and an amphipathic peptide from the *Antennapedia* homeodomain (Ant). Researchers working with Ant found that internalization in cultured cells was independent of temperature, occurring at both 37 °C and 4 °C (Derossi *et al.*, 1994). Because endocytosis does not occur at 4 °C, this finding indicated that

PTDs did not enter cells through an endocytic mechanism. This result was also observed by a group studying HIV-1 Tat peptide (Thoren *et al.*, 2003). Norden and coworkers showed that Ant was able to cross pure lipid bilayers (Thoren *et al.*, 2000), suggesting a novel mechanism for PTD internalization involving direct interaction with the plasma membrane. Models were proposed that involved either localized disruption of the bilayer or transient pore formation induced by peptide binding to the surface Figure 1-1 (Prochiantz, 2000). In Chapter 2, we directly test the ability of polyarginine to cross lipid bilayers utilizing a liposome-leakage assay.

Dowdy and coworkers showed that the internalization of HIV-Tat β -gal constructs was also independent of temperature (Schwarze *et al.*, 1999). They subsequently noted that for entry of protein fusions, the entire cargo had to be denatured (Vocero-Akbani *et al.*, 2000; Vocero-Akbani *et al.*, 2001). They proposed that upon cellular entry, chaperones would allow for proper refolding of proteins.

Fixation Artifacts

In 2001, Lebleu and coworkers reported that HIV-Tat localization was different in fixed and living cells (Richard *et al.*, 2003). Previously, all mechanistic studies concerning HIV-TAT had been done with fixed, cultured cells. In fixed cells, peptide localized to all regions of the cell with much peptide being localized to the nucleolus (Mitchell *et al.*, 2000; Suzuki *et al.*, 2002). In living cells, however, peptides were not seen in the nucleus. Rather, peptides were found in the cytoplasm and vesicles (Richard *et al.*, 2003). Further studies showed that internalization was temperature- and ATP-dependent, suggesting that internalization occurred via an endocytic mechanism, contradicting many of the earlier studies (Futaki, 2005). Similar results were found

for R₉ (Fuchs and Raines, 2004) and β -peptides (Potocky *et al.*, 2003). Hence, the validity of all early experiments concerning PTD mechanism was called into question and live-cell microscopy became the obligate tool for studying the PTD internalization mechanism.

Cell-Surface Binding – Role of Cell-Surface Glycosaminoglycans

The surface of mammalian cells is negatively charged due mainly to their anionic polysaccharides (Iozzo, 2005). For example, polysaccharides such as heparan sulfate (HS) are attached to cell-surface proteins in the Golgi apparatus to form glycosaminoglycans (GAGs) (Whitelock and Iozzo, 2005). HS is usually found attached to one of two proteins in mammalian cells; syndecan – a transmembrane protein, or glypican – a GPI-anchored protein most often associated with lipid rafts. After their biosynthesis in the Golgi, these proteins are transported to and displayed on the plasma membrane.

GAGs mediate important cell–cell signaling interactions and are turned over frequently (Yanagishita, 1998). Syndecan and glypican are internalized in separate endocytic pathways. Whereas glypican is rapidly targeted to the lysosome, syndecan is internalized via clathrin-mediated endocytosis. In early endosomes, the GAGs are cleaved from their protein scaffold by proteases and then suffer partial degradation of the GAGs by glycosylases. In what seems to be a rather slow endocytic process (1-2 h), GAGs are eventually degraded in an acidic lysosomal compartment (Yanagishita, 1992; Yanagishita and Hascall, 1992).

Cell–surface polysaccharides often act as important molecules for cell signaling and adhesion (Hacker *et al.*, 2005). Many viruses, including herpesviruses, require the presence of HS for efficient infection (Spear, 2004). Further, signaling molecules including FGF require the

presence of HS for stable signal transduction (Roghani and Moscatelli, 1992; Gleizes *et al.*, 1995). In fact, GAGs have been determined to be essential for the cellular entry of many proteins. For example, members of the fibroblast growth factor (FGF) superfamily require binding to HS and their cognate FGF-receptor protein for productive endocytosis (Roghani and Moscatelli, 1992). It has also been noted that HS mediates the internalization of polycations such as cationic lipids (Mislick and Baldeschwieler, 1996). Because of the well-established link between HS and polycation transport, GAGs such as HS became candidate receptors for PTDs.

Tyagi and coworkers were the first to show the importance of HS in PTD internalization. Using the entire HIV-Tat protein, they showed that internalization was not only an endocytic process but also requires the presence of HS (Tyagi *et al.*, 2001). Several groups have characterized the interaction between HIV-Tat and HS (Hakansson *et al.*, 2001; Ziegler and Seelig, 2004). In Chapter 2, we describe the role of GAGs in R₉ uptake. From our data, and that of others, we developed a model for cationic peptide internalization based on interactions with cell-surface carbohydrates (Figure 1-3).

Internalization in Living Cells

It is clear from a number of studies that PTD internalization in living cells is an endocytic process (Potocky *et al.*, 2003; Richard *et al.*, 2003; Fuchs and Raines, 2004). Yet, endocytosis is a general term that refers to a number of cellular processes. Therefore, many groups have tried to delineate the exact pathway of PTD entry into cells.

Dowdy and coworkers used a live-cell reporter assay to show that Tat-conjugated proteins were internalized via macropinocytosis (Wadia *et al.*, 2004). Macropinocytosis is a pathway that

involves invaginations of lipid raft regions of the plasma membrane (Johannes and Lamaze, 2002). They furthered showed that the Tat peptide alone followed the same pathway (Kaplan *et al.*, 2005).

Several groups have attributed internalization to other endocytic processes. Beaumelle and coworkers reported that HIV-TAT internalization occurred in clathrin-coated pits (Vendeville *et al.*, 2004). Further, Melikov and coworkers also showed that unconjugated TAT peptide internalization involves HS and is clathrin dependent (Richard *et al.*, 2005). Clathrin-mediated endocytosis does not occur in lipid rafts and therefore these results disagree with a model of macropinocytosis.

Most recently, Brock and coworkers have reported what they claim is a unifying model of peptide internalization. They found PTDs to be internalized via three mechanisms; macropinocytosis, clathrin-mediated endocytosis, and caveolae-mediated endocytosis (Fotin-Mleczek *et al.*, 2005). They showed that these three pathways competed with each other, but that internalization by the clathrin-mediated pathway had faster kinetics. Further, the clathrin-mediated pathway was only utilized at high ($> 5 \mu\text{M}$) peptide concentrations.

Delivery of PTDs to the cytoplasm

Current data suggest that both peptides and proteins fused to PTDs proceed into the cell via interactions with cellular polysaccharides (Zorko and Langel, 2005). Yet, the efficiency of delivery to the cytoplasm seems to be different for peptides and fusion proteins (Silhol *et al.*, 2002; Maiolo *et al.*, 2005). For delivery of macromolecules into the cytoplasm by endocytosis, the molecules must at some point cross a bilayer (plasma membrane, endosomal, or otherwise).

This step has been difficult to visualize and thus localize in live cells. Recently, Rothbard and coworkers suggested that guanidinium-containing peptides first form hydrogen bonds with anionic receptors (phospholipids) on the cell surface and then partition into the lipid bilayer in the direction dictated by the K^+ gradient present across the endosomal membrane (Rothbard *et al.*, 2004; Rothbard *et al.*, 2005). This model explained the ATP dependence of uptake as well as further defined the role of the guanidinium group. In contrast, Matile and coworkers examined the role of counterions in promoting exchange between surface-bound peptide and peptide partitioned into the bilayer (Sakai and Matile, 2003; Nishihara *et al.*, 2005). They found that in the presence of hydrophobic counteranions, the positive charges of polyarginine could be neutralized thus promoting bilayer partitioning. Their data suggest that, in the presence of the proper hydrophobic counterion, peptides should be able to translocate across a bilayer without the need for ATP hydrolysis.

Another model proposed by several labs involves requisite endosomal acidification for peptide release into the cytoplasm (Fischer *et al.*, 2002; Koch *et al.*, 2003; Potocky *et al.*, 2003; Magzoub *et al.*, 2005). Graslund and coworkers showed that the release of PTDs from lipid vesicles could be induced by creating an artificial pH gradient mimicking the gradient that exists between endosomal vesicles and the cytosol (Magzoub *et al.*, 2005). Gellman and coworkers showed that endosomal release of β -TAT was blocked by the addition of ammonium chloride, which blocks endosomal acidification (Potocky *et al.*, 2003).

Current model

The plethora of data concerning PTD entry acquired in the last few years has begun to shed light on these remarkable peptides. We know that the initial attachment to the cell surface is mediated by carbohydrates; most likely heparan sulfate and other sulfated GAGs (Tyagi *et al.*, 2001; Fuchs and Raines, 2004). Internalization is an endocytic process as peptides are colocalized with vesicle markers within living cells (Fuchs and Raines, 2004). The route through which these reach the cytoplasm is unclear but could involve the activity of heparanases as well as ATP-dependent pumps to enable the release of peptides. Nonetheless, it is possible that the heparan sulfate pathway could be a non-productive pathway that competes with an ATP-independent mechanism of transport, possibly involving bilayer partitioning. We show a current model for cationic PTD entry in Figure 1-3.

1.5 Other Functions of Cationic peptides

Biochemists have tried to exploit the properties of polycations such as polyarginine for many years. In 1976, Mandel and Fasman showed that polylysine or histones could condense DNA and be used to facilitate DNA delivery to cells (Mandel and Fasman, 1976). This work was advanced with the discovery and development of cationic lipids for the delivery of molecules into mammalian cells (Magee and Miller, 1972). Cationic lipids are now commonly used for the cellular delivery of proteins and nucleic acids (Hart, 2005).

Cationic peptides have promise as simple tags for proteins. Sassenfeld and Brewer showed that they could take advantage of the cationic nature of arginine by using short polyarginine

sequences to facilitate purification of recombinant proteins (Sassenfeld and Brewer, 1984). They further showed this tag could be specifically removed by carboxypeptidase B, an exoprotease that sequentially cleaves basic amino acids from the C-terminus of polypeptides. Wagner and coworkers noted that short polyarginine tags allowed for reversible immobilization of proteins onto solid supports (Nock *et al.*, 1997). They were able to immobilize green fluorescent protein (GFP) on mica surfaces and show that binding required the presence of the polyarginine tag. High ionic strength buffer caused desorption of the GFP by competition for surface binding.

The use of polycations has not been limited to proteins. Several groups have reported that polycationic polymers can be complexed with DNA plasmids to form multilayer thin films for the release of DNA into cells (Klugherz *et al.*, 2000; Schuler and Caruso, 2001; Jewell *et al.*, 2005). Lynn and coworkers have made ester-containing cationic polymers that are hydrolyzed at a specific rate to release DNA in a controlled manner (Vazquez *et al.*, 2002).

In Chapter 3, we describe the use of polyarginine fusion tags not only for internalization, but also immobilization and purification. Appendix II describes ongoing work done in collaboration with the Lynn group on the synthesis and properties of multilayered films of anionic polymers with small molecules and proteins fused to a PTD.

1.6 Prospectus

The applications of small peptides that facilitate transport into the cell are seemingly endless. Still, much remains to be understood about how these molecules work. The following section describes some of these unresolved issues.

Visualizing and enhancing endosomal escape

How do PTDs cross a cellular membrane into the cytoplasm? This is both the most difficult question to answer and the most difficult question to begin addressing. While fluorescence microscopy has been the useful tool in following PTD transport, visualizing the crossing of a peptide through a membrane is complicated by the build-up of fluorescent peptide in vesicles. Therefore new tools need to be developed to mask fluorescence prior to membrane crossing. Recently, our lab has published the synthesis of a small-molecule latent fluorophore that is non fluorescent until the molecule is cleaved by an esterase (Chandran *et al.*, 2005). Others have developed probes with fluorescence that responds to changes in pH or redox potential (Rijkers *et al.*, 1990; Hanson *et al.*, 2002; Hanson *et al.*, 2004). All of these tools could be utilized to visualize the later stages of PTD internalization.

The fraction of internalized PTDs that actually reach the cytosol is unknown. It is likely that a significant amount of peptide is routed to the lysosome, and there suffers degradation. Thus, it would be beneficial to design peptides with better internalization efficiency. There are many toxic peptides that form pores in membrane bilayers. Wolff and coworkers were able to mask the pore-forming activity of the bee-venom toxin melittin until the peptide reached the endosome (Rozema *et al.*, 2003). Upon reaching the endosome these peptides were activated, and they efficiently lysed the endosomal bilayer, and entered the cytoplasm. This technique, termed “Endosomolysis by Masking of a Membrane-Active Agent” (EMMA), allowed for controlled activation of the toxic activity of the peptide without promoting lysis of the plasma membrane and subsequent cell death. This approach was limited by lack of affinity for the cell surface. One

could, however, envision combining EMMA with a PTD such as polyarginine to promote not only cell-surface binding but also endosomal release.

Engineered Cationic Proteins

Much of the work with polycation-mediated internalization has focused on cationic peptides. As noted above, the chemical conversion of acidic residues into amines increases protein uptake. Is it possible to install cationic residues within a protein so as to bestow the ability to enter cells without affecting wild-type function? We attempt to address this question in Chapter 4 and Appendix I by using green fluorescent protein (GFP) and RNase A as model proteins.

1.7 Conclusion

The field of PTD cellular translocation has progressed rapidly over the past decade. Although much remains to be understood about the mechanism(s) of uptake, the great promise of these peptides as tools for drug delivery and scientific discovery make them a worthwhile area for research. Gaining a good understanding of the potential of these peptides will require a multidisciplinary and multidirectional approach. In turn, illuminating PTD function will likely lead to the discovery of new and useful applications.

Table 1-1: Cationic Peptides with Translocation Activity

Name	Sequence	Reference
<i>Natural peptides</i>		
HIV-1 Tat	RKKRRQRRR	(Vives <i>et al.</i> , 1997)
HIV-1 Rev	TRQARRNRRRRWRERQRG	(Suzuki <i>et al.</i> , 2002)
FHV coat	RRRRNRTRNRNRKVRG	(Suzuki <i>et al.</i> , 2002)
Antennapedia (Ant)	RQIKIWFQNRRMKWKK	(Derossi <i>et al.</i> , 1994)
Nucleoplasmin	KRPAAIKV	(Suzuki <i>et al.</i> , 2002)
Buforin II	TRSSRAGLQFPVGRVHRLLRK	(Park <i>et al.</i> , 2000)
DPV3	RKKRRRESRKKRRRES	(De Coupade <i>et al.</i> , 2005)
DPV7	GKRKKKGKLGKKRDP	(De Coupade <i>et al.</i> , 2005)
DPV10	SRRARRSPRGLGSG	(De Coupade <i>et al.</i> , 2005)
DPV15b	GAYDLRRRRERQSRLRRRRERQSR	(De Coupade <i>et al.</i> , 2005)
DPV1047	VKRGLKLRHVRPRVTRMDV	(De Coupade <i>et al.</i> , 2005)
<i>Synthetic peptides</i>		
R ₉	RRRRRRRRR	(Mitchell <i>et al.</i> , 2000)
r ₉	rrrrrrrrr	(Mitchell <i>et al.</i> , 2000)
pVEC	LLIILRRRRIRKQAHASHK	(Elmqvist <i>et al.</i> , 2001)
SynB1	RGGRLSYSRRRFSTSTGR	(Rousselle <i>et al.</i> , 2000)
Pept4	YARAAARQARA	(Ho <i>et al.</i> , 2001)
Pep-1	KETWWETWWTEWSQPKKKRKV	(Morris <i>et al.</i> , 2001)

Figure 1-1: Mechanism for intracellular translocation of cationic peptides. (A) Peptides are trapped in inverted micelles within the plasma membrane. These micelles can reopen inside the cell releasing peptide cargo. (B) Micelles perturb the plasma membrane locally, allowing cationic peptides to cross directly into the cytosol. Figure adapted from (Prochiantz, 2000).

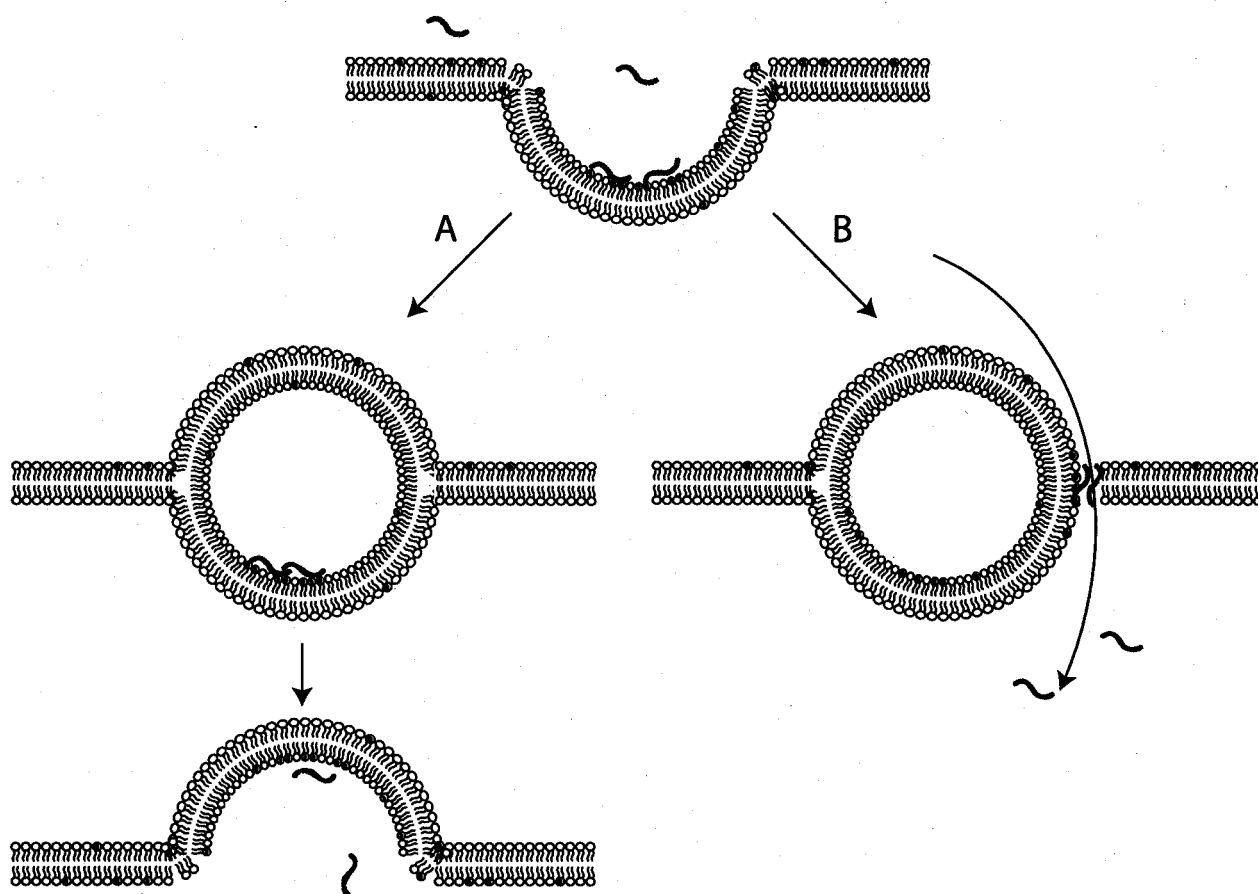


Figure 1-2: Pathway for the transduction of cationic peptides into cells. Cationic PTDs bind to HS proteoglycans on the cell surface. PTDs are internalized by endocytosis. HS is degraded by heparanases. Free PTDs leak from endocytic vesicles and enter the cytosol. Figure taken from (Fuchs and Raines, 2004).

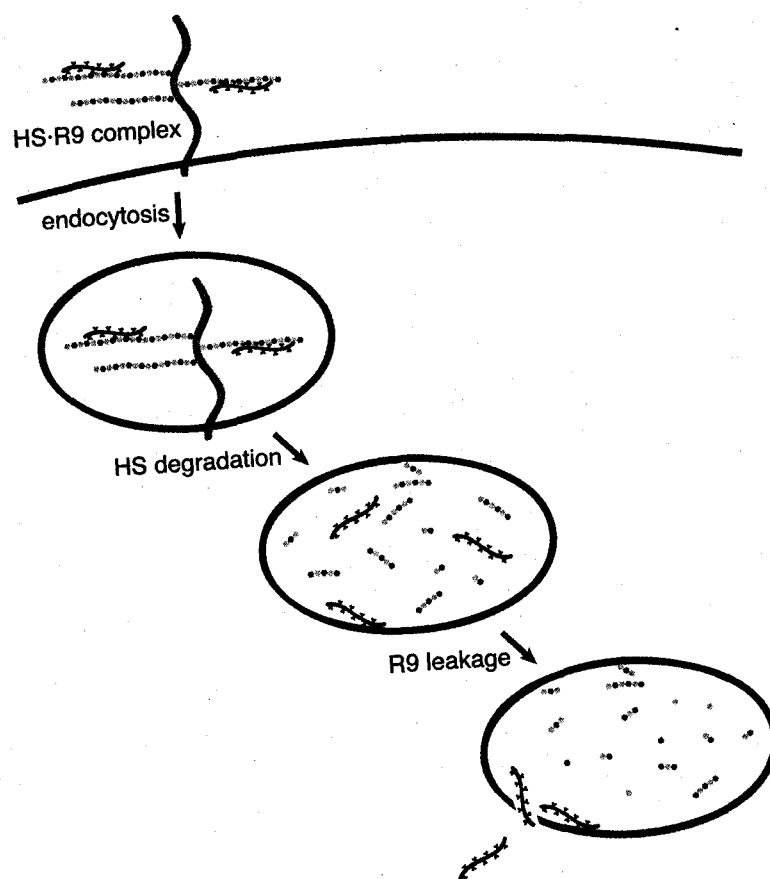
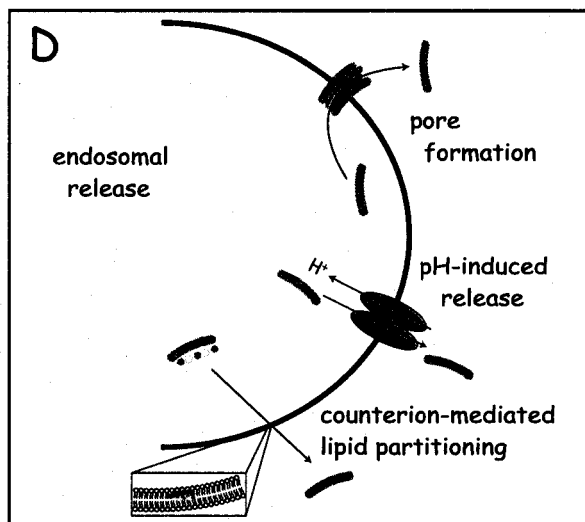
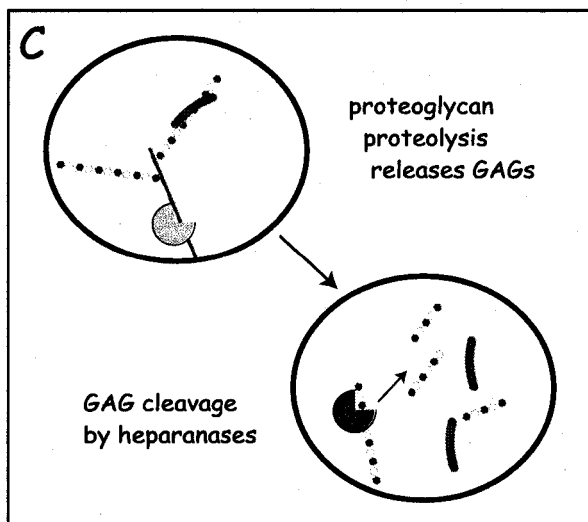
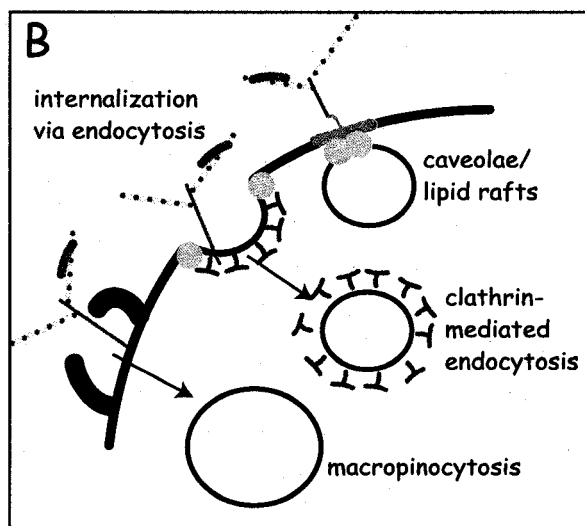
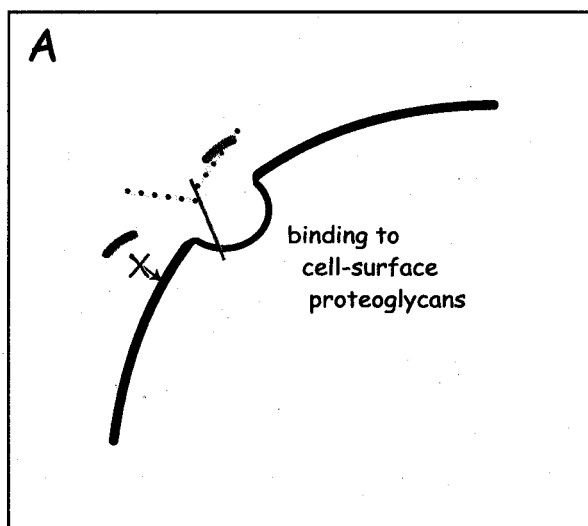
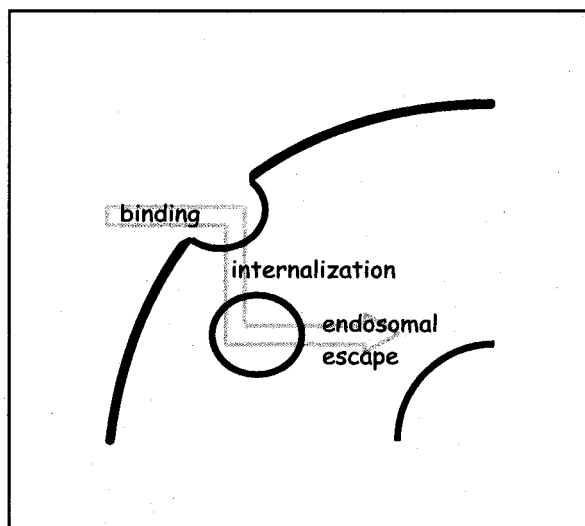


Figure 1-3: Current model of cationic peptide translocation into cells. Translocation consists of three steps: binding, internalization, and endosomal escape. Binding (A) of cationic peptides (purple) has been shown to be mediated by GAGs such as HS (green and yellow) and not occur through direct interaction with the plasma membrane. Internalization (B) probably occurs through several endocytic mechanisms including clathrin-mediated endocytosis, macropinocytosis and caveolae-mediated endocytosis. After their internalization, peptides are released from GAGs first by proteases (beige) and then heparanases (pink), which yield smaller GAG chains. Endosomal escape (D) can occur through a number of different mechanisms, including electropotential-mediated pore formation, pH-induced release, and counterion-mediated lipid partitioning.



Chapter Two

Pathway for Polyarginine Entry into Mammalian Cells

This chapter was published in part as:

Fuchs, S.M., and Raines, R.T. (2004) Pathway for polyarginine entry into mammalian cells.
Biochemistry, 43, 2438-2444.

2.1 Abstract

Cationic peptides known as protein transduction domains (PTDs) provide a means to deliver molecules into mammalian cells. Here, nonaarginine (R_9), the most efficacious of known PTDs, is used to elucidate the pathway for PTD internalization. Although R_9 is found in the cytosol as well as the nucleolus when cells are fixed, this peptide is observed only in the endocytic vesicles of live cells. Co-localization studies with vesicular markers confirm that PTDs are internalized by endocytosis rather than by crossing the plasma membrane. The inability of R_9 to enter living cells deficient in heparan sulfate (HS) suggests that binding to HS is necessary for PTD internalization. This finding is consistent with the high affinity of R_9 for heparin ($K_d = 109$ nM). Finally, R_9 is shown to promote the leakage of liposomes, but only at high peptide:lipid ratios. These and other data indicate that the PTD-mediated delivery of molecules into live mammalian cells involves: (1) binding to cell-surface HS, (2) uptake by endocytosis, (3) release upon HS degradation, and (4) leakage from endocytic vesicles.

2.2 Introduction

Facilitating the delivery of molecules into mammalian cells is of substantial interest (Denicourt and Dowdy, 2003; Green et al., 2003; Hallbrink et al., 2001; Leifert and Lindsay Whitton, 2003; Thierry et al., 2003; Vives et al., 2003). Developing the means to do so can generate both insights into cellular function and potential applications in biomedicine. As early as 1965, Ryser noted that mixing polylysine or other cationic macromolecules with proteins greatly increases the uptake of those proteins by cells (Ryser and Hancock, 1965). In 1988, Frankel and Green independently discovered that the RNA-binding HIV-TAT protein was capable of crossing lipid bilayers (Frankel and Pabo, 1988; Green and Loewenstein, 1988). The dissection of HIV-TAT function has revealed that a small cationic domain, residues 47–57, is responsible for transduction (Vives et al., 1997). Other cationic, nucleic acid-binding sequences are likewise capable of entering cells (Coeytaux et al., 2003; Suzuki et al., 2002). Peptide-like molecules and even non-peptidyl polycations are capable of crossing lipid bilayers (Mitchell et al., 2000; Suzuki et al., 2002). These cationic “protein transduction domains” (PTDs) are not only capable of entering cells but also can be used to deliver molecular cargo (Eguchi et al., 2001; Fawell et al., 1994; Schwarze et al., 1999), such as proteins, oligonucleotides, and small molecules (Backer et al., 2002; Hallbrink et al., 2001; Pooga et al., 2001; Schwarze and Dowdy, 2000; Wender et al., 2000).

What are the physicochemical characteristics of cationic PTDs? A natural backbone is not necessary for transduction, as D-amino acid (Derossi et al., 1996), peptoid (Wender et al., 2000), oligocarbamate (Wender et al., 2002), β -peptide (Rueping et al., 2002; Umezawa et al., 2002),

and 6-aminocaproic acid (Rothbard et al., 2002) analogs are capable of entering cells. In contrast, the positive charge of cationic PTD is essential for transduction, and arginine is preferred over lysine or histidine (Mitchell et al., 2000). Nonaarginine (R₉) is the most efficacious known PTD that is composed of natural L-amino acid residues (Wender et al., 2000).

Although the use of PTDs as macromolecular delivery devices has received much attention, the mechanism of PTD internalization remains controversial (Leifert and Lindsay Whitton, 2003). To date, most mechanistic studies have been performed with fixed cells (Futaki et al., 2002; Mai et al., 2002; Mitchell et al., 2000; Ragin et al., 2002; Rothbard et al., 2002; Rueping et al., 2002; Suzuki et al., 2002; Umezawa et al., 2002; Wender et al., 2002). Recently, Johansson, Lebleu, and their coworkers showed that cell fixation alters the transduction of cationic peptides (Lundberg and Johansson, 2002; Richard et al., 2003). Internalization was found to be energy-dependent, and the internalized peptide was observed in the endocytic vesicles of living cells (Richard et al., 2003). Dervan, Johansson, and their coworkers have reported similar cell-fixation artifacts for the transduction of N-methylpyrrole/N-methylimidazole polyamides (Belitsky et al., 2002) and PTD–green fluorescent protein fusions (Lundberg et al., 2003).

There have also been conflicting reports on whether PTDs bind to cell-surface glycosaminoglycans (GAGs) (Belting, 2003; Mai et al., 2002; Suzuki et al., 2002; Tyagi et al., 2001). The cell surface is coated with polysaccharides such as HS and sialic acid, and these molecules are known to mediate the binding of many proteins to cells (Belting, 2003). GAGs are actively internalized from the cell surface in vesicles (Yanagishita, 1998), and this turnover could allow for the passive uptake of interacting macromolecules. Tyagi has shown that the internalization of HIV-TAT protein is dependent on the presence of heparan sulfate

proteoglycans (HSPGs) (Tyagi et al., 2001). Subsequently, however, Sugiura reported that this constraint does not exist for polyarginine internalization into fixed cells (Suzuki et al., 2002).

Here, we examine the internalization of R₉ into both fixed and living cells. We also analyze R₉ internalization into living GAG-deficient Chinese hamster ovary (CHO) cells, and we extend those analyses with both qualitative and quantitative experiments on the binding of R₉ to heparin. Finally, we determine whether R₉ is able to promote the leakage of liposomes. Together, the data reveal provisions for the entry of a cationic PTD into mammalian cells.

2.3 Materials and Methods

Materials. Amino acids for peptide synthesis were from Novabiochem (Darmstadt, Germany). 5-(and 6-)Carboxytetramethylrhodamine (TAMRA), Hoescht 33342, and FM 1-43 were from Molecular Probes (Eugene, OR). Solvents were from Aldrich Chemical (Milwaukee, WI). Egg phosphatidylcholine (PC) and low-molecular weight heparin (M_r 3000) were from Sigma Chemical (St. Louis, MO). All other chemicals were from Fisher Scientific (Pittsburgh, PA) or Aldrich Chemical (Milwaukee, WI), and were used without further purification.

CHO-K1 cells were from the American Type Culture Collection (Manassas, VA). CHO-pgsD-677 cells (Lidholt et al., 1992) and CHO-pgsA-745 cells (Esko et al., 1985) were gifts of R. I. Montgomery. Cell culture medium and supplements were from Life Technologies (Gaithersburg, MD).

Peptide Synthesis. R₉ was synthesized by normal Fmoc-based solid-phase peptide synthesis with an Applied Biosystems Model 432A peptide synthesizer. R₉ was cleaved from the Rink acid

resin by incubation for 4 h in trifluoroacetic acid/ethanedithiol/phenol/thioanisole (32:4:3:1) and precipitated in diethylether. R₉ was purified by reversed-phase HPLC on a C4 column using a gradient of water:acetonitrile containing trifluoroacetic acid (0.1% v/v), and analyzed by matrix-assisted laser desorption ionization–time-of-flight (MALDI–TOF) mass spectrometry using a Bruker Biflex III instrument (m/z 1424.97; expected: 1423.69).

Peptide Labeling. R₉ was labeled on resin by incubation for 4 h with TAMRA (4 equivalents) in dimethylformamide containing benzotriazole-1-yl-oxy-tris-pyrolidino-phosphonium hexafluorophosphate (4 equivalents) and diisopropylethylamine (8 equivalents). The resin was washed with dimethylformamide and dichloromethane before deprotection as described above. TAMRA–R₉ was purified by reversed-phase HPLC and analyzed by MALDI–TOF mass spectrometry (m/z 1837.92; expected: 1837.13).

Liposomal Leakage. Egg phosphatidyl choline liposomes containing carboxyfluorescein (100 mM) were formed as described previously (Medina et al., 2002). Liposomes of 100- μ m diameter were generated by passage (≥ 10 times) through a mini-extruder (Avanti Polar Lipids). Promotion of vesicular leakage by R₉ was monitored by an increase in fluorescence intensity at 515 nm (excitation: 495 nm) using a QuantaMaster 1 photon-counting fluorometer from Photon Technology International (South Brunswick, NJ). Experiments were performed in 20 mM HEPES–NaOH buffer, pH 7.2. Percent leakage (%L) was calculated as $100 \cdot (I - I_0) / (I_{\text{detergent}} - I_0)$ where I_0 is the initial fluorescence intensity and $I_{\text{detergent}}$ is the intensity following the addition of Triton X-100 (to 0.1% v/v). Following each experiment, exact phospholipid concentrations were measured by using the method of Ames (Ames, 1966).

Cell Culture. CHO cell lines were cultured in Ham's F-12 medium supplemented with fetal calf serum (to 10% v/v) and antibiotics. Cells were grown in a CO₂(g) (5% v/v) atmosphere at 37 °C.

Peptide Internalization. CHO cells were seeded in 4-well Lab-Tek-II chamber slides (Nalge Nunc International, Naperville, IL) in Ham's F-12 medium. Labeled peptide was added to each slide, which was then incubated at 37 °C. After 60 min, cells were washed (6 times) with PBS containing Ca²⁺ (0.1 g/L) and Mg²⁺ (0.1 g/L). Fixed cells were prepared according to the procedure that we described previously (Umezawa et al., 2002). Cellular localization was visualized using an Eclipse E800 fluorescence microscope from Nikon (Tokyo, Japan) equipped with a 60X or 100X lens.

Heparin-Affinity Chromatography. The interaction of R₉ and heparin was assessed qualitatively by affinity chromatography. A 1.0-mL HiTrap Heparin HP column from Amersham Pharmacia Biotech (Piscataway, NJ) was equilibrated with 50 mM sodium acetate buffer (pH 5.0). Labeled peptide (~2 mg) was loaded onto the column, and eluted with a linear gradient of NaCl (0–2 M) in the same buffer. Peptide elution was monitored by absorbance at 280 and 535 nm.

Binding of TAMRA-R₉ to Heparin. An increase in the fluorescence of TAMRA-R₉ at 590 nm (excitation: 531 nm) accompanies its binding to soluble heparin. This increase was used to quantitate the affinity of TAMRA-R₉ (1.0 nM) for heparin (*M_r* 3000) in 20 mM HEPES–NaOH buffer, pH 7.5, using an EnVision multilabel plate reader from PerkinElmer (Wellesley, MA).

2.4 Results

R₉ Internalization in CHO Cells. Earlier this year, the intracellular localization of HIV-TAT peptide in fixed cells was reported to differ from that in living cells (Richard et al., 2003). To explore whether this dichotomy is a general feature of cationic PTDs, TAMRA-R₉ internalization was examined in living and fixed CHO-K1 cells. In living cells, TAMRA-R₉ was found in what appeared to be vesicles within the cell (Figure 2-1A). Upon fixing with paraformaldehyde (4% w/v), TAMRA-R₉ migrated to the nucleolus and diffused throughout the cytoplasm (Figure 2-1B). Similar results were observed when cells were fixed with acetone/methanol (1:1) (data not shown).

To confirm that TAMRA-R₉ did indeed localize to the vesicles of living cells, the localization of TAMRA-R₉ was compared to that of the dyes FM 1-43 (which is a marker for endocytotic vesicles) and Hoescht 33342 (which is a cell-permeable nuclear stain). Both TAMRA-R₉ and FM 1-43 appeared in punctate vesicular structures (Figure 2-2). No TAMRA-R₉ was visible in the nucleus of living cells.

R₉ Uptake by Glycosaminoglycan-Deficient CHO Cells. The CHO-pgsD-677 and CHO-pgsA-745 cell lines have mutations in the glycosaminoglycan (GAG) biosynthetic pathway. Specifically, CHO-pgsD-677 cells do not produce HS (Lidholt et al., 1992), and CHO-pgsA-745 cells produce neither HS nor chondroitin sulfate (CS) (Esko et al., 1985). TAMRA-R₉ was incubated with these mutant cells and wild-type CHO-K1 cells (positive control experiment), and its uptake was examined by fluorescence microscopy. Although TAMRA-R₉ was clearly visible in CHO-K1 cells, there was almost no detectable fluorescence from TAMRA-R₉ in GAG-deficient cell lines (Figure 2-3). These data indicate that interaction with GAGs on the cell

surface is critical for TAMRA-R₉ internalization. Adding exogenous heparin to CHO-K1 cells prior to the addition of TAMRA-R₉ leads to results similar to that with the GAG-deficient cell lines (data not shown), presumably because the exogenous heparin competes with cell-surface GAGs for TAMRA-R₉.

Binding of TAMRA-R₉ to Heparin. The interaction of R₉ with heparin (Figure 2-4A), which mimics the GAGs on the surface of a mammalian cell,² was probed in both qualitative and quantitative assays. The qualitative assay used affinity chromatography with immobilized heparin. TAMRA-R₉ was found to bind extremely tightly to immobilized heparin, eluting at approximately 1.5 M NaCl in 50 mM sodium acetate buffer, pH 5.0 (Figure 2-4B). This affinity is comparable to that of the HIV-TAT peptide under similar conditions (Hakansson et al., 2001).

The affinity of TAMRA-R₉ for soluble heparin was quantitated with a direct titration monitored by fluorescence spectroscopy. To determine the value of the equilibrium dissociation constant (K_d), binding data were fitted by nonlinear regression analysis to the equation:

$K_d^n = [\text{heparin}][\text{TAMRA-R}_9]^n / [\text{heparin} \cdot n\text{TAMRA-R}_9]$ with the program Prism 4 from GraphPad (San Diego, CA). Because heparin (M_r 3000) and TAMRA-R₉ (M_r 1836) are essentially homopolymers of similar mass, the value of n is likely to be near unity. For $n = 1$, $K_d = 109 \pm 13$ nM (Figure 2-4C). Allowing the value of n to vary gave $n = 0.87 \pm 0.05$ and $K_d = 119 \pm 16$ nM, which is not distinguishable from the value of K_d calculated with $n = 1$.

Liposomal Leakage. Some cell-permeating peptides enter mammalian cells by interacting directly with the lipid bilayer (Prochiantz, 2000). The ability of peptides to disrupt membrane integrity can be measured with a liposomal leakage assay (Medina et al., 2002).

Carboxyfluorescein was encapsulated in liposomes at a high concentration (>100 mM), which

quenches its intrinsic fluorescence. Upon vesicle disruption, leakage occurs, resulting in an increase in fluorescence. In a negative control experiment, no leakage of carboxyfluorescein from egg PC vesicles was observed in buffer alone (data not shown). R₉-Induced leakage in a peptide concentration-dependent manner (Figure 2-5A). This result indicates that R₉ is capable of disrupting the lipid bilayer. Yet, a peptide:lipid molar ratio of nearly 1:1 was required to induce leakage by R₉ (Figure 2-5B). In a positive control experiment, melittin (which forms pores in lipid bilayers (Yang et al., 2001)) caused more rapid leakage at 30 nM than did R₉ at 260 nM (data not shown).

2.5 Discussion

The efficacy of nascent chemotherapeutics can be limited by their ability to enter mammalian cells (Rojas et al., 1998; Schwarze et al., 1999). PTDs can expedite delivery (Denicourt and Dowdy, 2003; Green et al., 2003; Hallbrink et al., 2001; Leifert and Lindsay Whitton, 2003; Thierry et al., 2003; Vives et al., 2003). Determining the requirements for PTD entry into cells could enable the creation of even better molecular devices to effect internalization, as well as reveal new aspects of cellular biochemistry and biophysics.

Previous work has led to conflicting conclusions regarding the interaction of PTDs with cells. The mechanism by which peptide toxins, such as mellitin and magainin, interact with cells has been studied extensively, and these peptides are known to form pores in the plasma membrane (Yang et al., 2001). Penetratin, which is a cationic peptide corresponding to the third α -helix of the Antennapedia homeodomain, is capable of crossing membranes without causing vesicle

disruption. In the presence of a lipid bilayer, penetratin appears to form an amphipathic α -helix, which facilitates its insertion into the bilayer (Fischer et al., 2000; Thoren et al., 2000). HIV-TAT peptide has likewise been found in a helical structure by NMR spectroscopy, suggesting that HIV-TAT and perhaps other PTDs could act in a manner similar to penetratin (Silhol et al., 2002).

Early mechanistic studies on the cellular entry of PTDs were performed with fixed cells (Futaki et al., 2002; Mai et al., 2002; Mitchell et al., 2000; Ragin et al., 2002; Rothbard et al., 2002; Rueping et al., 2002; Suzuki et al., 2002; Umezawa et al., 2002; Wender et al., 2002). Fixation is believed to permeate membranes (Richard et al., 2003), and allows vesicle-entrapped peptides and proteins to travel to new locations (Lundberg and Johansson, 2002; Lundberg et al., 2003; Richard et al., 2003). Likewise, we find that TAMRA-R₉ is found in different cellular locations in fixed and living cells. Specifically, TAMRA-R₉ localizes in the nucleolus and cytoplasm of fixed cells (Figure 2-1B). In living cells, however, TAMRA-R₉ is found primarily in vesicles (Figures 2-1A and 2-2). As a result, our efforts to elucidate the requirements for PTD internalization have focused on living cells.

In living cells, cationic proteins such as HIV-TAT protein and some analogues of ribonuclease A (which is a small cationic protein (Raines, 1998)) are thought to bind to anionic carbohydrates on the cell surface (Ogawa et al., 2002; Tyagi et al., 2001). Moreover, polysaccharides such as heparan sulfate are believed to play important roles in cellular signaling by initiating the binding of certain proteins to their cellular receptors {Renato, 2001 #1512; Bernfield, 1999 #1513; Belting, 2003 #12}. On the cell surface, heparan sulfate is attached to either transmembrane proteins to form syndecans or GPI-anchored proteins to form glypicans

(Sasisekharan and Myette, 2003; Varki et al., 1999). The HS side chains of these heparan sulfate proteoglycans (HSPGs) undergo hydrolytic degradation by heparanases *en route* to the lysosome (Yanagishita and Hascall, 1984).

A number of proteins are known to bind to specific HSPGs. For some of these proteins, HS is believed to act as the receptor for cellular entry (Hashimoto et al., 1997). We find that the entry of a cationic PTD into living mammalian cells relies on the presence of HSPGs. Specifically, the entry of TAMRA-R₉ into CHO cells that are deficient in HS is decreased greatly relative to that into wild-type cells (Figure 2-3). Similar results have been observed with the intact HIV-1 TAT protein (Hashimoto et al., 1997).

HS and heparin are analogous glycosaminoglycans (Sasisekharan and Venkataraman, 2000; Varki et al., 1999).² Accordingly, heparin has been used as a surrogate for HS in a wide variety of biochemical experiments (Bilozur and Biswas, 1990; San Antonio et al., 1994; Zhou et al., 1999). We reasoned that if HSPGs mediate the cellular entry of PTDs, then cationic peptides such as TAMRA-R₉ should have a measurable affinity for heparin. Indeed, we find that TAMRA-R₉ binds strongly to immobilized heparin (Figure 2-4B), which mimics the HS side chains of cell-surface HSPGs. Moreover, the soluble heparin-TAMRA-R₉ complex has a value of K_d near 0.1 μ M (Figure 2-4C), which is similar to that of a typical receptor-ligand interaction.

How does R₉ release from HS and escape from endocytic vesicles? HS is cleaved by heparanases, first in vesicles of neutral pH and then in acidic endosomes (Belting, 2003; McKenzie et al., 2003; Yanagishita and Hascall, 1984). HS cleavage would diminish its anion valency and should thus diminish its affinity for R₉. We find that free R₉ is capable of disrupting a lipid bilayer and causing a liposome to leak (Figure 2-5). This leakage is maximal between pH

7.5 and 9.5 (data not shown), suggesting that R₉ could escape from endosomes prior to their acidification. Regardless, R₉-induced liposomal leakage occurs at a peptide:lipid molar ratio that is 10- to 100-fold greater than that for known pore-forming peptides (Medina et al., 2002). Thus, the disruption of lipid bilayers is likely to play a limited role in transduction at low concentrations of R₉, and a relatively high concentration could be necessary for efficient transduction.

Our findings are consistent with a four-step pathway for the entry of cationic PTDs into the cytoplasm of mammalian cells (Figure 2-6). First, peptides bind to HSPGs on the cell surface. These peptides are then taken up into a cell by heparan sulfate-mediated endocytosis. Once in vesicles, HS is degraded by heparanases, releasing the PTD. Finally, unbound PTD escapes from the vesicles after achieving a concentration high enough to promote vesicular leakage. This pathway bears some analogy to those proposed for the cellular entry of other HS-binding proteins, such as bFGF (Sperinde and Nugent, 2000) or follistatin (Sugino et al., 1997). The identity of the rate-limiting step for PTD entry (Figure 6) is not known. Identifying that step could lead to more efficacious PTDs or to transduction agonists.

Figure 2-1 Localization of TAMRA-R₉ in living and fixed cells. The internalization of TAMRA-R₉ (1.0 μM) was analyzed by fluorescence microscopy. Cells were counterstained with Hoescht 33342. (A) living CHO-K1 cells. (B) CHO-K1 cells fixed with paraformaldehyde. Bar, 10 μm.

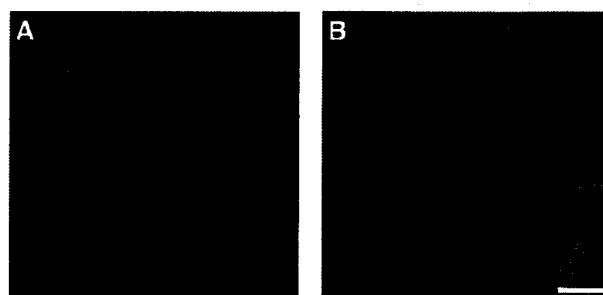


Figure 2-2 Co-localization of TAMRA-R₉ in living cells. The internalization of TAMRA-R₉ (1.0 μ M) and marker dyes into living CHO-K1 cells was analyzed by fluorescence microscopy. (A) TAMRA-R₉. (B) FM 1-43. (C) TAMRA-R₉, FM 1-43, and Hoescht 33342. (D) Bright-field image of CHO-K1 cells. Bar, 10 μ m.

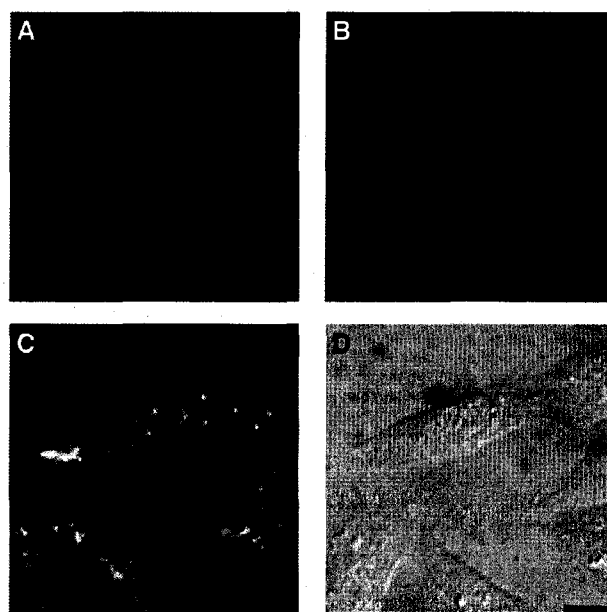


Figure 2-3 Dependence of TAMRA-R₉ internalization into living cells on glycosaminoglycans. Internalization of TAMRA-R₉ (1.0 μ M) into living wild-type and mutant CHO cells. (A) CHO-K1 cells (wild-type). (B) CHO-pgsD-677 cells (which lack HS). C, CHO-pgsA-745 cells (which lack HS and CS). Bar, 10 μ m.

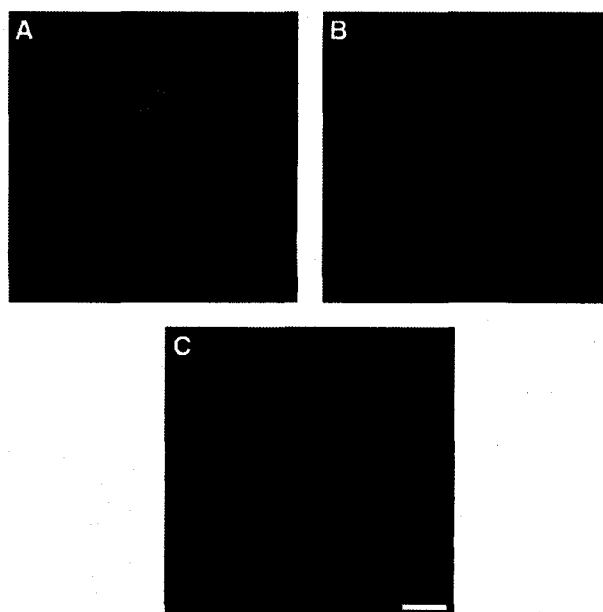


Figure 2-4 Affinity of TAMRA-R₉ for heparin. (A) Prevalent structural motif in heparin.²
(B) Elution profile from affinity chromatography of TAMRA-R₉ on immobilized heparin. TAMRA-R₉ was eluted with a linear gradient of NaCl (0–2 M) (conductivity, thin line), and monitored by its absorbance at 280 nm (thick line).
(C) Fluorescence titration of TAMRA-R₉ (1.0 nM) with heparin (*M_r* 3000) in 20 mM HEPES–NaOH buffer, pH 7.5. The equilibrium dissociation constant is $K_d = 109 \pm 13$ nM.

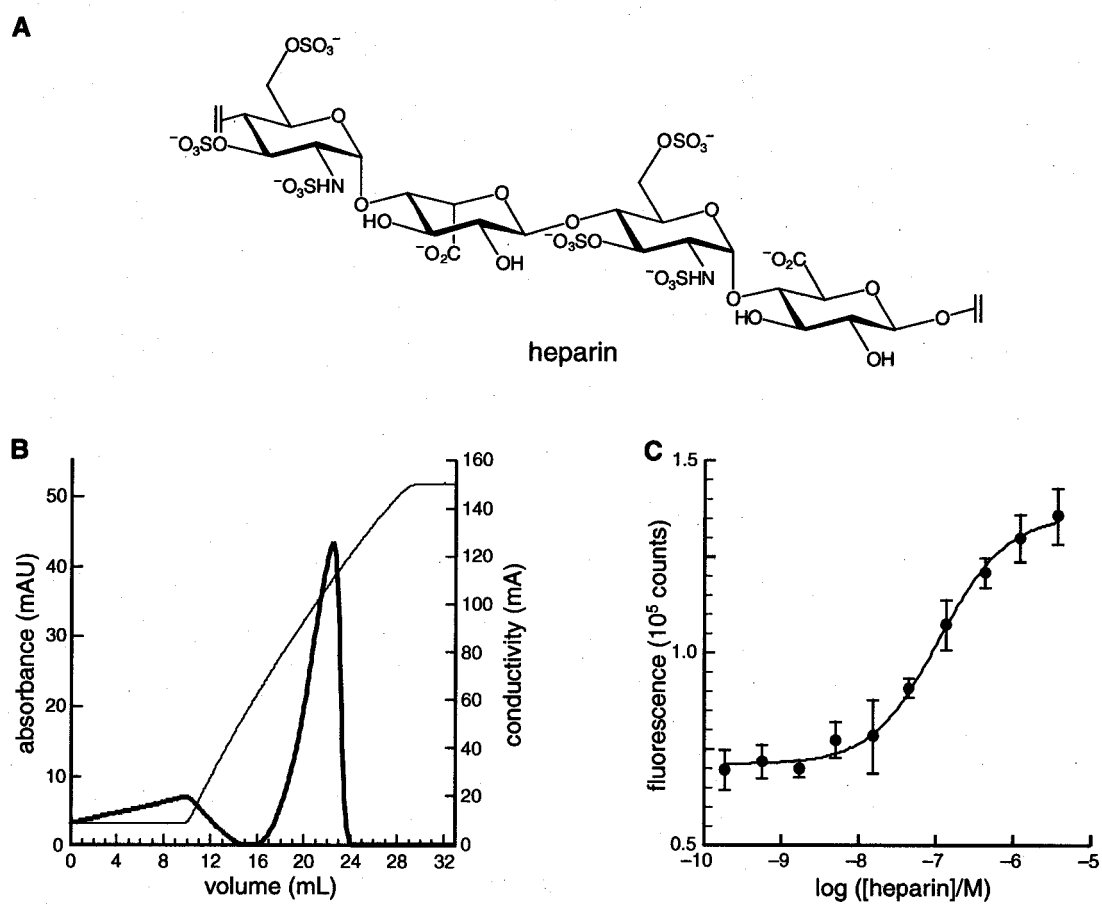


Figure 2-5 **R₉-Induced leakage of egg PC liposomes. (A)** Time course for the leakage of carboxyfluorescein from egg PC liposomes (100- μ m diameter) upon exposure to various concentrations of R₉. **(B)** Leakage of carboxyfluorescein from egg PC liposomes (100- μ m diameter) as a function of peptide:lipid molar ratio. Data in panel B are derived from data in panel A at 180 s.

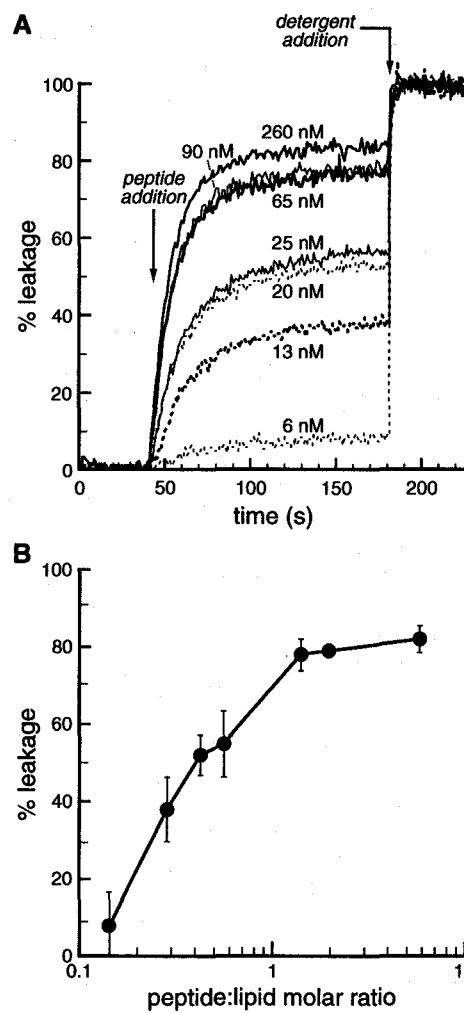
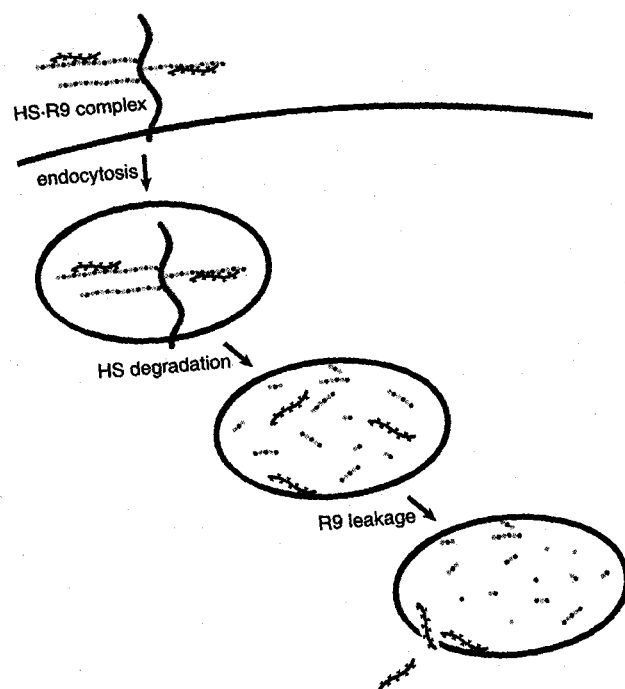


Figure 2-6 Pathway for the transduction of R_9 into cells. Cationic PTDs such as R_9 bind to HSPGs on the cell surface. PTDs are internalized by endocytosis. HS is degraded by heparanases. Free PTDs leak from endocytic vesicles and enter the cytosol.



Chapter Three

Polyarginine as a Multifunctional Fusion Tag

This chapter was published in part as:

Fuchs, S.M., and Raines, R.T. (2005) Polyarginine as a multifunctional fusion tag. *Protein Science*, 14, 1538-1544.

3.1 Abstract

Fusion to cationic peptides, such as nonaarginine (R_9), provides a means to deliver molecular cargo into mammalian cells. Here, we provide a thorough analysis of the effect of an R_9 tag on the attributes of a model protein: bovine pancreatic ribonuclease (RNase A). The R_9 tag diminishes the conformational stability of RNase A ($\Delta T_m = -8$ °C in phosphate-buffered saline). This effect is nearly mitigated by the addition of salt. The tag does not compromise the enzymatic activity of RNase A. An R_9 tag facilitates the purification of RNase A by cation-exchange chromatography and enables the adsorption of RNase A on glass slides and silica resin with the retention of enzymatic activity. The tag can be removed precisely and completely by treatment with carboxypeptidase B. Finally, the R_9 tag increases both the cellular uptake of RNase A and the cytotoxicity of G88R RNase A, a variant that evades the cytosolic ribonuclease inhibitor protein. Thus, polyarginine is a very versatile protein fusion tags.

3.2 Introduction

Numerous cationic peptides have been shown to permeate mammalian cells (Vives et al. 1997; Suzuki et al. 2002; Coeytaux et al. 2003). These peptides can serve as protein transduction domains (PTDs) to carry both small-molecule drugs and macromolecules such as proteins into cells (Schwarze et al. 1999; Rothbard et al. 2002). Although details of the internalization mechanism are unclear, the positive charge of these peptides is known to be critical for internalization (Mitchell et al. 2000). This requirement is probably due to favorable Coulombic interactions between the peptide and anionic cell-surface molecules, especially heparin sulfate (Fuchs and Raines 2004). The length and composition of the cationic peptide is important for internalization, as 7–9 cationic charges are optimal and arginine residues are preferred over lysine (Wender et al. 2000).

Despite the substantial interest among protein scientists in using PTDs, we are not aware of a detailed analysis of the effect of a PTD on the intrinsic properties of a protein cargo. Unlike small molecules, proteins have fragile conformations that are essential for their function. The addition of a nonaarginine (R₉) fusion tag could disrupt that conformation, and hence compromise function.

While much work has focused on the utility of an R₉ fusion tag in mediating cellular internalization, there is evidence that similar tags confer other useful attributes. Over twenty years ago, conjugation to short oligomers of arginine was used to facilitate protein purification (Sassenfeld and Brewer 1984). More recently, green fluorescent protein (GFP) containing a hexaarginine tag was adsorbed reversibly onto mica surfaces (Nock et al. 1997). Cationic

peptides have also been shown to interact strongly with both plastic and glass (Chico et al. 2003).

Here, we report on the impact of an R₉ fusion tag on the conformational stability and biological function of its protein cargo. We also describe numerous applications for an R₉ tag that are unrelated to cellular internalization, as well as a means to remove the tag precisely and completely. As a model protein, we use bovine pancreatic ribonuclease (RNase A; EC 3.1.27.5), which was perhaps the most studied enzyme of the 20th century (Raines 1998) and is now the basis for a new class of cytotoxins (Leland and Raines 2001). The intrinsic enzymatic and cytotoxic activities of RNase A provide a sensitive measure of the effect of an R₉ tag on both physical and biological attributes of a protein cargo. We find that R₉ has an ensemble of virtues that is unique among known fusion tags.

3.3 Materials and Methods

Cells and chemicals *Escherichia coli*. strain BL21 (DE3) PlysS and the pET22b(+) expression vector were from Novagen (Madison, WI). Human erythroleukemia cells (line K-562) and Chinese hamster ovary (line CHO-K1) were from the American Type Culture Collection (Manassas, VA). [methyl-³H]Thymidine (6.7 Ci/mmol) was from NEN Life Science Products (Boston, MA). All other chemicals and reagents were of commercial reagent grade or better and were used without further purification.

Terrific Broth (TB) liquid medium contained (in 1 L) tryptone (12 g), yeast extract (24 g), glycerol (4 mL), KH₂PO₄ (2.31 g), and K₂HPO₄ (12.54 g). Phosphate-buffered saline (PBS)

was 10 mM sodium phosphate buffer, pH 7.4, containing NaCl (138 mM) and KCl (2.7 mM).

Instruments. The mass of ribonuclease variants was confirmed by matrix-assisted laser desorption ionization–time-of-flight (MALDI–TOF) mass spectrometry using a Voyager-DE-PRO Biospectrometry Workstation (Applied Biosystems, Foster City, CA) using 3,5-dimethoxy-4-hydroxycinnamic acid as a matrix. Fluorescence measurements were performed with a QuantaMaster 1 photon counting fluorometer equipped with sample stirring (Photon Technology International, South Brunswick, NJ). Radioactivity was quantified with a Microbeta TriLux liquid scintillation counter (Perkin Elmer, Wellesley, MA).

Site-directed mutagenesis. Oligonucleotides were obtained from Integrated DNA Technology (Coralville, IA). cDNA encoding variants of RNase A were created in plasmid pBXR, which directs the production of RNase A in *E. coli* (delCardayré et al. 1995) by using the QuikChange mutagenesis kit from Stratagene (La Jolla, CA). All variants of RNase A possessed an N-terminal methionine residue, which has been reported to have no effect on ribonucleolytic activity (Arnold et al. 2002). An R₉ tag was separated from the remainder of a protein by a triglycine linker.

Production and purification of protein variants. Untagged variants of RNase A and Onconase™ (which is the most cytotoxic known homolog of RNase A (Matousek et al. 2003)) were produced in *E. coli* and purified as described previously (Leland et al. 1998). Variants of RNase A containing a C-terminal R₉ tag were prepared as follows. BL21(DE3)PlysS cells containing a plasmid that encodes an RNase A variant were grown at 37 °C with shaking (250 rpm) in TB containing ampicillin (200 µg/mL) and chloramphenicol (35 µg/mL) to an OD = 1.6

at 600 nm. cDNA expression was induced by adding isopropyl β -D-thiogalactopyranoside (IPTG; to 1 mM). Cells were grown for an additional 4 h before harvesting. Cell pellets were resuspended in lysis buffer, which was 10 mM Tris-HCl buffer, pH 8.0, containing ethylenediaminetetraacetic acid (EDTA; 1.0 mM), NaCl (0.10 M), and phenylmethylsulfonyl fluoride (1.0 mM), and lysed by sonication. Inclusion bodies were isolated by centrifugation at 11,000g for 45 min and solubilized in denaturing solution, which was 20 mM Tris-HCl buffer, pH 8.0, containing guanidine hydrochloride (7.0 M) and EDTA (10 mM), for 4 h at room temperature. Solubilized inclusion bodies were diluted ten-fold with acetic acid (20 mM) and clarified by centrifugation. The supernatant was dialyzed overnight against the same buffer. The resulting protein was then folded overnight at 4 °C in a redox buffer, consisting of 100 mM Tris-HCl buffer, pH 8.0, containing EDTA (10 mM), L-arginine (0.5 M), reduced glutathione (1 mM), and oxidized glutathione (0.2 mM). Refolded protein was purified by cation-exchange chromatography on a 5-mL HiTrap SP-sepharose FF column (Amersham Biosciences, Piscataway, NJ) in 50 mM sodium acetate buffer, pH 5.0, with a linear gradient (50 + 50 mL) of NaCl (0–1.5 M). The identity of each variant was verified by MALDI-TOF mass spectrometry.

Assays of enzymatic activity. Ribonucleolytic activity was measured by monitoring the increase in the fluorescence of 6-FAM-dArU(dA)₂-6-TAMRA (Integrated DNA Technologies, Coralville, IA) upon enzyme-catalyzed cleavage, as described previously (Kelemen et al. 1999) with minor modifications. Polyarginine-containing peptides are known to bind to glass surfaces (Chico et al. 2003). We observed this phenomenon (data not shown), and so performed all assays in 10 mM Bis-Tris-HCl buffer, pH 6.0, containing NaCl (0.50 M). In this high-salt buffer, the binding of protein to a quartz cuvette was found to be insignificant.

Assays of cytotoxicity. The effect of ribonucleases on cell proliferation was determined by measuring the incorporation of [methyl- ^3H]thymidine into cellular DNA. K-562 cells were grown in RPMI 1640 medium containing fetal bovine serum (10% v/v), penicillin (100 units/mL), and streptomycin (100 $\mu\text{g/mL}$). Cytotoxicity assays were performed using asynchronous log-phase cultures grown at 37 °C in a humidified incubator containing $\text{CO}_2(\text{g})$ (5% v/v). To assay toxicity, cells (95 μL of a solution of 5×10^4 cells/mL) were incubated with PBS containing a ribonuclease (5 μL) in a 96-well plate. The cells were grown for 44 h and then pulsed for 4 h with radiolabeled thymidine (0.25 $\mu\text{Ci/well}$), which is only incorporated into the DNA of living cells. DNA was harvested onto glass fiber filters using a PHD cell harvester (Cambridge Technology, Watertown, MA). Filters were washed with water and dried with methanol, and their ^3H content was quantified with liquid scintillation counting.

Semisynthesis of fluorescent proteins. RNase A were labeled with fluorescein at one specific residue in a surface loop by using variants in which Ala19 was replaced with a cysteine residue (Haigis and Raines 2003). A19C RNase A–R₉ or A19C RNase A (100 μM) were incubated in PBS containing a 20-fold molar excess of 5-iodoacetamidofluorescein (Molecular Probes, Eugene, OR) and a 3-fold molar excess of tris[2-carboxyethylphosphine] hydrochloride (TCEP) for 4 h at room temperature. The resulting solution was dialyzed overnight against 50 mM sodium acetate buffer, pH 5.0, and then purified by cation-exchange chromatography using a HiTrap CM-Sepharose Fast Flow column (5 mL) with a linear gradient (50 + 50 mL) of NaCl (0–1.00 M for A19C RNase A; 0–2.00 M for A19C RNase A–R₉). Conjugation to the fluorophore was confirmed by MALDI–TOF mass spectrometry.

Fluorescence microscopy. Fluorescence microscopy was used to follow the internalization of

fluorescent proteins by mammalian cells. CHO-K1 cells were maintained in Ham's F-12 Medium containing fetal bovine serum (5% v/v), penicillin (100 units/mL), and streptomycin (100 µg/mL). Cells were seeded onto glass-bottom culture dishes and grown overnight in the same medium. The medium was replaced with fresh medium (100 µL) immediately before the addition of fluorescein-labeled proteins. Cells were allowed to incubate with fluorescein-labeled RNase A–R₉ or RNase A for 15 min, and were then washed three times with the same medium containing *n*-propyl gallate (1 mM) to protect against photobleaching. Images were obtained with a Nikon C1 laser-scanning confocal microscope equipped with 60x and 100x lenses.

Thermal denaturation. As RNase A is denatured, its six tyrosine residues become exposed to solvent and its molar absorptivity at 287 nm decreases significantly (Hermans and Scheraga 1961). RNase A–R₉ or RNase A (25 µM) was placed in PBS or 50 mM sodium phosphate buffer, pH 7.2, containing NaCl (0–1.00 M). Unfolding was monitored by the change in absorbance at 287 nm as the temperature was raised at a rate of 0.15 °C/min. Data were fitted to a two-state model to calculate the value of T_m , which is the temperature at the midpoint of the transition between the folded and unfolded states (Pace and Scholtz 1997).

Adsorption of proteins to glass slides. Fluorescein-labeled RNase A–R₉ and RNase A were adsorbed on glass microscope slides by adding 5 µL of a solution of protein in PBS to wells formed by secure-seal hybridization chambers (Schleicher & Schuell Bioscience, Keene, NH). After 15 min, the wells were washed three times with PBS. The adsorption of proteins was visualized with a Typhoon 9410 variable mode fluorimager (Amersham Biosciences). Similarly, slides with adsorbed fluorescein-labeled RNase A–R₉ were washed with 50 mM sodium phosphate buffer, pH 7.2, containing NaCl (1.00 M) in an attempt to desorb the protein.

Adsorption of proteins to silica resin. A solution of RNase A–R₉ or RNase A (10 μM) in PBS was allowed to adsorb to acid-washed silica resin (10 mg; Sigma Chemical, St. Louis, MO) for 1 h. The resulting resin was washed extensively with 50 mM sodium phosphate buffer, pH 7.2, containing NaCl (1.00 M). The activity of the adsorbed enzyme was measured by adding resin (1 μL of a 1 mg/mL suspension) to a cuvette containing assay buffer, which was 50 mM MES–NaOH buffer, pH 6.0, containing NaCl (0.10 M) and the fluorogenic substrate 6-FAM–dArU(dA)₂–6-TAMRA. The MES in the assay buffer was purified prior to use by anion-exchange chromatography to remove the potent ribonuclease inhibitor oligo(vinylsulfonic acid) that contaminates buffers derived from ethanesulfonic acid (Smith et al. 2003). Substrate cleavage was monitored by the change in fluorescence (excitation: 495 nm, emission: 515 nm).

3.4 Results

Purification of an R₉-tagged protein and proteolytic degradation of the R₉ tag. One impetus for the development of novel peptide tags is to facilitate the purification of proteins produced by recombinant DNA (rDNA) technology (Nilsson et al. 1997; Stevens 2000; Hearn and Acosta 2001). Tags that can be utilized for purification and then removed are especially desirable. The addition of R₉ to RNase A increased the positive charge of the protein and thus strengthened its interaction with inexpensive, cation-exchange resins (Figure 3-1A). A concentration of NaCl exceeding 1 M was required for the elution of RNase A–R₉ from a HiTrap SP column. The resulting RNase–R₉ was homogeneous according to SDS–PAGE (Figure 3-1B), and had MS (MALDI) *m/z* 15,404 (expected for Met–RNase A–Gly₃–Arg₉: 15,390).

The C-terminal R₉-tag was removable by incubation with the exoprotease carboxypeptidase B (CPB), which catalyzes the sequential hydrolysis of peptide bonds of C-terminal basic residues. Removal of the tag was complete in less than 1 h. The resulting protein eluted at a lower salt concentration from SP Sepharose (Figure 3-1A), had greater mobility during SDS-PAGE (Figure 3-1B), and had MS (MALDI) m/z 14,000 (expected for Met-RNase A-Gly₃: 13,985), such that $(m/z) - 1404$ (expected for the loss of Arg₉: -1406).

Effect of R₉ tag on conformational stability and enzymatic activity. To be useful, a tag cannot greatly diminish the stability or activity of a protein. We measured the effect of an R₉ tag on the conformational stability of RNase A. The value of T_m for RNase A decreased from (62.1 ± 1.0) to (54.0 ± 1.0) °C upon addition of the R₉ tag (Figure 3-2A). RNase A is a cationic protein with a measured $pI = 9.3$ (Ui 1971). Adding additional cationic residues is likely to decrease the conformational stability of RNase A by increasing unfavorable Coulombic interactions within the protein (Shaw et al. 2001; Ramos and Baldwin 2002). To test this hypothesis, we measured the T_m of the two proteins at increasing concentrations of NaCl, which can ameliorate unfavorable Coulombic interactions. The value of T_m for RNase A increased gradually as a function of salt concentration (Figure 3-2B). In contrast, the value of T_m for RNase A-R₉ increased dramatically between 0.10 and 0.50 M NaCl, approaching that of RNase A. This result indicates that the destabilization does indeed arise from unfavorable Coulombic interactions.

The enzymatic activity of RNase A and RNase A-R₉ was determined by using a continuous assay with a fluorogenic substrate. The addition of R₉ had no noticeable effect on the activity of RNase A (Table 3-1). It is noteworthy, however, that these assays were performed in a buffer containing 0.50 M NaCl to minimize adsorption to the quartz cuvette.

Cellular uptake of an R₉-tagged protein. The most often noted function of cationic peptides such as R₉ is as a protein transduction domain. The uptake of RNase A and RNase A–R₉ into CHO-K1 cells was visualized by confocal microscopy. The uptake of RNase A–R₉ was evident after 30 min at 37 °C (Figure 3-3A). In contrast, the uptake of RNase A was not apparent under the same conditions (Figure 3-3B).

Cytotoxicity of R₉-tagged variants of ribonuclease A. In addition to being well-studied model protein, ribonucleases are potentially useful as cancer chemotherapeutics (Leland and Raines 2001). Although RNase A itself is not cytotoxic, its G88R variant is known to be toxic toward a wide variety of cancer cell types by virtue of its ability to evade ribonuclease inhibitor (RI) (Leland et al. 1998; Antignani et al. 2001; Haigis et al. 2003). RI is a cytosolic protein that binds to wild-type RNase A with nearly fM affinity, but has 10⁴-fold less affinity for G88R RNase A. Adding the R₉ tag to G88R RNase A resulted in a 3-fold increase in its cytotoxic activity (Figure 3-4; Table 3-1). This result suggests that cellular uptake limits the cytotoxicity of G88R RNase A. Interestingly, adding the R₉ tag did not endow wild-type RNase A with cytotoxic activity (Figure 3-4), despite an evident increase in cellular uptake (Figure 3-3). This result suggests that the concentration of RNase A–R₉ in the cytosol does not reach 4 μM, which is the cytosolic concentration of RI (Haigis et al. 2003).

Adsorption of an R₉-tagged protein. The immobilization of proteins on surfaces is enabling the creation of protein microarrays for probing protein–ligand and protein–protein interactions (Kabsch 1988; Kodadek 2001; Zhu and Snyder 2003). We used an R₉ tag to adsorb RNase A to glass slides and silica resin (Figure 3-5).

The R₉ tag enhances the binding of fluorescein-labeled RNase A by more than 30-fold (Figure 3-5A). The tagged protein remains associated with a glass slide, even in the presence of 1 M NaCl (data not shown). Adsorption of RNase A–R₉ to silica resin affords active enzyme on a solid support (Figure 3-5B). All detectable enzymatic activity is associated with the silica resin, rather than the supernatant. Virtually no wild-type RNase A adsorbed to silica resin under the same conditions.

3.5 Discussion

A great benefit of rDNA technology is the ability to fuse peptide sequences with useful attributes to a protein of interest. Until recently, such peptide tags have been used solely to facilitate purification or detection (Nilsson et al. 1997; Stevens 2000; Hearn and Acosta 2001). A few tags, such as the S-peptide of RNase A (Kim and Raines 1993), can play both roles. Recently, new tags have emerged that endow additional functions, such as cellular internalization or surface immobilization (Elia et al. 2002; Kabouridis 2003). We have shown that a polyarginine (R₉) tag can provide all of these attributes.

We fused R₉ to the C-terminus of RNase A by using rDNA technology. There, the R₉ tag greatly increased the affinity of RNase A for a cation-exchange resin (Figure 3-1). Further, the tag was removable precisely and completely by the addition of carboxypeptidase B. In additional experiments, we fused the R₉ tag to the N-terminus of RNase A. The resulting fusion protein had a degraded tag (data not shown). This result has precedent, as the endogenous ompT protease of *E. coli* has been shown to cleave proteins between adjacent basic residues (Ford et al. 1991).

Because protein biosynthesis begins at the N-terminus, a C-terminal R₉ tag on RNase A (which forms inclusion bodies in *E. coli* (delCardayré et al. 1995)) is less vulnerable to degradation by the ompT protease than is an N-terminal tag.

Enzymatic catalysis provides an extremely sensitive measure of native protein structure (Knowles 1987). We conclude that the addition of an R₉ tag appears to have little effect on the three-dimensional structure of wild-type RNase A or its G88R variant, based on a <2-fold change in values of k_{cat}/K_m for RNA cleavage (Table 3-1). The R₉ tag does, however, decrease the conformational stability of RNase A at physiological salt concentration (Figure 3-2). This effect is mitigated by the addition of salt, indicating that it originates from unfavorable Coulombic interactions between the cationic tag and the cationic protein. Because RNase A is an especially cationic protein, the destabilizing effect of an R₉ tag is likely to be less severe in most proteins.

One major hurdle in the development of protein chemotherapeutics is the inability to deliver them into cells. Some success has been achieved by fusing proteins to molecules that have cell surface receptors, such as folate or transferrin (Leamon and Low 1991; Rybak et al. 1991; Suzuki et al. 1999). A more recent approach has been to fuse proteins to peptide tags that are capable of entering cells (Beerens et al. 2003; Green et al. 2003). Indeed, we observed that RNase A–R₉ is internalized more efficiently than is RNase A (Figure 3-3). More rapid uptake is consistent with the 3-fold increase in cytotoxic activity conferred by an R₉ tag to G88R RNase A (Figure 3-4). This increase is noteworthy, given that approximately 99% of RNase A suffers lysosomal degradation before reaching the cytoplasm (Kothandaraman et al. 1998).

Finally, we find that RNase A–R₉ but not RNase A is adsorbed strongly on glass or silica

surfaces (Figure 3-5). The RNase A–R₉ remains adsorbed in the presence of 1 M NaCl, and is thus irreversibly immobilized for many purposes. Most significantly, the adsorbed RNase A retains enzymatic activity, as had been observed previously upon covalent immobilization of RNase A at a specific site (Sweeney et al. 2000; Soellner et al. 2003).

Summary

We provide a thorough analysis of the effect of an R₉ tag on the attributes of a model protein: RNase A. We find that the R₉ tag diminishes the conformational stability of the protein ($\Delta T_m = -8$ °C) but that this effect is ameliorated by the addition of salt. The tag has a negligible effect on the structure of the protein, as evidenced by the retention of full enzymatic activity. We find that an R₉ tag facilitates protein purification by cation-exchange chromatography and enables the adsorption of functional protein on glass slides and silica resin. The tag can be removed precisely and completely by treatment with carboxypeptidase B. Finally, the R₉ tag increases both the cellular uptake of the protein and the cytotoxicity of a protein variant (which is manifested in the cytosol). We conclude that polyarginine has potential as a very versatile protein fusion tags.

Table 1. *Biochemical parameters of ribonuclease A and its variants*

Ribonuclease	pI ^a	T_m ^b (°C)	k_{cat}/K_M ^c (10 ⁶ M ⁻¹ s ⁻¹)	IC ₅₀ ^d (μM)
RNase A	8.6	63.7	1.8 ± 0.2	>25
RNase A-R ₉	9.6	56	1.0 ± 0.2	>25
G88R RNase A	8.8	60	12.6 ± 0.4	5.8 ± 1.0
G88R RNase A-R ₉	9.8	54.0	9.6 ± 0.2	2.0 ± 0.4

^a Values of pI were estimated from amino acid composition (Bjellqvist et al. 1993; Bjellqvist et al. 1994). ^b Values of T_m (± 2 °C) were determined in PBS by UV spectroscopy. ^c Values of k_{cat}/K_M (± SE) are for the catalysis of 6-FAM-dArU(dA)₂-6-TAMRA cleavage at 25 °C in 10 mM Bis-Tris-HCl buffer, pH 6.0, containing NaCl (0.50 M). ^d Values of IC₅₀ (± SE) are for the incorporation of [methyl-³H]thymidine into the DNA of K-562 cells.

Figure 3-1 Effect of an R₉ tag on the purification of a protein by cation-exchange chromatography. (A) RNase A–R₉ was purified by cation-exchange chromatography before (– CPB) and after (+ CPB) the addition of carboxypeptidase B. (B) SDS–PAGE gel of RNase A–R₉ before (– CPB) and after (+ CPB) the addition of carboxypeptidase B. Purified RNase A is a standard.

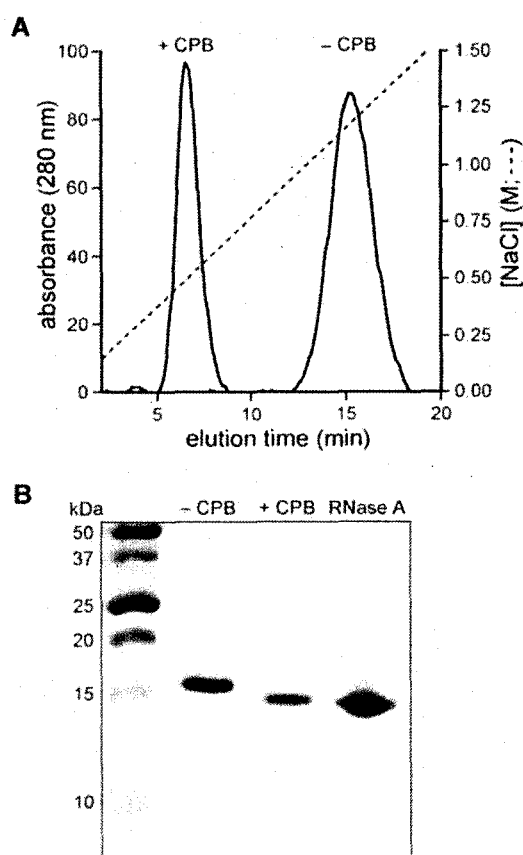


Figure 3-2 Effect of an R₉ tag on the conformational stability of a protein. (A) Thermal denaturation of RNase A (□) ($T = 63.2 \pm 1.0$ °C) and RNase A-R₉ (■) ($T = 54.0 \pm 1.0$ °C) in PBS. (B) Conformational stability of RNase A (□) and RNase A-R₉ (■) in 50 mM sodium phosphate buffer, pH 7.2, containing NaCl (0–1.00 M).

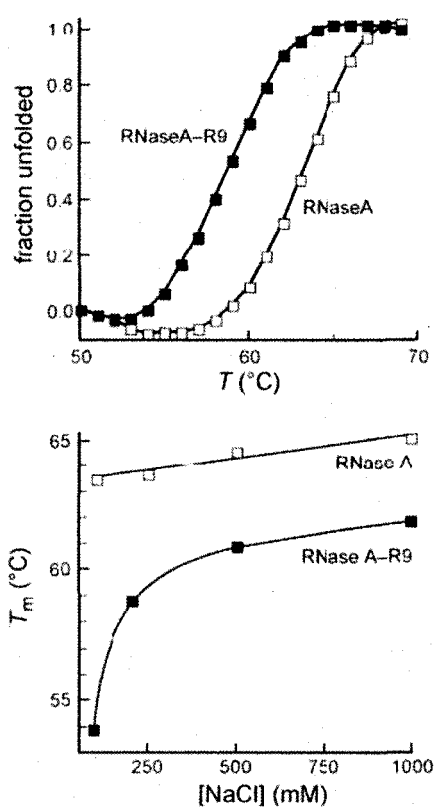


Figure 3-3 Effect of an R₉ tag on the uptake of a protein by living mammalian cells.

CHO-K1 cells were incubated with fluorescein-labeled RNase A–R₉ (A; 10 μM) or fluorescein-labeled RNase A (B; 10 μM) for 1 h at 37 °C before visualization by fluorescence microscopy. Scale bar: 10 μm.

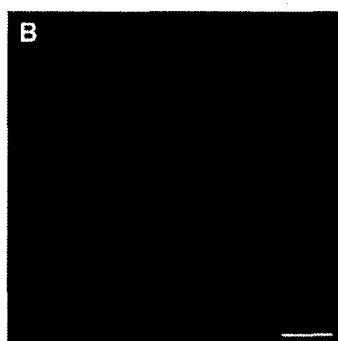
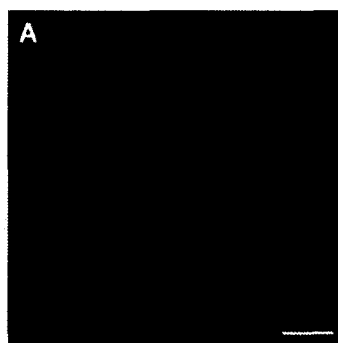
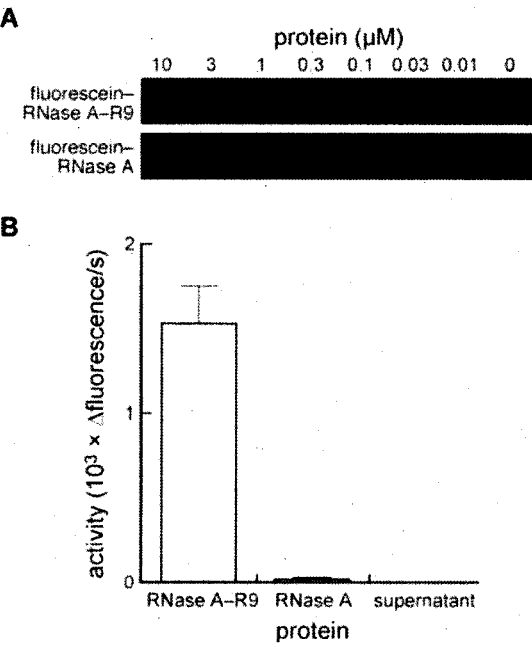


Figure 3-4 Effect of an R₉ tag on the cytotoxicity of wild-type ribonuclease A, its G88R variant, and Onconase™. Cell proliferation was determined by incorporation of [methyl-³H]thymidine into cellular DNA after a 44-h incubation with a ribonuclease. Each data point is expressed as a percentage of a PBS control. Variants with R₉ tags are denoted with filled symbols: RNase A–R₉ (●) and G88R RNase A–R₉ (■). Variants without R₉ tags are denoted with open symbols: RNase A (○), G88R RNase A (□), and ONC (◊). IC₅₀ values are listed in Table 1.

Figure 3-5 Effect of an R₉ tag on the adsorption of a protein to a glass slide and silica resin.

(A) Fluorescent images of fluorescein-labeled RNase A-R₉ and RNase A (10–0.01 μM) adsorbed on to a glass slide. (B) Ribonucleolytic activity in a solution containing silica resin with adsorbed RNase A-R₉ or RNase A, and in the supernatant upon removal of the silica resin with adsorbed RNase A-R₉.



Chapter Four

Cell-Permeable Variant of Green Fluorescent Protein

4.1 Abstract

Methods of delivering proteins and small molecules to cells are highly sought after for the design and development of new therapeutics. Peptides capable of transporting macromolecules into cells are well described (Wadia and Dowdy, 2005). Further, chemical methods of modifying proteins to improve cellular uptake have been developed (Pardridge *et al.*, 1990). Both methods rely highly on the presence of positive charge. Here, we describe a technique we refer to as site-specific cationization that involves modifying specific protein residues to basic residues, specifically arginine. We use green fluorescent protein (GFP) as a model protein for these studies. We show that a variant of GFP retains the biophysical properties of the wild-type protein while gaining the ability to enter cells. Further, internalization is dependent on protein concentration and is likely mediated by cell-surface glycosaminoglycans (GAGs) such as heparan sulfate (HS).

4.2 Introduction

The plasma membrane is designed as a natural barrier to exclude most molecules (Wadia and Dowdy, 2005). Breaching this barrier is a limiting factor in the development of proteins as therapeutics and diagnostic tools (Marafino and Pugsley, 2003). Accordingly, there is much interest in developing novel ways to deliver proteins and other macromolecules into cells.

In the early 1960s, Ryser described the phenomenon by which cationic molecules are internalized by cells (Ryser, 1967). Further, these molecules can be used to increase the uptake of other small molecules (Shen and Ryser, 1979). Pardridge and coworkers furthered this work by showing that proteins could be chemically modified to be more cationic and cell-permeable (Triguero *et al.*, 1989; Pardridge *et al.*, 1990). Diamines will react with solvent-accessible carboxylic acids on proteins to increase the basic character of these proteins. Chemical cationization is of limited utility, however, because essential residues are vulnerable to modification as has been observed in bovine pancreatic ribonuclease (RNase A) (Futami *et al.*, 2001; Futami *et al.*, 2002; Futami *et al.*, 2005) and other proteins (Triguero *et al.*, 1989; Bass *et al.*, 1990).

Many groups have shown that small cationic peptides are capable of cellular entry (Mitchell *et al.*, 2000; Suzuki *et al.*, 2002; Fuchs and Raines, 2004; Futaki, 2005). Further, non-linear scaffolds containing basic sidechains are also internalized (Futaki *et al.*, 2002). Recently Gellman and coworkers demonstrated that internalization of cationic β -peptides was enhanced when the charges were preorganized into a rigid structure in which the charges were all

displayed on the same face (Potocky *et al.*, 2005). We hypothesized that we could create a cationic surface or face on a protein that would facilitate cellular entry.

We chose to employ enhanced green fluorescent protein (eGFP) for our studies. Wu and coworkers were the first to show that a HIV-Tat peptide fused to GFP enhanced uptake by cells (Yang *et al.*, 2002). Recently, Yamada and coworkers reported the cytosolic entry of a chemically modified GFP (Futami *et al.*, 2005). To our knowledge, however, no one has ever created a cell-permeable variant of GFP or, indeed, any protein purely by site-directed mutagenesis.

eGFP is a variant of the native green fluorescent protein (GFP) from *Aequorea victoria* with several mutations to enhance green fluorescence (S65T, etc) (Cormack *et al.*, 1996) and optimized codons for expression in *E. coli* (Haas *et al.*, 1996). It has many properties that facilitate both structure–function analyses and studies of cellular entry. First, the β -barrel fold of eGFP is extremely stable with respect to thermal and chemical denaturation (Ormo *et al.*, 1996; Yang *et al.*, 1996; Verkhusha *et al.*, 2003). Thus, modifications to the protein surface, while potentially destabilizing, should not affect the ability of the protein to remain folded. Further, because the eGFP fluorophore forms after the protein folds, the ability of eGFP to accommodate substitutions can be monitored simply by following chromophore formation (Waldo *et al.*, 1999). Lastly, in order to follow cellular entry we need a way to monitor uptake. We can follow the entry of eGFP variants into cells using a number of fluorescence-based techniques, including microscopy and flow cytometry (Merilainen *et al.*, 2005).

Here, we describe the first eGFP variant that is capable of self-sufficient cellular entry. Fewer than five substitutions are sufficient to enable cellular uptake. We show that uptake

occurs through endocytosis and is facilitated by cell surface GAGs. We expect that this cationic eGFP can be used for *in vivo* and *in vitro* fluorescence applications without the need for classical transfection.

4.3 Materials and Methods

Materials. The pRSET_B plasmid containing a cDNA for eGFP was obtained from S.J. Remington (University of Oregon). Primers for making mutations in the eGFP cDNA were obtained from Integrated DNA Technologies (Coralville, IA) and had the sequences 5' CACTGGAGTTGTCCCAATTCTTGTTCGTTTACGTGGTCGTGTTAATGGGCACAAATT TTCTGTCAGTGG 3' and its reverse complement (in which sites of mutation are underlined for the E17R, D19R, D21R substitutions), 5' CGGGAAGTACAAGACACGTGCTCGTGTCAGTTTGAAGGTGATACCC 3' and its reverse complement (for the E111R substitution), and 5' CCCTTGTTAATAGAATCCGGTTTAAAAGGTATT GATTTTAAAG 3' and its reverse complement (for the E124R substitution). DH5 α and BL21(DE3) competent cells were from Stratagene (La Jolla, CA).

Site-directed mutagenesis. cDNA encoding eGFP variants were obtained using the QuikChange mutagenesis kit (Stratagene, La Jolla CA) using the primer pairs described above. Three successive rounds of mutagenesis yielded eGFP with five substitutions, E17R, D19R, D21R, E111R, and E124R. This cationic variant is referred to as "cGFP".

Protein production. Plasmids containing the sequences for eGFP and variants of eGFP were transformed into BL21(DE3) cells, and colonies were selected for on Luria-Bertani (LB) agar

plates by their ampicillin (Amp) resistance. Small cultures (25 mL of LB medium containing 200 μ g/mL Amp) were started from a single colony and grown at 37 °C with shaking at 200 rpm to an optical density of $OD = 0.6$ at 600 nm. One-liter cultures of the same medium were inoculated with 4 mL of the starter culture and grown at 37 °C with shaking at 300 rpm to an $OD_{600} = 0.6$. Cultures were then cooled to 15 °C and GFP cDNA expression was induced by the addition of isopropyl β -D-1-thiogalactopyranoside (IPTG) (1 mM final concentration). Cultures were grown at 15 °C with shaking at 300 rpm for 18 hours and harvested by centrifugation (5,000 rpm for 10 min) in a Beckman Coulter Avant J-20 XPI centrifuge using a JLA 8.1 rotor. Cell pellets were either frozen or used immediately in protein purification.

Protein purification. Cell pellets from 1 L of cell culture were resuspended in ~10 mL of ice-cold cell lysis buffer (50 mM sodium phosphate buffer, pH 7.2, containing 500 mM NaCl and 1 mM PMSF). Cells were lysed by sonication (50% duty/ 50% output) five times for 30 s. Cell debris was removed by centrifugation at 22,000 x g for 60 min at 4 °C in a Beckman Optima XL-80K ultracentrifuge using a 60Ti rotor. Clarified cell lysate was dialyzed for at least 2 h against phosphate-buffered saline containing 500 mM NaCl (PBS+) (50 mM sodium phosphate buffer, pH 7.2, containing 636 mM NaCl) before loading onto a Ni-NTA agarose (Qiagen, Germany). The column was washed with the same buffer containing 20 mM imidazole before eluting with 50 mM sodium phosphate buffer, pH 7.2, containing 636 mM NaCl and 500 mM imidazole. The fractions containing green-colored protein were pooled and diluted 1/10 with water to lower the salt concentration. cGFP was then loaded onto a 5-mL HiTrap SP FF sepharose column (Amersham Biosciences, Piscataway NJ). Protein was eluted with a 100 mL linear gradient (50 + 50 mL) of 50 mM sodium phosphate buffer, pH 7.5,

containing 0–1 M NaCl. Fractions containing green-colored protein were pooled and dialyzed against 50 mM sodium phosphate buffer, pH 7.5, containing 652 mM NaCl. The N-terminal histidine tag was removed as described previously (Hanson et al. 2004). Briefly, protein was incubated with 1:50 (w/w) α -chymotrypsin for 20 h at room temperature. Chymotrypsin degrades the N-terminal tag but does not cleave the GFP protein (Hanson et al. 2004). Protein was concentrated using Vivascience 5000 MW spin columns and protein concentration was determined by optical absorbance at 280 nm ($\epsilon_{280} = 19890 \text{ cm}^{-1} \text{ M}^{-1}$) or by the BioRad protein assay.

Fluorescence Properties. Fluorescence measurements were performed with a QuantaMaster 1 photon counting fluorometer equipped with sample stirring (Photon Technology International, South Brunswick, NJ). Fluorescence excitation and emission spectra were obtained in PBS+ buffer using a 2-nm slit width and scanning at a rate of 1 nm/s. Quantum yield (Φ) was determined following a method described previously (Cubitt et al. 1999). Briefly, the UV absorbance at 490 nm for cGFP in PBS+ was matched to a fluorescein standard in 0.1 N NaOH of known quantum yield ($\Phi_f = 0.95$ in 0.1 N NaOH). The area under the emission spectra from 500–700 nm after excitation at 490 nm was determined, and the ratio (cGFP area/fluorescein area) was used to calculate the quantum yield of cGFP (cGFP area/fluorescein area = $\Phi_{\text{cGFP}} / \Phi_f$).

Guanidinium-Induced Equilibrium Unfolding. The stability of cGFP and other GFP variants was determined by following the change in fluorescence as a function of denaturant concentration (Stepanenko et al., 2004). GFP proteins (1–5 nM) were incubated in 96-well flat-bottom plates (total volume 100 μL) in 50 mM sodium phosphate buffer, pH 7.5, containing

NaCl (500 mM) and guanidine hydrochloride (Gdn-HCl) (0–6.3 M) for 24 h at room temperature. Fluorescence intensity was determined using a Tecan Ultra 384 fluorescence plate reader. Data were fitted to a two-state unfolding mechanism and could be used to calculate the standard free energy of denaturation, $\Delta G^\circ (= -RT \ln K)$. Here, R is the gas constant, T is the absolute temperature and K is the equilibrium constant which can be calculated from the experimental data using the standard equation: $K = [(y)_N - (y)] / [(y) - (y)_D]$ (Tanford, 1968). The (y) value is the observed fluorescence value, and $(y)_N$ and $(y)_D$ are the (y) values for the native and denatured states, respectively.

Cell Internalization. Chinese hamster ovary cells (CHO-K1), glycosaminoglycan-deficient cell lines (CHO-677 and CHO-745) and HeLa cells were obtained from the American Type Culture Collection (ATCC) and maintained according to recommended instructions. The day before protein incubation, cells were seeded onto 4- or 8-well Lab-Tek II Chambered Coverglass tissue culture dishes (Nalge Nunc International, Naperville, IL) to yield 75% confluency on the next day. The following day, protein solutions (in PBS containing 500 mM NaCl) were added to cells in 200 μ L (protein volume added was less than 1/20 total volume) of media or PBS containing magnesium (1 mM) and calcium (1 mM). Protein was incubated with cells for known times and the cells were then washed with PBS containing magnesium and calcium three times prior to visualization. In some samples, cell nuclei were counterstained with Hoescht 33342 for 5 min prior to washing. Internalization was visualized with a Nikon C1 laser scanning confocal microscope equipped with 60X and 100X lenses.

4.4 Results

Design of cationic GFP (cGFP). We believed that mutations could be made to the surface residues of a protein structure that would endow the protein with the ability to enter cells without compromising native function. We chose eGFP as a model protein for these experiments because it has a very stable fold and the surface-exposed residues are not important for native fluorescence. Our next goal was to choose residues on the eGFP surface for mutation. We chose to modify five residues (E17, D19, D21, E111, and E124) to the basic residue arginine. These residues reside on three adjacent β -strands and are in close proximity to five basic residues (K107, R109, K113, K122, and K126) (See Figure 4-1). Making these five mutations would afford a protein with a highly basic patch over part of its surface. We believed this basic area would facilitate cellular uptake.

Fluorescence properties of cGFP. cGFP was over-produced in *E. coli* and purified by published methods (Hanson *et al.*, 2002; Hanson *et al.*, 2004). We characterized the fluorescence of cGFP relative to eGFP to ensure that cGFP spectral properties that were similar to wild-type protein. Figure 4-2a shows excitation and emission spectra for cGFP and eGFP. Both proteins show excitation maxima at 470, 480, and 488 nm. Further both proteins exhibit maximal emission at ~507 nm. We further determined the quantum yield of cGFP. Using fluorescein as a standard, we found the quantum yield of cGFP to be 0.44 ± 0.02 (Figure 4-2b). eGFP has a quantum yield of 0.6 (Tsien, 1998).

GdmCl-induced unfolding of GFP variants. Modifying residues of a protein may alter the ability of the protein to fold and/or decrease the stability of the protein in solution. In the case of GFP, this is important because proper folding is necessary for chromophore formation. Further, the protein must be reasonably stable at physiological temperature for experiments in cell culture. Attempts to monitor unfolding by thermal denaturation were unsuccessful as cGFP tended to precipitate upon unfolding at high temperature (data not shown). We instead monitored unfolding of eGFP and cGFP as a function of Gdn-HCl concentration (Figure 4-3a). eGFP and cGFP had midpoints of unfolding of 3.1 ± 0.3 and 3.1 ± 0.3 M Gdn-HCl respectively. The dependence of the standard free energy of denaturation (ΔG°) on Gdn-HCl concentration can be determined by plotting ΔG versus [Gdn-HCl] (Figure 4-3b). Results show that ΔG° varied linearly with respect to Gdn-HCl concentration. Thus the conformational stability of the GFP variants can be estimated using the equation:

$$\Delta G^\circ = \Delta G(\text{H}_2\text{O}) - m [\text{Gdn-HCl}]$$

where $\Delta G(\text{H}_2\text{O})$ is an estimate of the conformational stability of a protein in the absence of denaturant assuming that unfolding continues to be linear with respect to denaturant concentration to 0 M denaturant (Pace, 1986). The slope of the line in Figure 4-3b corresponds to the value m and is a measure of the dependence of ΔG on Gdn-HCl concentration. Unfolding parameters for cGFP and eGFP are summarized in table 4-1.

Internalization of GFP variants in HeLa cells. Cellular internalization of GFP variants can be visualized by fluorescence microscopy. We incubated HeLa cells with increasing concentrations of either eGFP or cGFP for 4 h at 37 °C. After three washes with PBS+ buffer, we followed

internalization by confocal fluorescence microscopy (Figure 4-4). Fluorescence intensity within cells increased with increasing concentration of cGFP (0-5 μ M). Very little fluorescence intensity was observed in cells incubated with eGFP. Confocal images of only the highest concentration of eGFP used are shown in Figure 4-4f.

Role of GAGs in cGFP internalization. Several groups have shown that GAGs such as HS are important for initial binding of cationic peptides to the cell surface. We monitored cell-surface binding and cellular internalization of cGFP in CHO cells. Further, we repeated this experiment in CHO cell lines deficient in GAG biosynthesis. Typical results are shown in Figure 4-5. In wild-type CHO-K1 cells, cGFP binds to the cell surface and is internalized. In CHO 677 (deficient in HS), and CHO 745 (deficient in HS and CS), there is little internalization of cGFP.

4.5 Discussion

As the need for new drugs and biomaterials increases, the ability to engineer macromolecules with new and novel functions will become increasingly important (Pokala and Handel, 2001; Lilie, 2003). Designer proteins with new physiological functions will be important for drug development, diagnostic tools and many other applications. Towards that end, we show here initial efforts to create a green fluorescent protein (GFP) that is capable of entering cells.

Although their mechanism of entry is not completely understood, cationic peptides have become widely used for the delivery of molecules into cells (Futaki, 2005; Wadia and Dowdy, 2005). Suzuki and coworkers observed that non-linear, cationic polymers were readily internalized by cells (Futaki *et al.*, 2002). Further, Pardridge and coworkers showed that chemically modifying proteins with diamines to make the surface more basic increased uptake (Triguero *et al.*, 1989). We reasoned that we could make a protein cell permeable by site-specifically modifying surface residues to the basic amino acid arginine. By inspection, we located a densely-charged area of the GFP surface that we suspected was suitable for modification. We replaced five acidic residues to arginine, thus creating a GFP variant that has a net gain of ten positive charges. We showed that this variant of GFP, cGFP, could be expressed in *E. coli* and purified to near homogeneity. Further, the excitation and emission spectra of cGFP were determined to be identical to those of eGFP. The quantum yield of cGFP was, however, found to be 0.44, which is approximately 1/3 lower than that observed for eGFP (Tsien, 1998). Quantum yield is a measure of the efficiency of energy conversion to fluorescent light. Although cGFP is not as bright as eGFP, this quantum yield is similar to that of other fluorescent protein variants of GFP, such as YFP and BFP (Tsien, 1998).

Two like-charges will repel each other according to Coulomb's law (Pace *et al.*, 2000). We were concerned that creating a variant of GFP with ten positive charges, on three adjacent β -strands, would strongly destabilize the protein and affect its ability to fold. Hence we measured the conformational stability of both cGFP and eGFP in the presence of increasing concentration of the denaturant Gdn-HCl (Figure 4-3). Our results show that cGFP has similar stability to

eGFP. This result indicates that cGFP is well folded under physiological conditions and that the GFP protein scaffold is highly tolerant of mutations to its surface.

We measured the internalization of varying concentrations of cGFP and eGFP in HeLa cells (Figure 4-4). Our results show that cGFP is readily internalized at extracellular concentrations as low as 50 nM (Figure 4-4b). Further, internalization can be attributed to the mutations installed into cGFP, as eGFP is not internalized even at the highest concentration tried herein (Figure 4-4f). We observed that, similar to cationic peptides, cGFP is found within vesicles of living cells. We therefore hypothesized that, similar to cationic peptides, internalization was an endocytic process.

Glycosaminoglycans (GAGs) such as heparan sulfate (HS) and chondroitin sulfate (CS) are important for efficient cellular entry of cationic peptides (Hakansson *et al.*, 2001; Tyagi *et al.*, 2001; Fuchs and Raines, 2004). Hence, we tested the role of GAGs in cGFP internalization (Figure 4-5). Our results show that cGFP uptake is decreased in GAG-deficient cell lines. These data suggest that, like cationic peptides, interactions with GAGs on the cell surface are important for cGFP entry.

Our data indicate that we have been able to design a variant of GFP that is capable of cellular entry. GFP variants are widely used for a number of applications in cell biology due to their robust and diverse fluorescence properties (Miyawaki, 2005). Having a GFP variant capable of cell entry may in the future eliminate the need to for transfection to express GFP fusions within mammalian cells. Further, a cell-permeable GFP may be useful for monitoring a number of cellular processes in living cells both *in vitro* and *in vivo* (Hoffman, 2005). Beyond

the scope of GFP, site-specific cationization may be a useful technique for the development of more cell permeable proteins.

**Table 4-1: Thermodynamic Parameters of Gdn-HCl-induced
Unfolding of eGFP and cGFP**

Protein	$\Delta G(\text{H}_2\text{O})$ (kcal/mol)	m (kcal/mol•M)	$C_{1/2}(\text{M})$
eGFP	6.7 ± 0.2	2.1 ± 0.2	3.1 ± 0.3
cGFP	7.1 ± 0.9	2.2 ± 0.2	3.1 ± 0.3

Figure 4-1: Design scheme for the cell-permeable GFP variant (cGFP). A charged surface of GFP was chosen by inspection. Acidic residues (in red) were mutated to the basic residue arginine to yield a protein surface with ten basic charges (in blue). Heterologous production yielded cGFP, a cell-permeable variant of GFP.

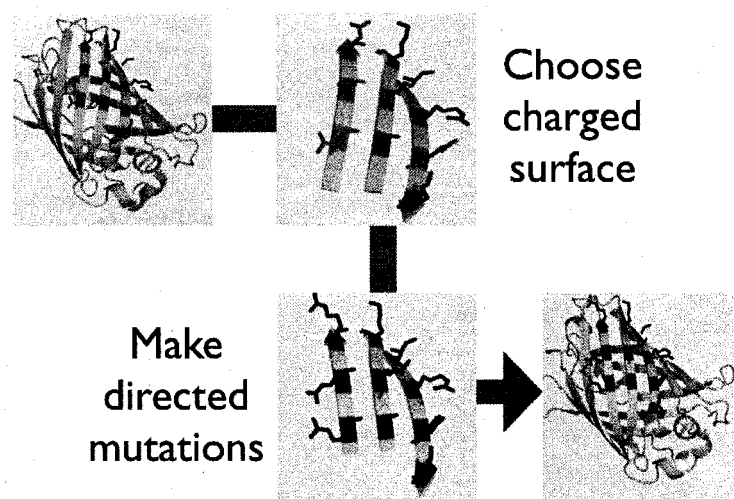


Figure 4-2: Characterization of the fluorescence properties of cGFP. (A) Fluorescence

excitation (----) and emission (—) spectra for cGFP (blue) and eGFP (green).

Data were collected in increments of 1 nm with a scan rate 5 nm/s. (B) Raw data for determination of the quantum yield (Φ) for cGFP. Solutions of cGFP (blue) and fluorescein (green) ($\Phi_f = 0.95$ in 0.1 N NaOH) of equal absorbance at 490 nm were diluted in PBS+ (for cGFP) or 0.1 N NaOH (for fluorescein) and the area under the emission spectra curve from 500–700 nm was determined. The quantum yield of cGFP (Φ_{cGFP}) was determined by the difference in area (cGFP area / fluorescein area = $(\Phi_{\text{cGFP}}) / \Phi_f$).

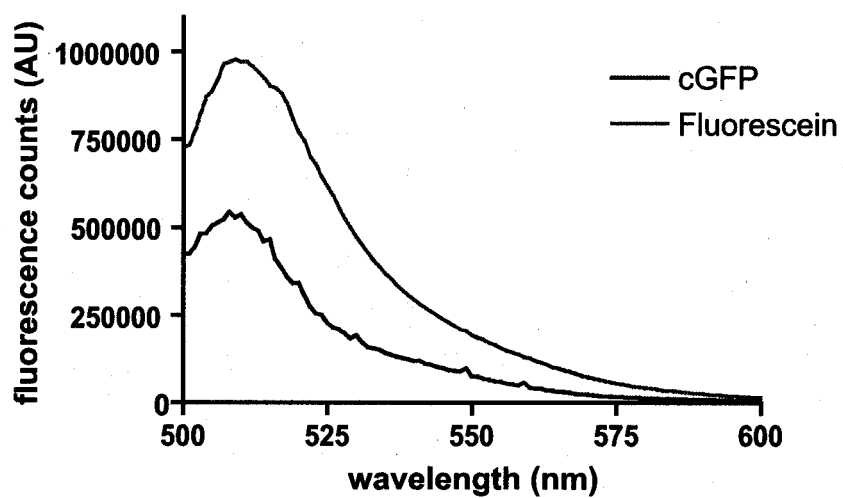
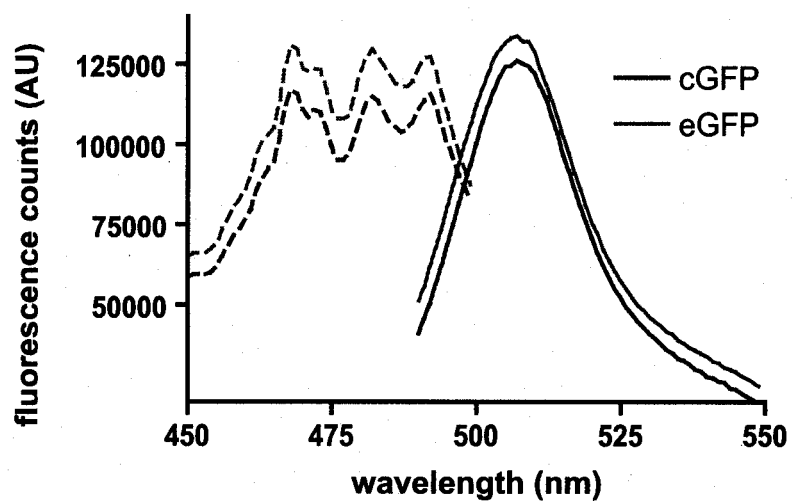


Figure 4-3: Gdn-HCl-induced unfolding of cGFP (blue) and eGFP (green). (A) Plot of normalized fluorescence intensity versus denaturant concentration. The midpoint of the transformation was fitted to a sigmoidal dose-response curve using Prism Graphpad software. The midpoint of the transition corresponds to the $C_{1/2}$ or the concentration of denaturant at which the protein is 50% unfolded at equilibrium. (B) Dependence of ΔG on Gdn-HCl concentration. Data were fitted to a linear regression model in which the slope (m) is the dependence of ΔG° on denaturant and the y-intercept approximates the free energy of the protein in the absence of denaturant ($\Delta G^\circ \sim \Delta G(\text{H}_2\text{O})$).

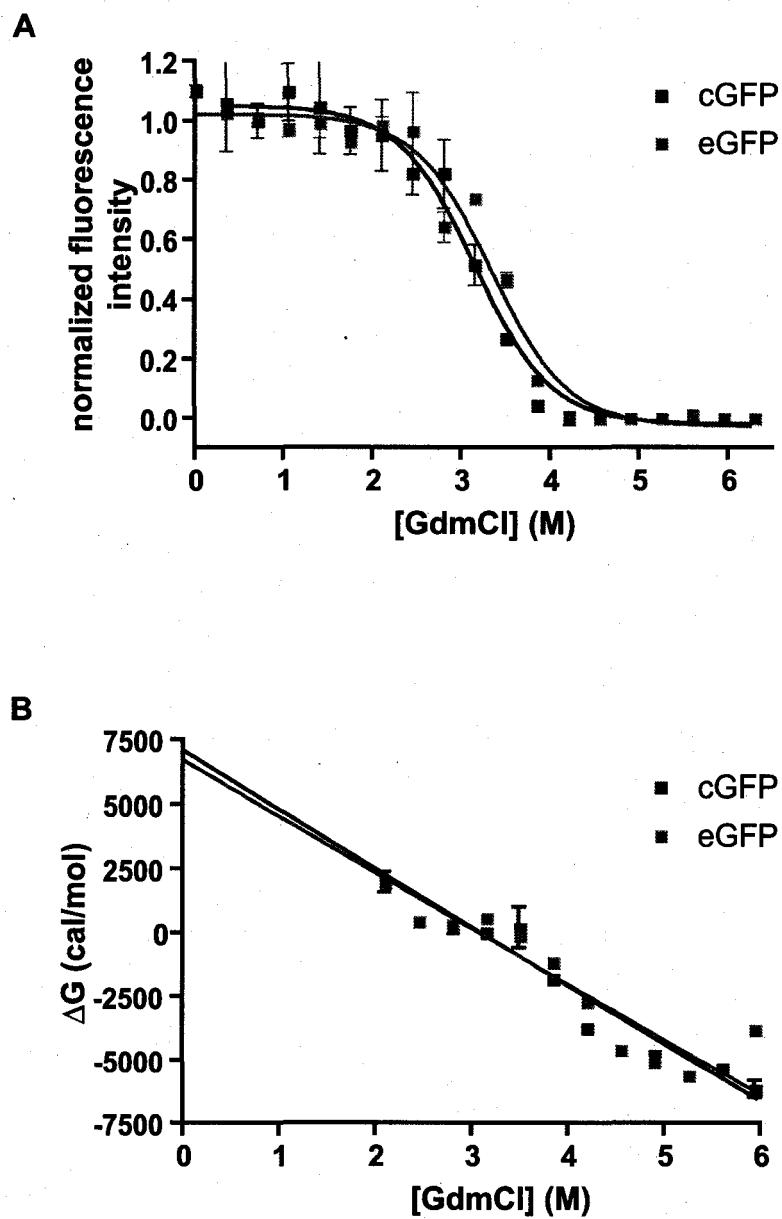


Figure 4-4: Dose-dependence of the internalization of GFP variants in HeLa cells. Proteins were incubated with HeLa cells for 4 h at 37 °C and washed three times with PBS+ prior to visualization. (A–E) cGFP was incubated at 0, 0.05, 0.5, 1 and 5 μ M, respectively. (F) eGFP was incubated at 5 μ M for 4 h at 37 °C. (G) Stacked series of cGFP (2 μ M) internalization in CHO cells after one hour of incubated at 37 °C.

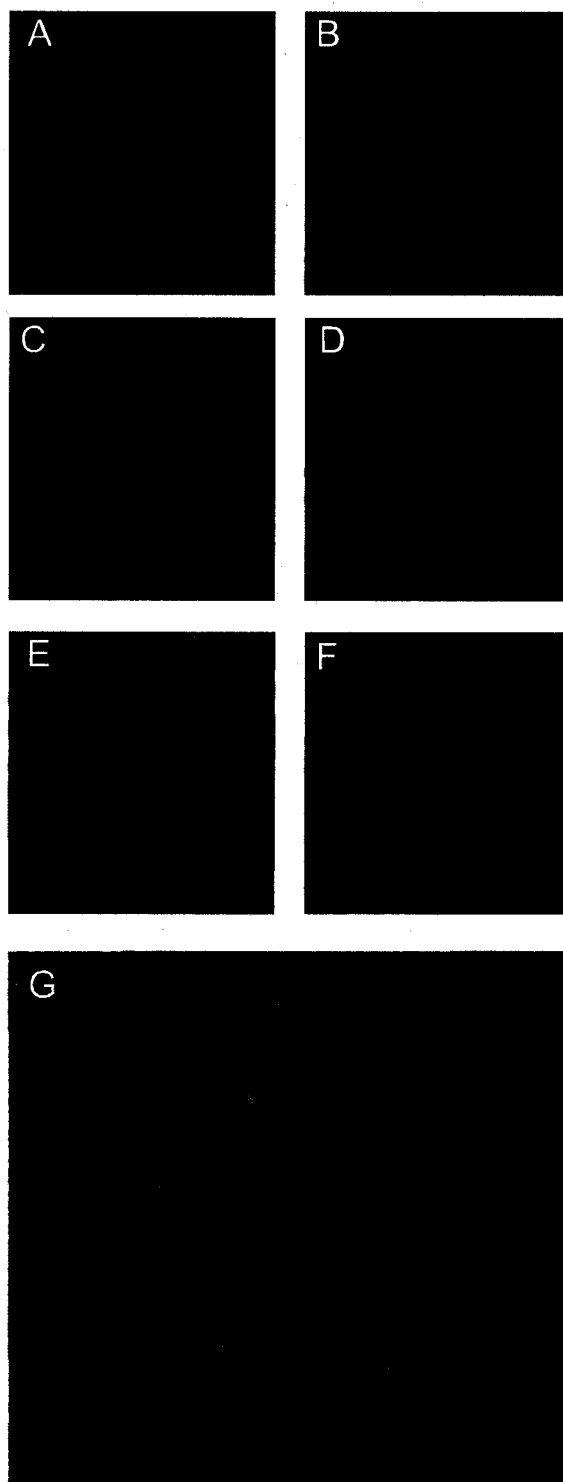
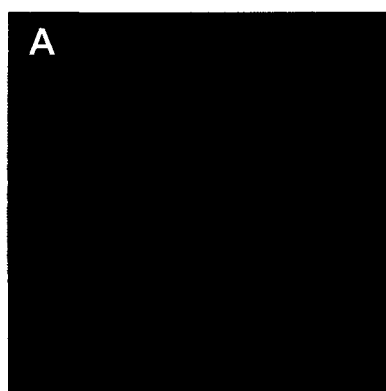
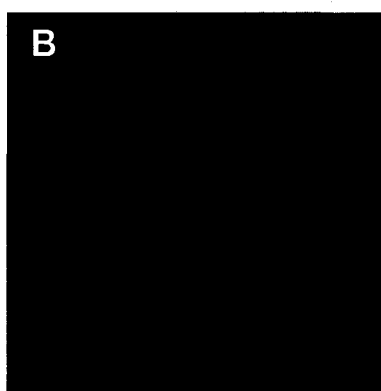


Figure 4-5: GAG-dependence of cGFP internalization. CHO-K1 and GAG deficient cell lines, CHO 677 and CHO 745, were incubated with cGFP (5 μ M) for 4 h at 37 °C and washed three times with PBS prior to visualization.

**A****CHO K1****B****CHO 677****C****CHO 745**

Chapter Five

Detection of HIV-1 Protease Activity with a Cell-Permeable Variant of Green Fluorescent Protein

5.1 Abstract

A novel, cell-permeable reporter of human immunodeficiency virus type 1 (HIV-1) protease (HIV-PR) activity was developed. A cell-permeable variant of green fluorescent protein (GFP) containing a peptide sequence cleaved by HIV-PR was linked to a small-molecule fluorophore, 5- (and 6-) tetramethylrhodamine isothiocyanate (TRITC), through a cysteine residue. The resulting protein exhibited fluorescence resonance energy transfer (FRET) between GFP and TRITC. In the presence of purified HIV-PR, the substrate was cleaved, resulting in a 2.5-fold reduction in TRITC emission coupled with a 5-fold increase in GFP emission. This substrate was used to monitor HIV-PR activity in living 293T/17 cells expressing either wild-type or inactive HIV-PR. This application demonstrates that this novel, cell-permeable GFP is a useful tool for monitoring HIV-PR activity in living cells.

5.2 Introduction

Viral proteases represent relevant targets for drug development due to their essential function in the viral life cycle (Bianchi and Pessi, 2002; Magden *et al.*, 2005). As such, methods to detect protease activity, either for diagnostic or screening purposes, are highly desirable. HIV-PR is one of the best-understood viral enzymes, and is an excellent model protein for the development of new activity-based assays (West and Fairlie, 1995; Gulnik *et al.*, 2000). HIV-PR is encoded within the HIV genome and is essential for the viral life cycle. HIV-PR, like other retroviral proteases, is responsible for processing the viral polyprotein into both functional structural proteins and enzymes (Patick and Potts, 1998). Inhibitors of HIV-PR, therefore, are of great interest as potential therapeutics (Wlodawer and Vondrasek, 1998). Accordingly, there is a need to develop better methods of measuring and/or detecting HIV-PR activity.

In addition to processing viral proteins, HIV-PR also cleaves several cellular proteins resulting in cytotoxicity (Shoeman *et al.*, 1991; Rizzo and Korant, 1994). Consequently, it has been difficult to develop cell-based or *in vivo* assays for HIV-PR activity (Sadaie and Hager, 1994; Westby *et al.*, 2005). Several cell-based assays have been developed for monitoring HIV-PR activity in mammalian cells (Lindsten *et al.*, 2001; Hu *et al.*, 2005). Although these assays are useful *in vitro*, they require the expression of reporter plasmids and therefore do not function in primary cells or tissues.

Methods of following biological processes in living cells are highly desirable for basic research, drug development, and as diagnostic tools (Blasberg and Tjuvajev, 2003; Roda *et al.*, 2004). One major limitation to working *in vivo* is the inability to easily introduce reporter

molecules. Therefore, there is also a need to develop new methods of delivering reporter molecules to living cells and tissues.

Over the past five years, cationic peptides capable of cellular entry have been described (Vocero-Akbani *et al.*, 2001a; Fittipaldi and Giacca, 2005; Futaki, 2005). These peptides known as protein transduction domains (PTDs) are capable of crossing cell barriers and carrying diverse molecular cargoes (Wadia and Dowdy, 2005). Many groups have shown that, similar to attaching cationic PTDs, increasing the positive charge of a protein by chemical modification can facilitate cellular internalization (Triguero *et al.*, 1989; Futami *et al.*, 2001). These technologies have achieved some success in increasing uptake of modified proteins and small molecules (Vocero-Akbani *et al.*, 2001b; Futami *et al.*, 2005).

We demonstrated in Chapter four that we could design a cell-permeable green fluorescent protein (GFP) by selectively modifying surface residues of the protein to more basic residues. Fluorescent proteins, such as GFP, are often used as reporters for cellular activities due to their robust fluorescence properties and utility as protein fusion tags (Griesbeck, 2004; Chudakov *et al.*, 2005; Yuste, 2005). Fluorescence techniques are highly utilized as analytical tools because of the large number of available fluorophores and their high sensitivity (which can enable detection at nanomolar concentration) (Cummings *et al.*, 1999). Further, fluorescent proteins can be adapted for other applications such as fluorescence resonance energy transfer (FRET) to monitor enzymatic activity, protein-protein interactions, and other interactions (Zaccolo, 2004; Chudakov *et al.*, 2005). This newly described cell-permeable GFP (cGFP) expands the utility of fluorescence proteins because it facilitates use in living cells without the need for transfection.

New fluorescence imaging capabilities in living cells and tissues may be possible using cell-permeable fluorescent proteins such as cGFP.

Here we demonstrate the use of cGFP as a reporter in living cells. We created fluorescent resonance energy transfer (FRET) substrates based on cGFP and then, examined the ability of HIV-PR to cleave a number of cGFP-based FRET substrates that displayed HIV-PR substrate peptides at their C-terminus. We demonstrate that this substrate functions both *in vitro* and in cell cultured human cells to detect HIV-PR activity. This substrate provides a starting point for the development of more robust fluorescent substrates for *in cellulo* detection of proteolytic activity.

5.3 Materials and Methods

Materials. The pRSET_B plasmid containing a cDNA for eGFP was obtained from S. J. Remington (University of Oregon). The plasmid for the cell permeable variant of eGFP (cGFP) was constructed as described in Chapter 4. Primers for making mutations to introduce the HIV-PR recognition sequence into cGFP were obtained from Integrated DNA Technologies (Coralville, IA) and had the following sequence: 5' GGCATGGATGAACTATACAAAACGGTGTCGTTCAATTTCCCGCAGATCACGTGTTAATAAGGATCCGAGCTCGAGATCTG 3' and its reverse complement where the HIV-PR cleavage site is underlined (corresponding to amino acid sequence TVSFNFPQITC). The primers to delete residues 230–238 of eGFP had the following sequence: 5' GAGTTTGTAACAGCTGCTGGGATTACGGTGTCGTTCAATTTCCCG 3' and its reverse complement. The primers to make the C48S and C70V substitutions were 5' CCAATTGCTACCAGAGCAAGTCCACCATGAGAATCACCG 3' and

5' CTCTCACTTATGGTGTTC AAGTCTTTTCAAGATACCCAG 3' with their respective complements. The primers to add a C-terminal glycine to the HIVPR sequence were 5' CCCGCAGATCACGTGTGGCTAATAAGGATCCGAGCTCGAGC 3' and its reverse complement. DH5 α and BL21(DE3) competent cells were from Stratagene (La Jolla, CA).

Site-directed mutagenesis. eGFP variants were obtained using the QuikChange mutagenesis kit (Stratagene, La Jolla CA) using the primer pairs described above to make the given mutations.

Protein production. Protein was produced and purified as described in Chapter 4. Briefly, cultures were grown at 37 °C with shaking at 300 rpm to an $OD = 0.6$ at 600 nm. Cultures were then cooled to 15 °C, and cDNA transcription was induced by the addition of isopropyl β -D-1-thiogalactopyranoside (IPTG) (1 mM final concentration). Cultures were grown at 15 °C with shaking at 300 rpm for 18 h and harvested by centrifugation (5,000 rpm for 10 min) in a Beckman Coulter Avant J-20 XPI centrifuge using a JLA 8.1 rotor. Cell pellets were either frozen or used immediately for protein purification.

Protein purification. Cell pellets from 6 L of cell culture were resuspended in ~60 mL of ice-cold cell lysis buffer (50 mM sodium phosphate buffer, pH 7.2, containing 500 mM NaCl and 1 mM PMSF). Cells were lysed by sonication (50% duty/50% output) five times for 30 s. Cell debris was removed by centrifugation at 22,000 $\times g$ for 60 min at 4 °C in a Beckman Optima XL-80K ultracentrifuge using a 60Ti rotor. Clarified cell lysate was dialyzed for at least 2 h against phosphate-buffered saline containing 500 mM NaCl (PBS+) (50 mM sodium phosphate buffer, pH 7.2, containing 636 mM NaCl) before loading onto a column of Ni-NTA agarose resin (Qiagen, Germany). The resin was washed with the same buffer containing 20 mM

imidazole before elution with 50 mM sodium phosphate buffer, pH 7.2, containing NaCl (636 mM) and imidazole (500 mM). The fractions containing green-colored protein were pooled and diluted 1/10 with water to lower the salt concentration. Protein was then loaded onto a 5-mL column HiTrap SP FF sepharose resin (Amersham Biosciences, Piscataway NJ). Protein was eluted with a 100 mL linear gradient (50 + 50 mL) of 50 mM sodium phosphate buffer, pH 7.5, containing NaCl (0-1 M). Fractions containing green-colored protein were pooled and dialyzed against 50 mM sodium phosphate buffer, pH 7.5, containing NaCl (636 mM). Protein was concentrated using Vivascience 5000 MW spin columns, and protein concentration was determined by optical absorbance at 280 nm ($\epsilon_{280} = 19890 \text{ cm}^{-1}\text{M}^{-1}$) or by the BioRad protein assay.

Synthesis and purification of FRET substrates. Purified GFP in PBS+ buffer was incubated with dithiothreitol (DTT) (5 mM) for 30 min at RT to reduce the free thiol. DTT was removed by purification over a 5-mL column of HiTrap Desalting resin (Amersham) equilibrated in PBS+ buffer. The reduced protein (50 μM) was reacted immediately with a solution of TMR1A (500 μM) in DMF at 4 °C overnight. The resulting FRET substrate was dialyzed exhaustively against PBS+ followed by purification by cation-exchange chromatography using a 5-mL column of HiTrap SP resin with a 100 mL linear gradient (50 + 50 mL) of 50 mM sodium phosphate buffer, pH 7.5, containing NaCl (0-1 M) (Amersham).

Ex cellulo cleavage of FRET substrate by HIV-1 PR. The HIV substrates GFP TMR 1–8 (10 nM), purified above, were added to 2-mL PBS+ buffer. Fluorescence emission spectra (500–600 nm) were collected upon excitation at 470 nm. Purified HIV-PR (gift of R.F. Turcotte or from

NIH AIDS Research and Reference Reagent Program) was added to the cuvette (~5 nM), and fluorescence was monitored at several time points.

Transient Transfections. Two plasmids, VRC4200 and VRC4000 were obtained from Dr. Gary Nabel (NIH NIAID). These plasmids direct the production of the Gag/Pol region of the HIV-1 polyprotein with active HIV-1 PR (VRC 4200) or a protease with a point mutation in the active site (VRC 4000). 293T/17 cells (ATCC) were transfected with 2 μ g of either plasmid using the TransIT kit (Mirus). Protease activity was confirmed by immunoblotting looking for the cleavage of the p17 region of the Gag/Pol protein using sheep p17 antisera (1:1000) (NIH AIDS reagent resource) and a rabbit-anti sheep-HRP secondary antibody (1:5000) (Abcam).

Cell Internalization. 293T/17 cells were transfected in 6-well plates with plasmids VRC4200 or VRC4000 20 h prior to incubation with a FRET substrate. Eight hours after transfection, 100 μ L of cells were removed from the 6-well plate and were seeded onto 4 or 8-well Lab-Tek II Chambered Coverglass tissue culture dishes (Nalge Nunc International, Naperville, IL) to yield approximately 75% confluency the next day. Twenty hours post transfection, protein solutions (in PBS + 500 mM NaCl) were added to cells in 200 μ L (protein volume added was less than 1/20 total volume) of medium or PBS containing magnesium (1 mM) and calcium (1 mM). Protein was incubated with cells for known times, and cells were washed with PBS containing magnesium and calcium three times prior to visualization. In some samples, cell nuclei were counterstained with Hoescht 33342 for 5 min prior to washing. Internalization was visualized with a Nikon C1 laser scanning confocal microscope equipped with 60X and 100X lenses.

5.4 Results

Design of FRET substrate. Energy transfer between fluorescent molecules is dependent on a number of factors, including the spectral overlap of the donor and acceptor as well as the distance between the two molecules. Further, when designing for imaging applications, one must be concerned about direct excitation of the acceptor fluorophore by the laser. We chose to use cGFP as our donor molecule because it is cell-permeable and has fluorescence properties similar to wild-type eGFP (see Chapter 4). We chose to work with a derivative of tetramethylrhodamine (TMR) because it has some spectral overlap with cGFP but should not be excited by a 488 nm Argon laser. We engineered several variants of cGFP in which we removed native cysteine residues as well as shortened the distance between cGFP and the fluorophore by removing non-essential residues 230–238 of the GFP sequence (see Figure 5-1a for the relevant constructs). We linked TMR to cGFP via a C-terminal cysteine residue, forming a stable thioether linkage. The TMR and GFP are separated by a 10-residue sequence (TVSFNF/PQIT), that corresponds to a natural sequence cleaved by HIV-PR where cleavage occurs between the phenylalanine and proline residue. A schematic of the FRET substrate and cleavage by HIV-PR is shown in Figure 5-1b.

cGFP variants (Figure 5-1a) were produced in *E. coli* and purified. Following purification, proteins were labeled with 5-tetramethylrhodamineiodoacetimide (TMRiA) to form FRET substrates. In the purification of GFP–TMR 1, we determined that TMRiA was reacting with Cys48. Hence we replaced this residue with serine in subsequent variants. In addition, we found that Δ 230–238 cGFP (GFP–TMR 2,4,6,8) exhibited better FRET than did full-length cGFP. Replacing the other native cysteine residue, Cys70, with valine decreased the yield of fluorescent

protein in *E. coli* and was therefore not included in our final construct. We added a C-terminal glycine (GFP-TMR 7-8) to lower the pKa of the reactive cysteine, thus making it more reactive.

In vitro characterization of the FRET substrate GFP-TMR 8. We measured energy transfer for substrate GFP-TMR 8 in PBS+ buffer by collecting emission spectra from 500–600 nm upon excitation at 470 nm (Figure 5-2 red curve). Emission at 575 nm was approximately equal to emission at 510 nm. HIV-PR was added to a final concentration of 5 nM and fluorescence emission was monitored versus time. We observed a decrease in emission at 575 nm coupled to a larger increase in emission at 510 nm (Figure 5-2).

Monitoring HIV-PR activity in cell culture using GFP-TMR 8. Upon reaction with HIV-PR *in vitro*, GFP-TMR 8 exhibited decreased emission at 575 nm and increased emission at 510 nm (Figure 5-2). We transfected 293T/17 with a construct (Figure 5-3a) which expressed the HIV-1 polyprotein with the cDNA for the active HIV-PR (VRC4200). HIV-PR activity in these cells was monitored by the ability of the protease to cleave the p17 region of the polyprotein in the presence and absence of the protease inhibitor, as measured by immunoblotting (Figure 5-3b). We then incubated GFP-TMR 8 (2 μ M) with 293T/17 cells expressing either active or inactive protease and visualized these cells by confocal microscopy (Figure 5-4). We observed an increase in green fluorescence (510 nm emission) in cells producing active HIV-PR. Further, in cells lacking protease, green emission seems to colocalize with red fluorescence, suggesting that the FRET substrate, GFP-TMR 8, remains intact.

5.5 Discussion

Methods for monitoring processes in living cells are highly useful for many applications. Of particular interest are new methods for the detection of viral activity within cells. Here, we synthesize new fluorescent substrates and demonstrate their utility for monitoring HIV-PR activity in living cells.

We chose cationic GFP (cGFP) to act both as a FRET donor and also as the vehicle for delivering the substrate into cells. The choice of FRET donor and acceptor are key to efficient energy transfer. GFP variants have been used in many applications as FRET substrates for monitoring protease activity. In most cases, the donor and acceptor molecules are both fluorescent proteins (Chudakov *et al.*, 2005). We decided to use a small molecule as a fluorescence acceptor, as it would likely not affect the ability of cGFP to enter cells. Other groups have used dyes such as eosin as FRET acceptors with GFP donors (Suzuki *et al.*, 2004). These molecules are however, unsuitable for optical applications, as their fluorescence emission profiles overlap too closely with that of GFP. We therefore chose the dye TMR, as it is minimally excited by 488 nm argon lasers yet has been useful as a FRET partner with green donor fluorophores such as fluorescein (Kelemen *et al.*, 1999).

Another important factor in the design of FRET substrates is the distance between donor and acceptor molecules. Efficiency of energy transfer ($E\%$) is determined by the equation: $E = R_0^6 / (R_0^6 + R^6)$ where R_0 is the Förster radius of the donor fluorophore and R is the actual distance between donor and acceptor. We assume the Förster radius for cGFP is similar to that determined for wild-type eGFP ($R_0 = 5.04$ nm) (Tsien, 1998). We attached the acceptor

molecule, TMR, to cGFP via a free thiol on the C-terminus of the protein. To alter the distance between TMR and cGFP we made a full-length cGFP construct as well as one in which residues 230–238 were excised (Figure 5-1a). Others have shown that only residues 6–229 of GFP are essential for chromophore formation (Ormo *et al.*, 1996; Yang *et al.*, 1996).

As mentioned previously, we attached TMR to a cysteine residue inserted at the C-terminus of cGFP. eGFP has two native cysteine residues at positions 48 and 70. Cys48 is solvent accessible and can be modified by thiol-reactive probes (Ormo *et al.*, 1996; Yang *et al.*, 1996; Suzuki *et al.*, 2004). Hence, we replaced Cys48 with serine, a conservative mutation that had been shown previously not to affect chromophore formation (Suzuki *et al.*, 2004). Cys70 is buried in the interior of the protein and is not modified by thiol-reactive probes (Suzuki *et al.*, 2004).

We purified several TMR-labeled cGFP variants to determine which variant gave optimal energy transfer. GFP–TMR 8 was a variant of cGFP in which residues 230–238 deleted. Further, it had the C48S substitution and a C-terminal glycine residue. We deemed this glycine necessary to lower the pK_a of Cys249. Emission spectra for GFP–TMR 8 are shown in Figure 5-2. Upon excitation at 470 nm, this construct exhibited nearly identical fluorescence at 510 nm (from cGFP) and 575 nm (FRET to TMR). Upon cleavage of the substrate by HIV-PR, we observed a nearly 5-fold increase in cGFP emission as well as a coincident decrease in fluorescence emission from TMR (Figure 5-2). This result shows that GFP–TMR 8 is a capable FRET substrate for measuring HIV-PR activity.

Several attempts to develop cell-based assays for HIV-PR activity have been reported. Lindsten and coworkers used a GFP–HIV-PR fusion to monitor protease activity as a function of

its cytotoxicity (Lindsten *et al.*, 2001). Most recently, Mouland and coworkers used a GFP–luciferase bioluminescence resonance energy transfer (BRET) system to observe HIV-PR activity in cells (Hu *et al.*, 2005). These approaches, while useful, are limited by the need for transfection of the substrate. Because the substrate we have designed should be cell-permeable, our approach could be applicable to cultured or primary cells. To test our substrate in living cells we incubated GFP–TMR **8** with 293T/17 cells, producing the gag/pol regions of the HIV-1 polyprotein (Figure 5-3a). Plasmid VRC4200 expresses the native gag/pol region of the HIV-1 polyprotein under the control of a CMV promoter (Huang *et al.*, 1997; Huang *et al.*, 2001). HIV-PR activity in these cells was confirmed by following cleavage of p17, a structural gag protein, from the polyprotein precursor (Figure 5-3b).

Our FRET substrate for HIV-PR activity showed increased green emission in HIV-PR+ cells (Figure 5-4). This result was consistent with *ex cellulo* experiments that showed an increase in emission at 510 nm. We did not see, however, a marked decrease in red emission (575 nm), indicating that intracellular TMR can be excited to some extent by the 488-nm laser. Further, because cGFP is internalized via endocytosis, much of the fluorescence is localized in vesicles. To address these problems, we need to develop new acceptor molecules. Recently, Ilien and coworkers reported the synthesis of several quencher molecules that effectively quench the fluorescence of GFP (Tahtaoui *et al.*, 2005). We imagine that incorporating these functionalities would improve our results by giving a simplified fluorescence output (that is, only an increase in green fluorescence upon cleavage). Further, the substrate would have no fluorescence in vesicles, as no HIV-PR is present there, and would fluoresce only in the cytosol.

Using a novel cell-permeable variant of GFP, we have designed a cell-permeable FRET substrate for monitoring HIV-PR activity in living cells. Further optimization of the FRET pairs should allow this substrate to be used in primary cells and tissues. Because of the modularity of protease cleavage sequences, this substrate could also be useful in monitoring protease activity from a number of other viral and pathogenic sources.

Figure 5-1: Design of HIV-PR cleavable FRET substrates. (upper) pRSET plasmids encoding for the proteins GFP-TMR 1-8 are shown with the substitutions indicated. Proteins were labeled with TMRIA at the C-terminal cysteine residue. (lower) Design of a GFP-based FRET substrate. cGFP (green) is attached to a small-molecule fluorophore (red) via 10-residue loop, that is cleaved by HIV-PR (yellow).

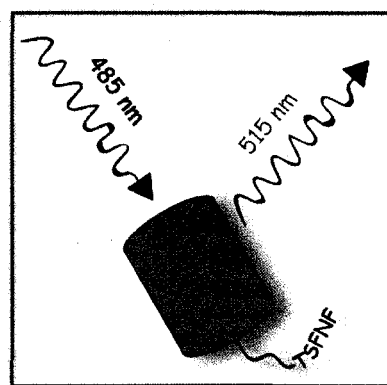
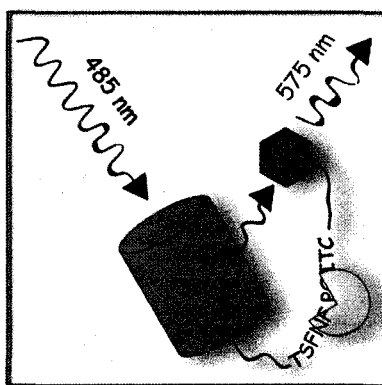
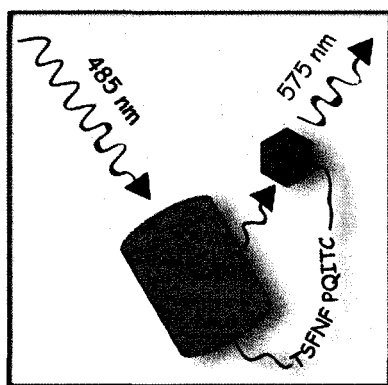
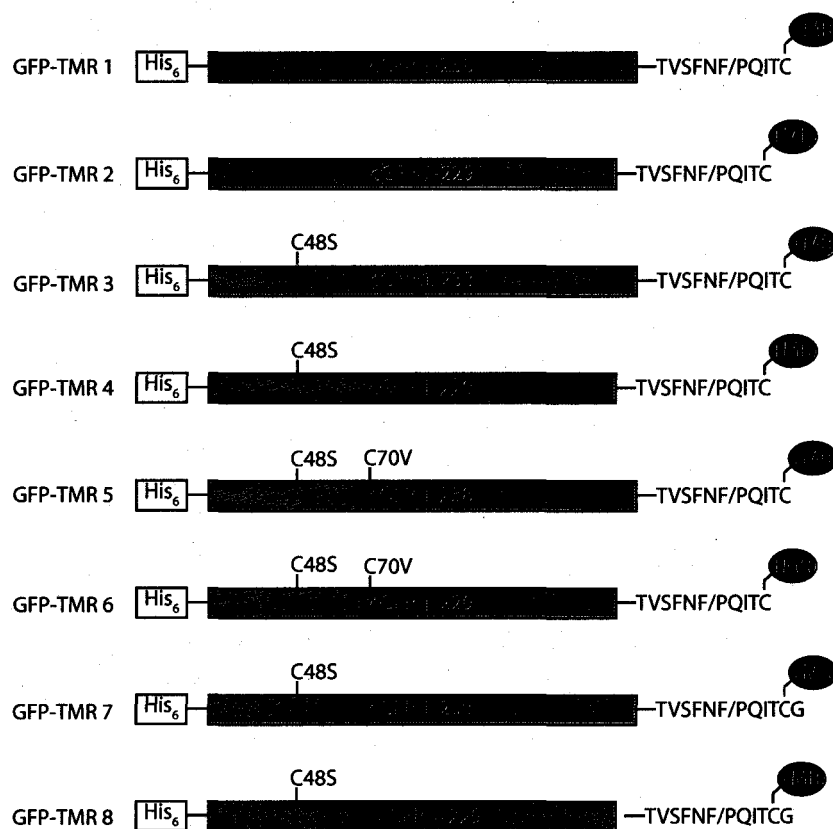


Figure 5-2: Cleavage of GFP-TMR **8** by HIV-PR *in vitro*. Emission spectra of GFP-TMR **8** (1 nM) during cleavage by HIV-PR (emission 470 nm). Scans were taken at 0 (red), 1 (red-orange), 3 (orange), 5 (yellow), 7 (green), 9 (aqua), 11 (blue), and 15 (purple) min.

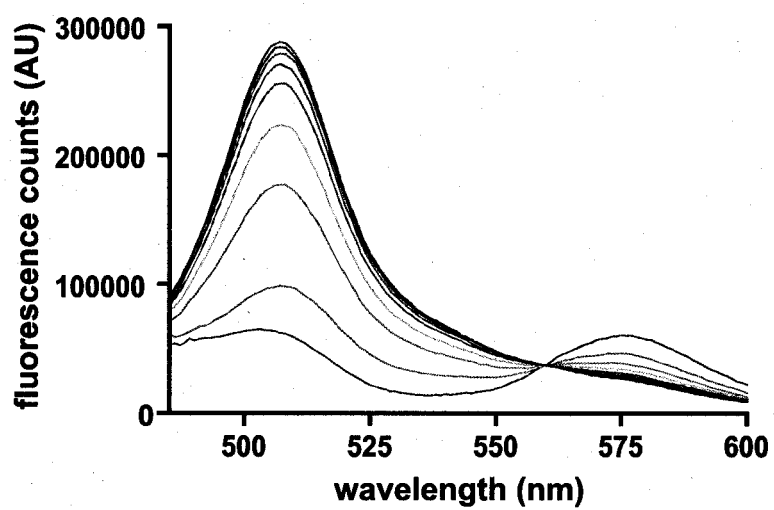


Figure 5-3: Cell lines for transient expression of HIV-PR. (A) Plasmid VRC4200 (gift of Dr. Gary Nabel) encodes the HIV-1 gag/pol region of the polyprotein under the control of the CMV viral promoter. (B) Schematic of the gag/pol region of the HIV-1 polyprotein. (below) Immunoblot of the processing of p17 from the gag region of the HIV-1 polyprotein by HIV-PR. The p17 protein is cleaved from the p55 precursor. In the presence of the inhibitor indinavir, the p55 protein remains unprocessed.

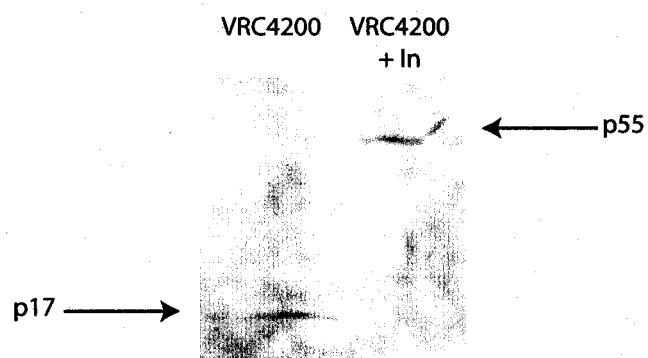
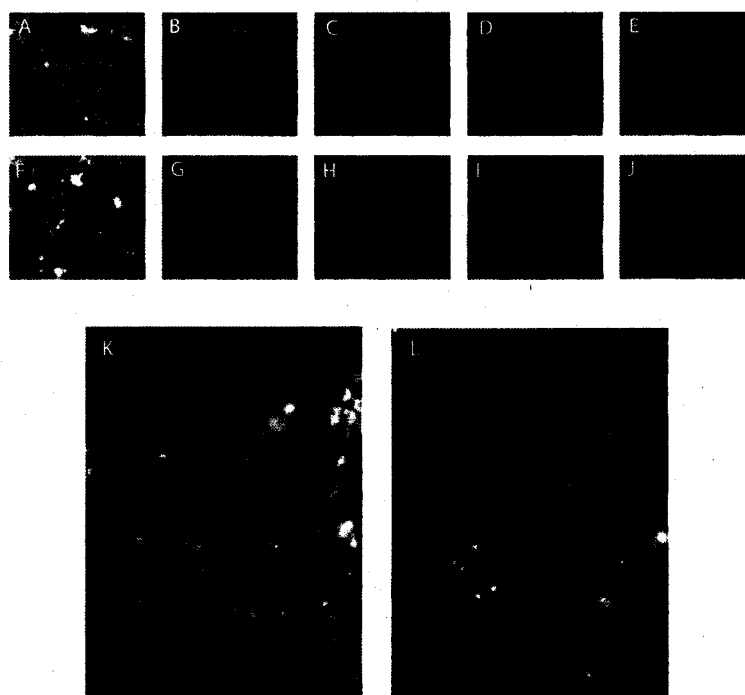


Figure 5-4: Confocal microscope images of GFP-TMR 8 in 293T/17 cells. 5 μ M GFP-TMR 8 was incubated with 293T/17 cells transfected with VRC4200 plasmid (A-E) or cells incubated with the HIV-PR inhibitor indinavir (1 mM) (F-J). Cells were excited with a 488-nm laser and emission in the green (B, G) and red (C,H) spectral regions are shown. Cells were counterstained with Hoechst 33342 dye (D, I). (A,F) Merge of red, green and blue channels. (E, J) Areas containing both green and red fluorescence were subtracted to show only emission due to cGFP. Twofold magnification of GFP-TMR 8 internalization in HIVPR-expressing (K) and HIVPR-negative (L) cells.



Appendix I

Design of Toxic Ribonuclease A Variants with Increased Cellular Uptake

This work was performed with undergraduate researcher Ryan T. Groeschl.

Introduction

Ribonucleases (RNases) have received much recent interest as potential chemotherapeutics due to their ability to catalytically degrade RNA and cause cell death (Leland and Raines, 2001). Bovine pancreatic ribonuclease (RNase A) is the best-studied member of the RNase A superfamily of proteins with respect to structure and function (Raines, 1998). Although RNase A is not toxic to mammalian cells, several variants have been shown to be cytotoxic (Matousek et al., 2003a; Matousek et al., 2003b; Youle and D'Alessio, 1997). Cytotoxicity is correlated to the ability to evade the cytosolic ribonuclease inhibitor protein (RI) (Haigis et al., 2003). Even single amino acid substitutions that weaken the affinity for RI make RNase A toxic to mammalian cells (Leland et al., 1998).

Ribonuclease toxicity is dependent on a number of factors in addition to the ability to evade RI. Catalytic activity is required for a ribonuclease to be toxic (Leland and Raines, 2001; Leland et al., 2001). Further, a ribonuclease must reach the cytoplasm to engage and degrade RNA, and the efficiency of internalization is a key to cytotoxicity. Indeed, Youle and coworkers showed that toxicity could be increased by fusing RNase A to transferrin (Youle et al., 1993). Further, we demonstrated that adding the protein transduction domain (PTD) nonaarginine (R₉) to the C-terminus increased cellular uptake and cytotoxicity (Fuchs and Raines, 2005).

Yamada and coworkers showed that chemical cationization of RNase A led to greater toxicity (Futami et al., 2002). Their most cytotoxic ribonucleases had 20-fold lower enzymatic activity than did the wild-type enzyme. This result highlights one of the limitations of chemical cationization. Because the reaction is non-specific, residues important for substrate binding or

catalysis can be modified, adversely affecting function. Further, their technique led to a mixture of products with a broad range of molecular weights.

Here, we use of the concept of site-specific cationization (See: Chapter 4) to design a more cell-permeable variant of RNase A. We expected that we could increase the positive charge of the protein while retaining catalytic activity, thus making a more cytotoxic variant of RNase A.

Materials and Methods

Cells and chemicals. *Escherichia coli* strain BL21 (DE3) PlysS and the pET22b(+) expression vector were from Novagen (Madison, WI). Human erythroleukemia cells (line K-562) and Chinese hamster ovary (line CHO-K1) were from the American Type Culture Collection (Manassas, VA). [methyl-³H]Thymidine (6.7 Ci/mmol) was from NEN Life Science Products (Boston, MA). All other chemicals and reagents were of commercial reagent grade or better, and were used without further purification.

Terrific Broth (TB) liquid medium contained (in 1 L) tryptone (12 g), yeast extract (24 g), glycerol (4 mL), KH₂PO₄ (2.31 g), and K₂HPO₄ (12.54 g). Phosphate-buffered saline (PBS) was 10 mM sodium phosphate buffer, pH 7.4, containing NaCl (138 mM) and KCl (2.7 mM).

Instruments. The masses of the ribonuclease variants were confirmed by matrix-assisted laser desorption ionization–time-of-flight (MALDI–TOF) mass spectrometry on a Voyager-DE-PRO Biospectrometry Workstation (Applied Biosystems, Foster City, CA) using 3,5-dimethoxy-4-hydroxycinnamic acid as a matrix. Fluorescence measurements were performed with a QuantaMaster 1 photon counting fluorometer equipped with sample stirring (Photon Technology

International, South Brunswick, NJ). Radioactivity was quantified with a Microbeta TriLux liquid scintillation counter (Perkin Elmer, Wellesley, MA).

Site-directed mutagenesis. Oligonucleotides were obtained from Integrated DNA Technology (Coralville, IA). cDNA encoding variants of RNase A were created in plasmid pBXR, which directs the production of RNase A in *E. coli*, (delCardayré et al., 1995) by using the QuikChange mutagenesis kit from Stratagene (La Jolla, CA). All variants of RNase A possessed an N-terminal methionine residue, which has been reported to have no effect on ribonucleolytic activity (Arnold et al., 2002). A C-terminal R₉ tag was separated from the remainder of a protein by a triglycine linker.

Production and purification of protein variants. Untagged variants of RNase A and Onconase™ (which is the most cytotoxic known homolog of RNase A (Matousek et al., 2003b)) were produced in *E. coli* and purified as described previously (Leland et al., 1998). Variants of RNase A containing a C-terminal R₉ tag were prepared as follows. BL21(DE3)PlysS cells containing a plasmid that encodes an RNase A variant were grown at 37 °C with shaking (250 rpm) in TB containing ampicillin (200 µg/mL) and chloramphenicol (35 µg/mL) to an *OD* = 1.6 at 600 nm. cDNA expression was induced by adding isopropyl β-D-thioglucopyranoside (IPTG; to 1 mM). Cells were grown for an additional 4 h before harvesting by centrifugation. Cell pellets were resuspended in lysis buffer, which was 10 mM Tris-HCl buffer, pH 8.0, containing ethylenediaminetetraacetic acid (EDTA; 1.0 mM), NaCl (0.10 M), and phenylmethylsulfonyl fluoride (1.0 mM), and lysed by sonication. Inclusion bodies were isolated by centrifugation at 11,000g for 45 min and solubilized in denaturing solution, which was 20 mM Tris-HCl buffer, pH 8.0, containing guanidine hydrochloride (7.0 M) and EDTA (10 mM), for 4 h at room

temperature. Solubilized inclusion bodies were diluted ten-fold with acetic acid (20 mM) and clarified by centrifugation. The supernatant was dialyzed overnight against the same buffer. The resulting protein was then folded overnight at 4 °C in a redox buffer, which 100 mM Tris-HCl buffer, pH 8.0, containing EDTA (10 mM), L-arginine (0.5 M), reduced glutathione (1 mM), and oxidized glutathione (0.2 mM). Refolded protein was purified by cation-exchange chromatography on a 5-mL HiTrap SP-sepharose FF column (Amersham Biosciences, Piscataway, NJ) in 50 mM sodium acetate buffer, pH 5.0, with a linear gradient (50 + 50 mL) of NaCl (0–1.5 M). The identity of each variant was verified by MALDI-TOF mass spectrometry.

Assays of enzymatic activity. Ribonucleolytic activity was measured by monitoring the increase in the fluorescence of 6-FAM-dArU(dA)₂-6-TAMRA (Integrated DNA Technologies, Coralville, IA) upon enzyme-catalyzed cleavage, as described previously (Kelemen et al., 1999) with minor modifications. Polyarginine-containing peptides are known to bind to glass surfaces (Chico et al., 2003). We observed this phenomenon (data not shown), and so performed all assays in 10 mM Bis-Tris-HCl buffer, pH 6.0, containing NaCl (0.50 M). In this high-salt buffer, the binding of protein to a quartz cuvette was found to be insignificant.

Assays of cytotoxicity. The effect of ribonucleases on cell proliferation was determined by measuring the incorporation of [methyl-³H]thymidine into cellular DNA. K-562 cells were grown in RPMI 1640 medium containing fetal bovine serum (10% v/v), penicillin (100 units/mL), and streptomycin (100 µg/mL). Cytotoxicity assays were performed using asynchronous log-phase cultures grown at 37 °C in a humidified incubator containing CO₂(g) (5% v/v). To assay toxicity, cells (95 µL of a solution of 5 × 10⁴ cells/mL) were incubated with PBS containing a ribonuclease (5 µL) in a 96-well plate. The cells were grown for 44 h and then

pulsed for 4 h with radiolabeled thymidine (0.25 $\mu\text{Ci}/\text{well}$), which is only incorporated into the DNA of living cells. DNA was harvested onto glass fiber filters using a PHD cell harvester (Cambridge Technology, Watertown, MA). Filters were washed with water and dried with methanol, and their ^3H content was quantified with liquid scintillation counting.

Thermal denaturation. As RNase A is denatured, its six tyrosine residues become exposed to solvent and its molar absorptivity at 287 nm decreases significantly (Hermans and Scheraga, 1961). Unfolding was monitored in PBS buffer containing NaCl (500 mM) by the change in absorbance at 287 nm as the temperature was raised at a rate of 0.15 $^{\circ}\text{C}/\text{min}$. Data were fitted to a two-state model to calculate the value of T_m , which is the temperature at the midpoint of the transition between the folded and unfolded states (Pace and Scholtz, 1987).

Results

Design of cationic RNase A variants. There are many factors that contribute to the toxicity of ribonuclease. Although we were seeking to improve ribonuclease uptake, we planned to use cytotoxicity as a measure of internalization. Therefore, all RNase A variants contained the G88R substitution which raises the K_d for the interaction with RI 10^4 -fold (Kobe and Deisenhofer, 1993; Leland et al., 1998). Previous results from Yamada and coworkers suggested that increasing the cationic surface of RNase A would make the protein more toxic (Futami et al., 2002). To increase the cationic character of RNase A without disrupting catalytic activity, we made specific point mutations to the RNase A surface. Using an electrostatic potential map of RNase A created with PyMol modeling software, we noted the presence of two acidic residues

on the molecular surface of RNase A (Figure AI-1). These residues, Glu49 and Asp53, are in close proximity to one another but are removed from the basic active site. We expected that substituting these residues with arginine would increase charge without affecting catalytic activity. Recently, we showed that adding a cationic tag to RNase A increased uptake as measured by fluorescence microscopy (Fuchs and Raines, 2005). Hence, in addition to the point mutations described, we also determined if a cationic PTD and site-specific cationization would have additive effects on the cytotoxicity of ribonuclease variants.

Biochemical chracterization of cationic RNase A variants. RNase variants were purified as described previously (Leland et al., 1998). We characterized both the catalytic activity and thermal stability of the purified proteins (Table AI-1). The E49R/D53R/G88R RNase A variant showed similar catalytic activity to that of G88R RNase A. Interestingly, this variant had a lower T_m value (54 °C) than did G88R RNase A (60 °C).. Addition of the polyarginine tag to either G88R or E49R/D53R/G88R RNase A resulted in a further decrease in stability. Likewise, catalytic activity is decreased slightly with the addition of the R₉ tag.

Cytotoxicity of RNase A variants. The toxicity of a ribonuclease increases as the efficiency of transport into the cell becomes more efficient (Fuchs and Raines, 2005). We therefore monitored the internalization of our RNase variants by measuring their toxicity in K-562 cells (Figure AI-2; Table AI-1). RNase A is not toxic to mammalian cells due to its affinity for the cytosolic RI protein. The toxic variant G88R RNase A had an IC₅₀ value of 5.8 μM. Adding the two substitutions, E49R and D53R, to this variant improved toxicity by 3-fold to 1.9 μM. The addition of the R₉-tag to either G88R RNase A or E49R/D53R/G88R RNase A increased their

cytotoxicity by approximately 3-fold with G88R RNase A–R₉ and E49R/D53R/G88R RNase A–R₉ exhibiting IC₅₀ values of 2.0 and 0.59 μ M, respectively.

Discussion

The ability of cationic character to affect cellular uptake of a macromolecule has been known for many years (Ryser, 1967; Ryser and Hancock, 1965). As described previously, a number of strategies have been developed to harness this effect and apply it to drug development. Here, we used a strategy called site-specific cationization to modify the surface charge of a protein, RNase A, without compromising normal enzyme function.

We chose to replace residues Glu49 and Asp53 of RNase A with arginine. Arginine has been shown to be the most effective amino acid for facilitating uptake of polybasic peptides (Mitchell et al., 2000; Suzuki et al., 2002). There are other acidic residues on the RNase A surface, such as Glu9 and Glu111, that are in closer proximity to the active site. In subsequent studies we modified these residues both to arginine without any considerable change in toxicity (S.M. Fuchs, T.Y. Chao, and R.T. Raines, unpublished results). These residues lie close to the substrate active site, and thus it is likely that these variants were less toxic due to diminished enzymatic activity.

The E49R/D53R variant of RNase A exhibited wild-type activity using a small nucleotide substrate (Table AI-1). Yet, these substitutions caused a measurable change in the stability of the protein ($\Delta T_m \approx 9^\circ\text{C}$). It is possible these residues participate in hydrogen bonds or Coulombic interactions that are important to conformational stability. Further it is possible that

the installation of arginine residues results in unfavorable interactions. Regardless, the variant is still sufficiently stable to be a useful cytotoxin with a T_m much greater than 37 °C.

Increasing the surface charge of RNase A by modifying Glu49 and Asp53 to arginine resulted in a 3-fold increase in toxicity of the already toxic G88R variant of RNase A. This change, though small, is significant. We made these cognate mutations in RNase A, but this variant showed no change in toxicity (data not shown). These modifications do not affect RI binding and therefore, RI would sequester an internalized variant that lacks the G88R mutation.

We showed previously that adding an R₉-tag to the C-terminus of RNase A increased the internalization of that protein (Fuchs and Raines, 2005). We, therefore, made an R₉-tagged version of both G88R RNase A and E49R/D53R/G88R RNase A. The R₉-tag improved the toxicity of both variants by approximately 3-fold. This result suggests that distinct strategies for cationization can be combined to enhance cytotoxicity.

Several other substitutions have been made to optimize RNase A cytotoxicity mainly by decreasing the affinity for RI (Bretscher et al., 2000; Rutkoski et al., 2005). Future work will combine approaches for improving internalization with others that disrupt the RI•RNase A complex. We expect that these strategies will yield even more toxic RNase A variants.

Table AI-1. Biochemical parameters of RNase A and its variants

Ribonuclease	pI ^a	T_m ^b (°C)	k_{cat}/K_M ^c ($10^6 \text{ M}^{-1} \text{ s}^{-1}$)	IC ₅₀ ^d (μM)
RNase A	8.6	63.7	1.8 ± 0.2	>25
RNase A-R ₉	9.6	56	1.0 ± 0.2	>25
G88R RNase A	8.8	60	12.6 ± 0.4	5.8 ± 1.0
G88R RNase A-R ₉	9.8	54.0	9.6 ± 0.2	2.0 ± 0.4
E49R/D53R/G88R RNase A	9.3	53	1.7 ± 0.05	1.9 ± 0.6
E49R/D53R/G88R RNase A-R ₉	10.1	49	3.59 ± 0.05	0.56 ± 0.06

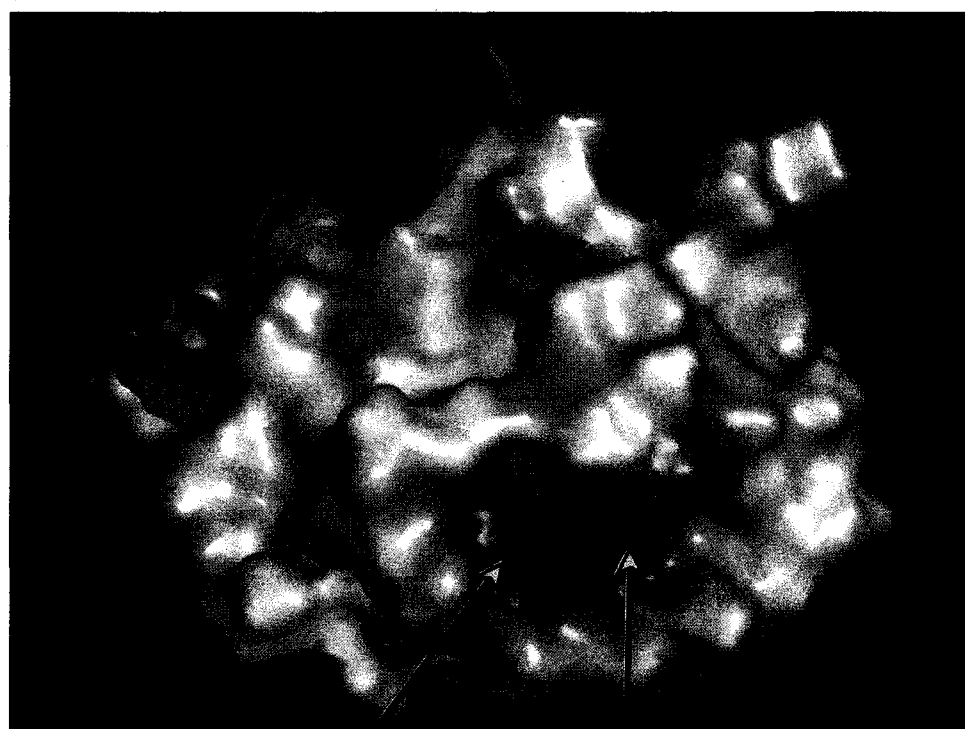
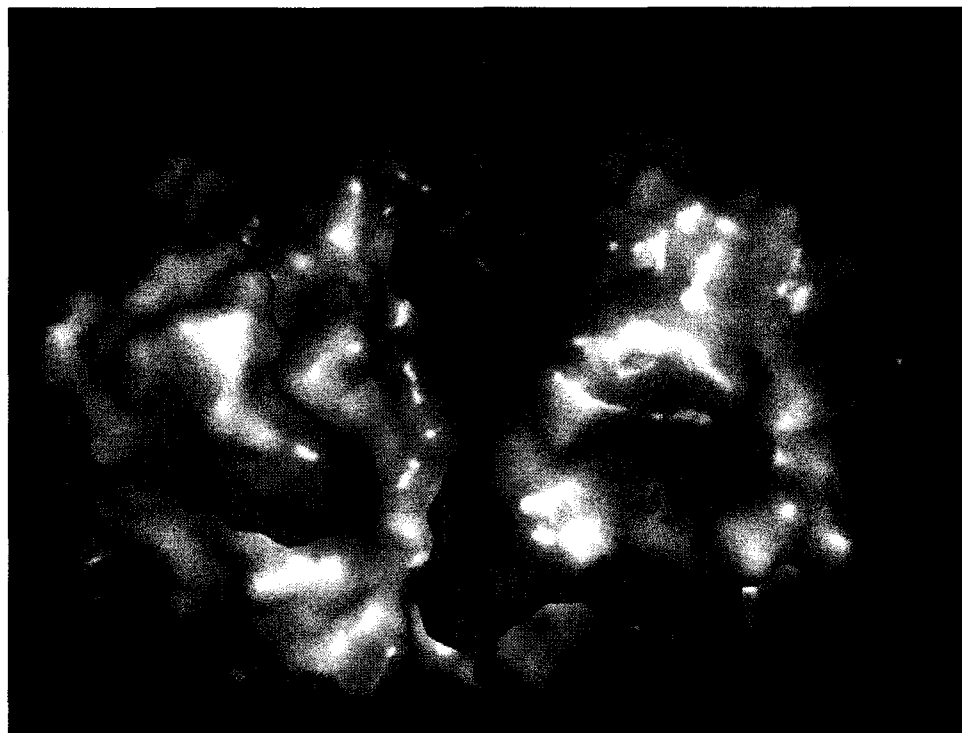
a Values of pI were estimated from amino acid composition (Bjellqvist et al., 1994; Bjellqvist et al., 1993).

b Values of T_m (± 2 °C) were determined in PBS by UV spectroscopy.

c Values of k_{cat}/K_M (\pm SE) are for the catalysis of 6-FAM-dArU(dA)2-6-TAMRA cleavage at 25 °C in 10 mM Bis-Tris-HCl buffer, pH 6.0, containing NaCl (0.50 M).

d Values of IC₅₀ (\pm SE) are for the incorporation of [methyl-³H]thymidine into the DNA of K-562 cells.

Figure AI-1. Electropotential model of RNase A. An electropotential map of RNase A was created with the program PyMol (top) View of RNase A active site. Basic areas are shown in blue, and acidic areas are shown in red. (bottom) Reverse view of RNase A showing the acidic patch corresponding to residues Glu49 and Asp53.



E49

D53

Figure AI-2. Cytotoxicity of wild-type RNase A and its cationic variants in K-562 cells. Cell viability was measured by ^3H -thymidine incorporation after 44 h of incubation with RNases. Toxicity was plotted as % cell viability versus concentration. RNase A (red) and ONC (green) were plotted as controls. G88R RNase A is shown in purple while E49R/D53R/G88R RNase A is shown in aqua.

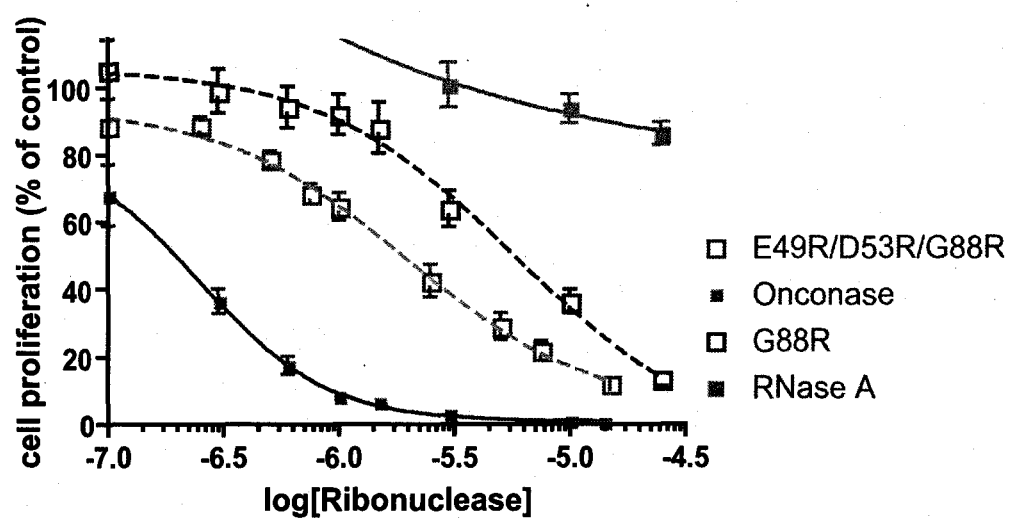
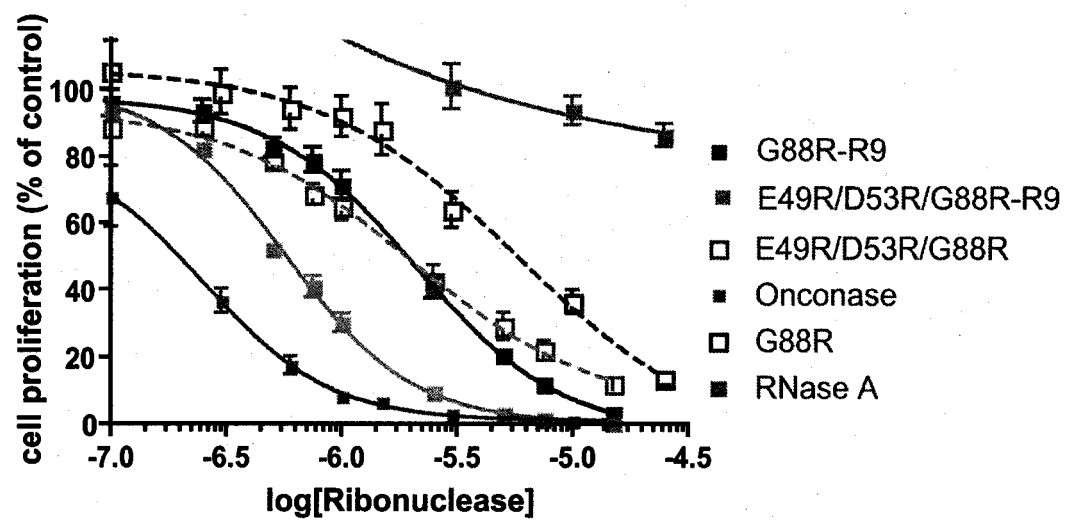


Figure AI-3. Cytotoxicity of cationic and R₉-tagged variants in K-562 cells. Cell viability was measured by ³H-thymidine incorporation after 44 h of incubation with RNases. Toxicity was plotted as % cell viability versus concentration. RNase A (red) and ONC (green) were plotted as controls. G88R RNase A variants are shown in purple (+ R₉: solid line and filled squares; - R₉: dashed line with open squares) and E49R/D53R/G88R RNase A variants are shown in aqua (+R₉: solid line and filled squares; - R₉: dashed line with open squares).



Appendix II

Release of Cationic Peptides and Proteins from Multilayered Thin Films

This work is done in collaboration with Dr. David M. Lynn (University of Wisconsin-Madison department of Chemical Engineering) Christopher M. Jewell and David Balachandran were responsible for all of the chip preparations and analyses.

Introduction

One important aspect of drug delivery is the ability to deliver molecules in a controlled manner. Controlled and sustained release systems are of great importance allowing for enhanced targeting, improved pharmacokinetics, lower toxicity, and greater patient convenience (Wood *et al.*, 2005). Still, many challenges exist particularly with the controlled delivery of larger molecules, such as proteins.

Over the past decade, thin films of oppositely charged polyelectrolytes have been developed that have diverse applications including drug delivery (Decher, 1997). Multilayer films are formed by the sequential layer-by-layer (LBL) absorption of oppositely charged polymers onto a solid substrate. Interestingly, these films are amenable to incorporation of a number of biomolecules, including small molecules, DNA, and proteins. In aqueous solution, these films can release encapsulated contents over time, allowing for controlled release of the biomolecule. Currently, many groups are working to tune the release properties of these polymers to release their contents over longer times or to release in response to environmental changes such as pH and ionic strength (Sukhishvili *et al.*, 2000; Schuler and Caruso, 2001).

Lynn and coworkers have shown that plasmid DNA itself was capable of acting as the negatively charged polyelectrolyte and could be used in conjunction with polycations such as polyethylenimine to form stable films (Zhang *et al.*, 2004). In aqueous solution, these films release plasmid DNA that is then capable of transfecting cells in culture.

The use of basic peptides to deliver conjugated target molecules is well established (Wadia and Dowdy, 2005). These peptides, known as protein transduction domains (PTDs), are able to interact with the cell surface and facilitate internalization of attached cargo (see Chapter 1).

Further, PTDs such as nonaarginine, R₉, can be utilized as tags for more diverse biotechnical applications such as purification or immobilization (Fuchs and Raines, 2005).

Our approach was to develop a system in which a positively-charged protein or peptide would be incorporated into films along with a negatively-charged polymer, such as sulfonated polystyrene. Further, the presence of cationic protein transduction domains (PTDs), would facilitate cellular entry of encapsulated cargoes upon release from films.

Here, we employ a PTD, nonaarginine (R₉), to facilitate encapsulation in thin films of tetramethylrhodamine as well as the enzyme bovine pancreatic ribonuclease (RNase A). Further, we show that these films release the R₉-conjugates and that the resulting molecules are capable of cellular entry upon release from films. We expect that these cationic tags could be useful in developing controlled release strategies for protein therapeutics.

Materials and Methods

Cells and chemicals. *Escherichia coli* strain BL21 (DE3) PlysS and the pET22b(+) expression vector were from Novagen (Madison, WI). All other chemicals and reagents were of commercial reagent grade or better, and were used without further purification.

Terrific Broth (TB) liquid medium contained (in 1 L) tryptone (12 g), yeast extract (24 g), glycerol (4 mL), KH₂PO₄ (2.31 g), and K₂HPO₄ (12.54 g). Phosphate-buffered saline (PBS) was 10 mM sodium phosphate buffer, pH 7.4, containing NaCl (138 mM) and KCl (2.7 mM).

Instruments. The mass of ribonuclease variants was confirmed by matrix-assisted laser desorption ionization–time-of-flight (MALDI–TOF) mass spectrometry using a Voyager-DE-

PRO Biospectrometry Workstation (Applied Biosystems, Foster City, CA) using 3,5-dimethoxy-4-hydroxycinnamic acid as a matrix. Fluorescence measurements were performed with a QuantaMaster 1 photon counting fluorometer equipped with sample stirring (Photon Technology International, South Brunswick, NJ).

Peptide synthesis. R₉, CR₉, and acetylated-R₉ were synthesized by Fmoc-based solid-phase peptide synthesis with an Applied Biosystems Model 432A peptide synthesizer. R₉ was cleaved from the Rink acid resin by incubation for 4 h in trifluoroacetic acid/ethanedithiol/phenol/thioanisole (32:4:3:1) and precipitated in diethylether. Peptides was purified by reversed-phase HPLC on a C4 column using a gradient of water:acetonitrile containing trifluoroacetic acid (0.1% v/v), and analyzed by matrix-assisted laser desorption ionization–time-of-flight (MALDI–TOF) mass spectrometry using a Bruker Biflex III instrument.

Synthesis of TMR–R₉. R₉ was labeled on resin by incubation for 4 h with TAMRA (4 equiv) in dimethylformamide containing benzotriazole-1-yl-oxy-tris-pyrolidino-phosphonium hexafluorophosphate (4 equiv) and diisopropylethylamine (8 equiv). The resin was washed exhaustively with dimethylformamide and dichloromethane before deprotection. TMR–R₉ was purified by reversed-phase HPLC and analyzed by MALDI–TOF mass spectrometry (*m/z* 1837.92; expected: 1837.13).

Synthesis of tetramethylrhodamine derivative (3). 5-carboxytetramethylrhodamine (1) was purified from a mixture of 5- (or 6-) carboxytetramethylrhodamine (Sigma Chemical) by C-18 reversed-phase HPLC using a gradient of water:acetonitrile containing trifluoroacetic acid (0.1% v/v). To a solution of (1) (0.23 mmol) in DMF was added PyBOP (0.5 mmol), DIEA (0.5 mmol),

and N-boc-diaminoethane (0.5 mmol), and the resulting solution was stirred overnight. The resulting mixture was purified by flash chromatography using MeOH/CH₂Cl₂ (5:95) to give **2** in 40% yield. The boc group was deprotected using TFA (2 mL) for 3 h. The resulting compound **3** was dried by rotary evaporation and washed three times with hexanes to remove residual *t*-butyl alcohol. The identity of (**3**) was confirmed by mass spectrometry (m/z 473.4 m/z , expected: 473.4) and by ¹H NMR.

Synthesis of TMR-CR₉ (5). N-(3-carboxy)maleimide was a generous gift of L.D. Lavis. To a solution of DCC (0.11 mmol), DMAP (0.011 mmol) and DIEA (0.11 mmol) in DMF was added N-(3-carboxy)maleimide (0.1 mmol), and the mixture was stirred for 40 min at rt. Compound **3** (0.10 mmol) was added, and the reaction mixture was stirred for 24 h. The peptide was purified by reversed-phase HPLC, and the mass was verified by MALDI-TOF mass spectrometry.

Synthesis of Ac-R₉-TMR ester isostere (6). To Ac-R₉ (0.01 mmol) in dry DMF (1 mL) was added DCC (0.011 mmol) at 0 °C under Ar(g). After 40 min, DMAP (0.011 mmol), DIEA (0.1 mmol), and **3** (0.011 mmol) were added, and the resulting solution was stirred overnight at room temperature. The product, **6**, was purified by reversed-phase HPLC using a gradient of water:acetonitrile containing TFA (0.1% v/v). The identity of the product was confirmed by MALDI-TOF mass spectrometry (m/z 1922 m/z ; expected: 1922.9).

Synthesis of tetramethylrhodamine derivative (8). To a solution of **1** (0.69 mmol) in DMF was added PyBOP (1.4 mmol), DIEA (1.4 mmol) and *t*-butoxyaminoethanol (1.4 mmol) and the solution was stirred overnight. The resulting mixture was purified by flash chromatography with a solvent system of MeOH/CH₂Cl₂ (5:95) to give **7** in 40% yield. The *t*-butyl group was removed by treatment with TFA (5 mL) overnight to give (**8**), which was recovered by rotary evaporation

and washed three times with hexanes to remove residual *t*-butyl alcohol. The identity of (7) was confirmed by mass spectrometry (m/z 474.2, expected 474.4) and by ^1H NMR spectroscopy.

Synthesis of Ac-R₉-TMR amide isostere (9). To Ac-R₉ (0.01 mmol) in dry DMF (1 mL) was added DCC (0.011 mmol), DIEA (0.04 mmol), and 8 (0.011 mmol), and the resulting solution was stirred overnight at room temperature. The product, 9, was purified by reversed-phase HPLC using a gradient of water:acetonitrile containing TFA (0.1% v/v). The identity of the product was confirmed by MALDI-TOF mass spectrometry (m/z 1921: expected:1921.9 m/z).

Production and purification of RNase A and RNase A-R₉. Untagged variants of RNase A were produced in *E. coli* and purified as described previously (Leland *et al.*, 1998). Variants of RNase A containing a C-terminal R₉ tag were constructed as described in Chapter 3 and prepared as follows. BL21(DE3)PlysS cells containing a plasmid that encodes an RNase A variant were grown at 37 °C with shaking (250 rpm) in TB containing ampicillin (200 µg/mL) and chloramphenicol (35 µg/mL) to an $OD = 1.6$ at 600 nm. cDNA expression was induced by adding isopropyl β-D-thiogalactopyranoside (IPTG; to 1 mM). Cells were grown for an additional 4 h before harvesting. Cell pellets were resuspended in lysis buffer, which was 10 mM Tris-HCl buffer, pH 8.0, containing ethylenediaminetetraacetic acid (EDTA; 1.0 mM), NaCl (0.10 M), and phenylmethylsulfonyl fluoride (1.0 mM), and lysed by sonication. Inclusion bodies were isolated by centrifugation at 11,000g for 45 min and solubilized in denaturing solution, which was 20 mM Tris-HCl buffer, pH 8.0, containing guanidine hydrochloride (7.0 M) and EDTA (10 mM), for 4 h at room temperature. Solubilized inclusion bodies were diluted ten-fold with acetic acid (20 mM) and clarified by centrifugation. The supernatant was dialyzed overnight against the same

buffer. The resulting protein was then folded overnight at 4 °C in a redox buffer, which 100 mM Tris-HCl buffer, pH 8.0, containing EDTA (10 mM), L-arginine (0.5 M), reduced glutathione (1 mM), and oxidized glutathione (0.2 mM). Refolded protein was purified by cation-exchange chromatography on a 5-mL column of HiTrap SP-sepharose FF resin (Amersham Biosciences, Piscataway, NJ) in 50 mM sodium acetate buffer, pH 5.0, with a linear gradient (50 + 50 mL) of NaCl (0–1.5 M). The identity of each variant was verified by MALDI-TOF mass spectrometry.

Semisynthesis of fluorescent proteins. RNases were labeled with fluorescein at one specific residue in a surface loop by using variants in which Ala19 was replaced with a cysteine residue (Haigis and Raines, 2003). A19C RNase A-R₉ or A19C RNase A (100 μM) were incubated in PBS containing a 20-fold molar excess of 5-iodoacetamidofluorescein (Molecular Probes, Eugene, OR) and a 3-fold molar excess of tris[2-carboxyethylphosphine] hydrochloride (TCEP) for 4 h at room temperature. The resulting solution was dialyzed overnight against 50 mM sodium acetate buffer, pH 5.0, and then purified by cation-exchange chromatography using a 5-mL HiTrap CM-Sephacrose Fast Flow column with a linear gradient (50 + 50 mL) of NaCl (0–1.00 M for A19C RNase A; 0–2.00 M for A19C RNase A-R₉). Conjugation to the fluorophore was confirmed by MALDI-TOF mass spectrometry.

Fabrication of Multilayered Films. Prior to film construction, quartz or silicon substrates were cut to approximately 0.5 x 3.0 cm and dipped in acetone, ethanol, methanol, and water. Substrates were cleaned and charged by oxygen plasma treatment. Solutions of linear poly(ethylene imine) (LPEI) and poly(styrene sulfonate) (SPS) used for the fabrication of LPEI/SPS precursor layers (20 mM with respect to the molecular weight of the polymer repeat

unit) were prepared using 18M Ω water w/ added NaCl and HCl . Solutions of SPS for upper films layers were prepared without added salt, and the pH was adjusted to 5.0. Solutions of fluorescein-labeled RNaseA with or without an R₉ tag were diluted with water from a stock solution to a final concentration of ~20 μ M. Slides were robotically coated with 10 precursor bilayers of LPEI and SPS to provide a suitably charged surface for subsequent adsorption. Upper layers consisting of RNaseA/SPS were deposited on these foundation layers using a manual dipping process. For all deposition steps, the general protocol was: (1) Substrates were submerged in a solution of polycation for 5 min, (2) substrates were removed and immersed in a wash bath for 1 min followed by a second wash bath for 1 min (wash baths were deionized water or 100 mM sodium acetate buffer, pH = 5.0), (3) substrates were submerged in a solution of polyanion for 5 min, and (4) substrates were rinsed in the manner described above. This cycle was repeated until the desired number of bilayers had been deposited. Film thicknesses of silicon substrates were characterized during fabrication by using ellipsometry.

Release Experiments. Coated substrates were placed in 1 mL of PBS buffer and incubated at 37 °C. At specified times, substrates were removed, rinsed in deionized water, and dried under filtered air. Ellipsometric thickness was recorded for silicon substrates at each timepoint. Substrates were then placed in 1 mL of fresh PBS buffer and the incubation was continued. The PBS solutions assayed for ribonucleolytic activity and RNaseA concentrations were calculated.

Localized Cell Transfection Experiments. COS-7 cells were grown in 6-well plates at an initial seeding density of 450,000 cells/well in 3.0 mL of growth medium which was 90% v/v Dulbecco's modified Eagle's medium and 10% fetal bovine serum containing penicillin (100 μ g/mL) and streptomycin (100 μ g/mL). Cells were allowed to grow overnight to approximately

80% confluence, and coated substrates were placed manually into the wells on top of the cells. DMEM was aspirated and replaced with 3 mL of Opti-MEM medium just prior to slide addition. Cells were incubated for 4h with slides and fluorescence and phase-contrast images were recorded without substrate removal using an Olympus IX70 fluorescence microscope.

Preliminary Results

Synthesis and erosion of TMR-R₉ ester and amide films. LBL-polyelectrolyte films have been used to control the release of many types of molecules. We wanted to explore the ability of cationic peptides to form stable films. To achieve this we used a TMR-labeled R₉ peptide. The TMR label is necessary to follow the fate of the peptide both in and out of the film. Further, to explore the potential of these films to release small molecules, we made a labile TMR-CR₉ construct where the TMR was attached to CR₉ via an ester linkage (Figure AII-2). These two molecules were loaded into films using sulfonated polystyrene (SPS) as the anionic polymer. Both molecules made stable films that degraded over time in aqueous solution (Figure AII-3). Degradation of the films could be monitored by the amount of fluorescence in solution (Figure AII-3a) and by changes in chip thickness (Figure AII-3b). Both the amide and ester peptides were released over a very long period of time (~54 days). We observed a faster release of TMR from the TMR-CR₉ ester films than release of the TMR-R₉ amide film. Presumably this represents hydrolysis of the ester linkage as the thickness of the two films changed at approximately the same rate (Figure AII-3b).

Synthesis of Fl-RNase A and Fl-RNase A-R₉ films. Fluorescently-labeled variants of RNase A and RNase A-R₉ were incorporated into films with SPS as the counterion polymer (Figure AII-5a). We were able to attain stable films with approximately 100 nm-thickness with the R₉-containing proteins but not with RNase A alone. The RNase A-R₉ films degraded in aqueous solution very quickly (1–2 h) at pH 7.2 to release protein (Figure AII-5b). Further, we placed these films over COS-7 cells and monitored the release of RNase coupled to cellular uptake via fluorescence microscopy (Figure AII-6). Although we observed entry of RNase A-R₉ into cells (Figure AII-6d), no RNase A could be detected in cells (Figure AII-6c).

Discussion

We have previously shown that the cationic peptide nonaarginine, R₉, can be used for a number of biotechnological applications (Fuchs and Raines, 2005). The ability of R₉ to form stable electrostatic interactions with polyanions prompted us to attempt to incorporate these peptides into multilayer polyelectrolyte films (Decher, 1997). Previously, others have shown that the release of small molecules from polyelectrolyte films could be attained by attaching these molecules to polymers through labile linkages (Thierry *et al.*, 2005). In our study we sought to explore a number of questions centered on the use of cationic peptides in LBL polyelectrolyte films.

Using TMR-R₉ we first demonstrated that these small peptides were able to form stable films with the counterion, sulfonated polystyrene (SPS). These films degraded slowly in aqueous solution (Figure AII-3). Next, we explored the use of these peptides as handles for the

incorporation of small molecules into films. We synthesized TMR-CR₉ in which tetramethylrhodamine was attached to CR₉ via an ester linkage. We suspected that in aqueous solution the rate of ester hydrolysis would be more rapid than release of the peptide from the film. Comparing the fluorescence of the aqueous solution as a function of time we did indeed observe a more rapid release of TMR-CR₉ than TMR-R₉ (Figure AII-3a). Although we would like to attribute this faster release to hydrolysis of the ester, we cannot discount the possibility that the change was due to some greater structural difference between the two peptides, as the linkers between the TMR and the peptides are quite different in these two molecules. To address this problem we have synthesized two new peptides that differ by only one atom (Figure AII-4). Analyzing the rate at which the solution fluorescence changes as a result of the release of these two peptides from films will give a better understanding of the utility of cationic peptides in LBL films.

In a second study, we explored the ability of R₉ to facilitate the incorporation of a protein, RNase A, into a multilayer film. We synthesized two fluorescein-labeled variants of RNase A; one was the wild-type protein (Fl-RNase A) and one had a nonaarginine tag at the C-terminus of the protein (Fl-RNase A-R₉) (Fuchs and Raines, 2005). We explored the incorporation of these two proteins into films with SPS as a counterion. Without the R₉ tag, RNase A was not incorporated into films (Figure AII-5a). We were able to form 100-nm films containing Fl-RNase A-R₉, suggesting that the R₉ is necessary and sufficient to promote protein incorporation into a film (Figure AII-5a). We observed that even though Fl-RNase A-R₉ formed films, they degraded very quickly in water (Figure AII-5b) with a half-life of less than 1 h. Thus, while use of R₉ in making protein films is promising, our current formulation is not usable for any

biological applications. Others have shown that they can tune the stability of polyelectrolyte multilayer films by altering the composition of the two polymers (Mendelsohn *et al.*, 2003). For example, polycations such as poly(dimethyldiallylammonium chloride) or PDAC are fully charged in aqueous solution and are known to form very stable multilayer structures with strong polyanions such as SPS (Seyrek *et al.*, 2003). Incorporating PDAC layers between layers of R₉-tagged protein may increase the stability of the film and thus alter the release properties. Future experiments will be aimed at stabilizing the R₉-containing films as well exploring the ability of R₉ to facilitate incorporation of more diverse proteins into films.

Our initial findings have shown that R₉ could be a useful tool for incorporating non-charged small molecules and proteins into multilayer films. Further, the ability of R₉ to enter cells offers a second level of efficacy, as R₉-tagged molecules would also be more efficient at entering cells than would untagged molecules. Future work in this area could provide useful methods of delivering biomolecules to cells in a controlled manner.

Figure AII-1. Scheme depicting the formation of an LBL multilayer polyelectrolyte film. Figure taken from (Decher, 1997). (A) description of the dipping method wherein a solid surface is dipped into a solution of polyanion (blue) washed in buffer, dipped in a solution of polycation (red), and washed. These steps are repeated multiple times to make many alternating positive and negative layers on the surface (B). (C) Molecular structure of a representative polyanion, SPS, and polycation, polyethylenimine (PEI).

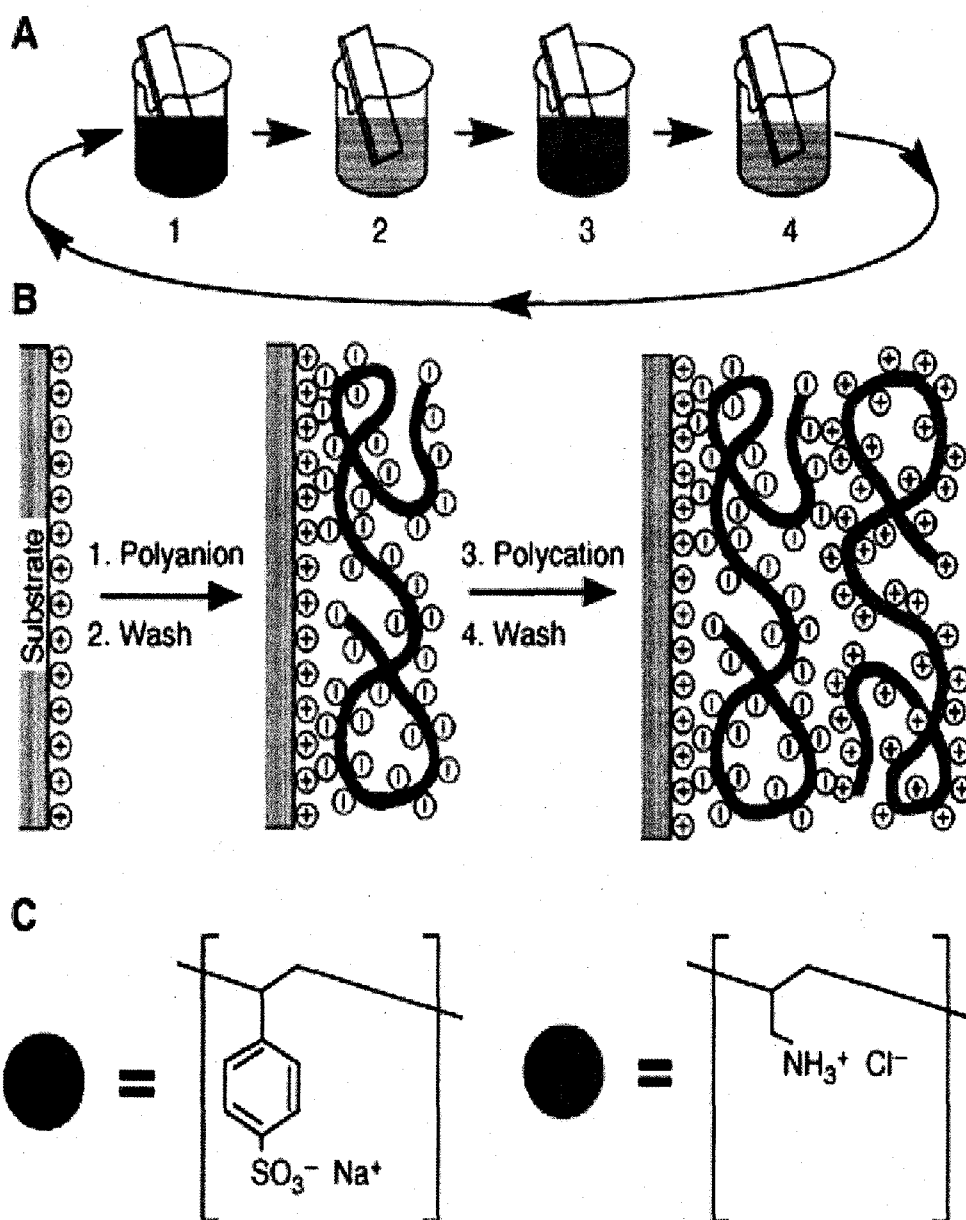


Figure AII-2. Synthetic scheme for TMR-CR₉ ester (5). A alcohol derivative of

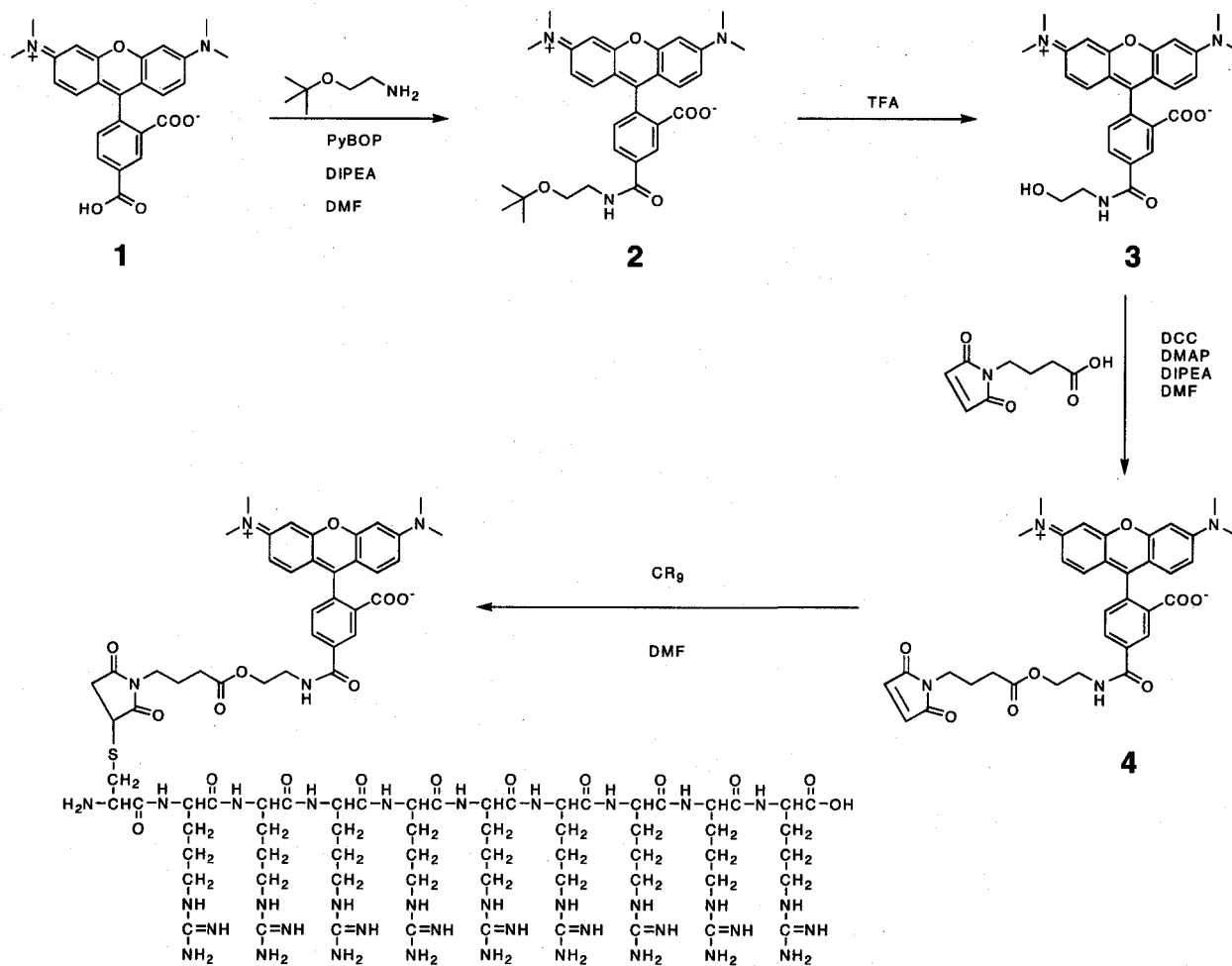
5-carboxytetramethylrhodamine (3) was formed in three steps from

5-carboxytetramethylrhodamine. This molecule was reacted with N-(3-

carboxy)maleimide to form a thiol reactive ester (4). This compound was coupled

to purified CR9 peptide to give an TMR-R₉ conjugated through a hydrolyzable

ester (5).



5

Figure AII-3. Release of TMR-R₉ and TMR-CR₉ from multilayer films. Silicon chips were dipped in solutions of either SPS or a peptide to form a multilayer film containing either the amide TMR-R₉ (solid line) or the ester TMR-CR₉ (dashed line). (A) The films were placed in an aqueous buffer, and release from the film was monitored at different time points by measuring total fluorescence of the aqueous solution and (B) the thickness of the chips by elipsometry. Figure courtesy of Christopher M. Jewell.

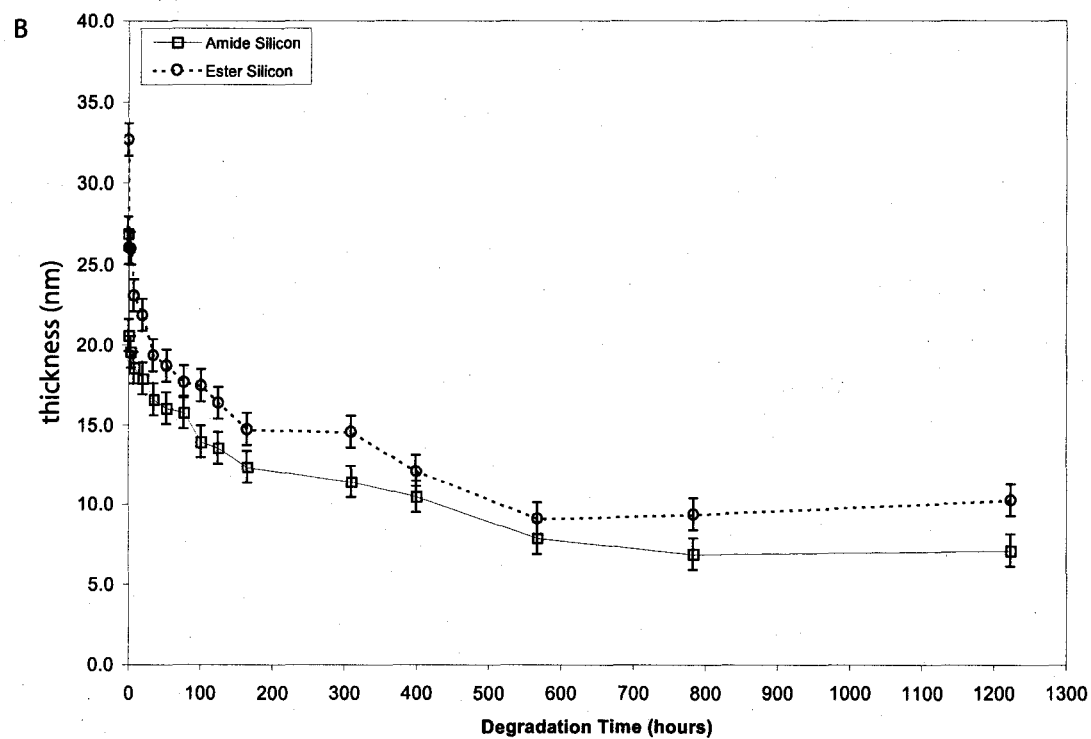
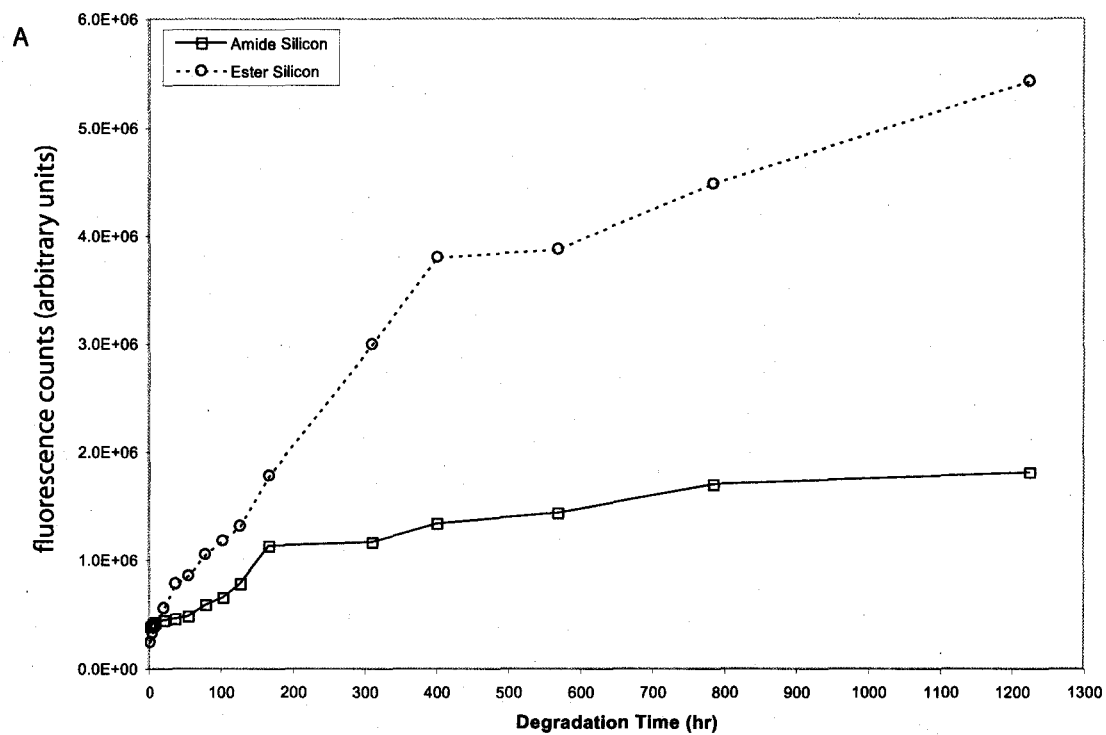


Figure AII-4. Improved synthetic scheme for TMR-R₉ amide and ester isosteres. TMR-derived alcohol (3) and amine (8) were coupled to the C-terminal carboxylate of Ac-R₉ peptide to give isosteric properties.

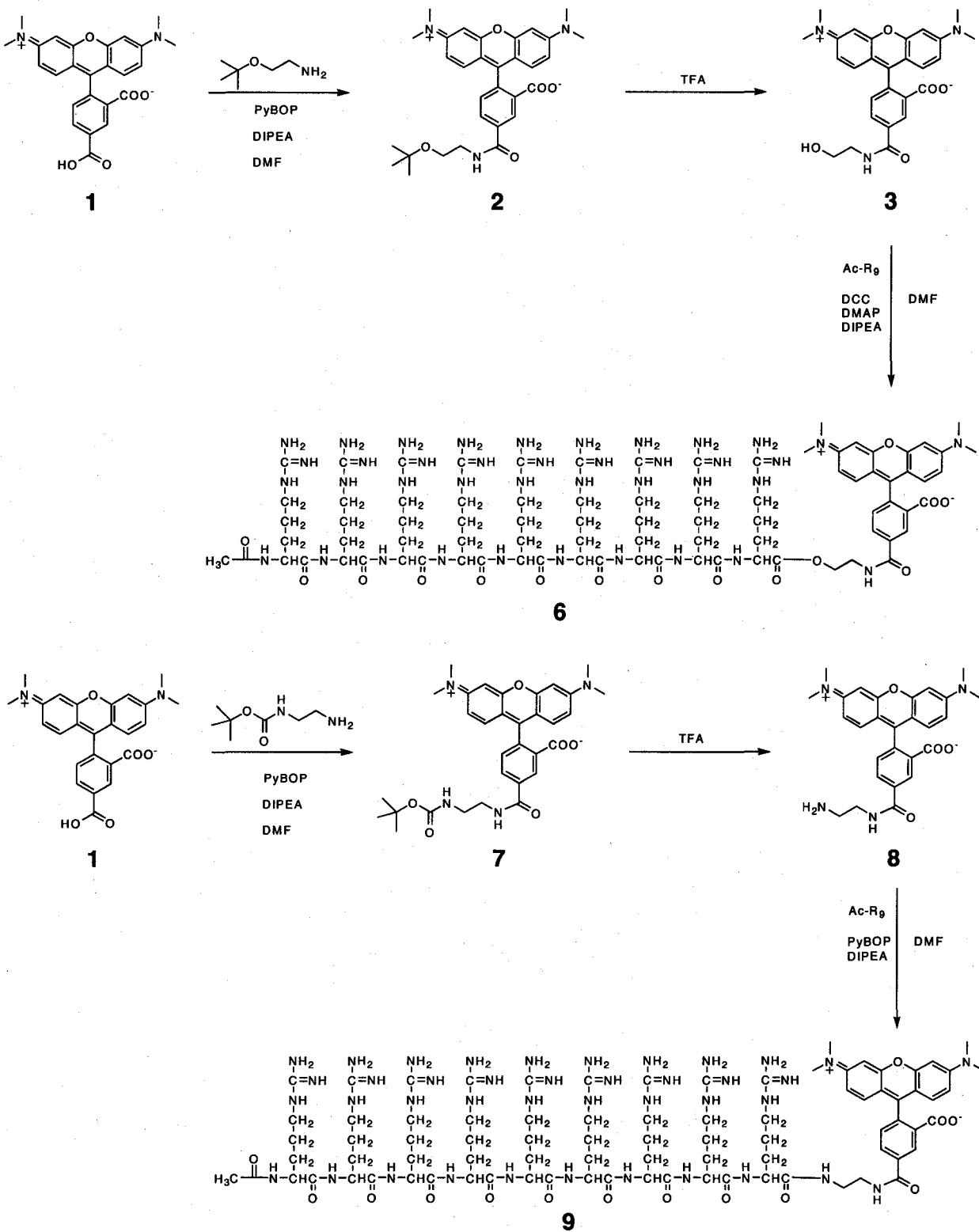


Figure AII-5. Synthesis and erosion of ribonuclease-containing films. F1-RNase A and F1-RNase A-R₉ were incorporated into multilayer films (top). The thickness of these films over time was monitored by ellipsometry (A). Release of fluorescein-labeled protein was monitored by measuring the total fluorescence in solution at different time points (B). Figure courtesy of Christopher M. Jewell.

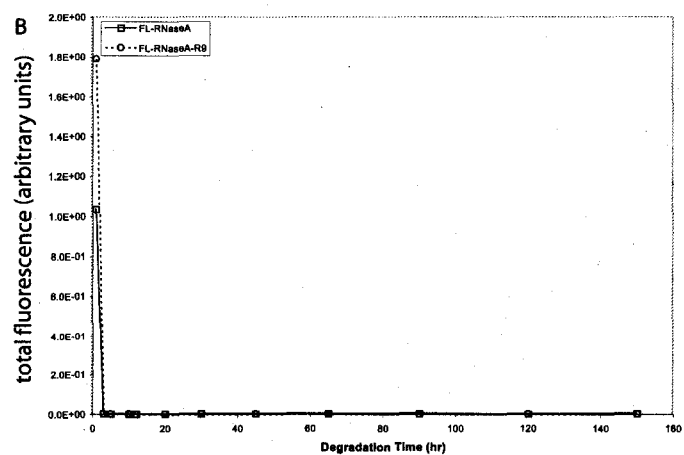
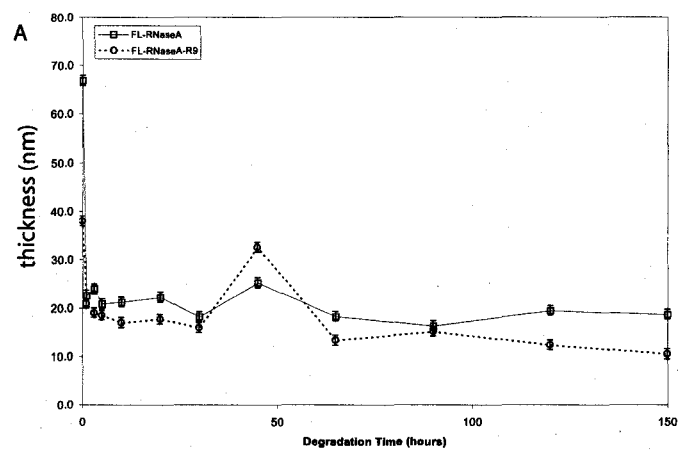
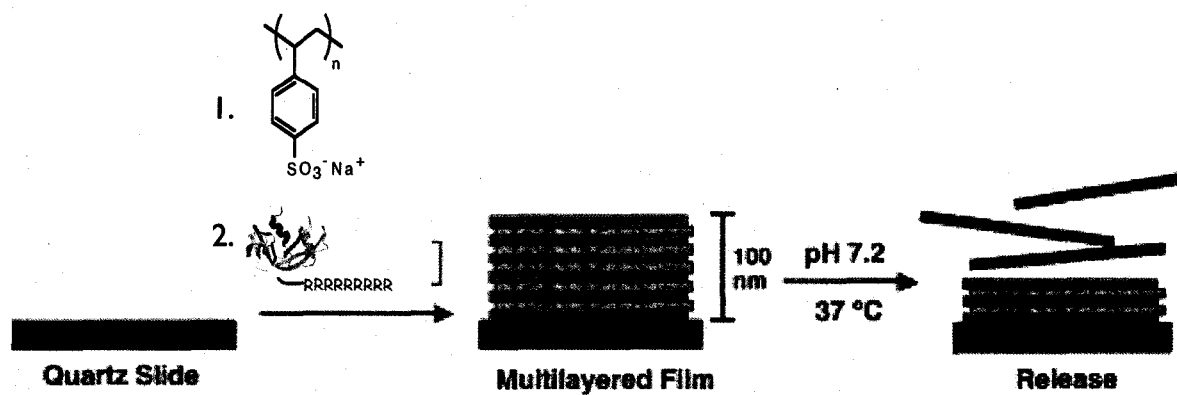
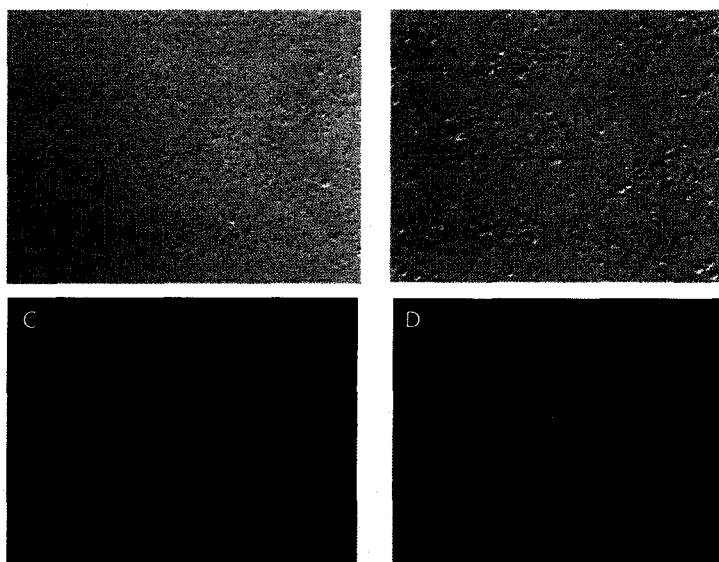
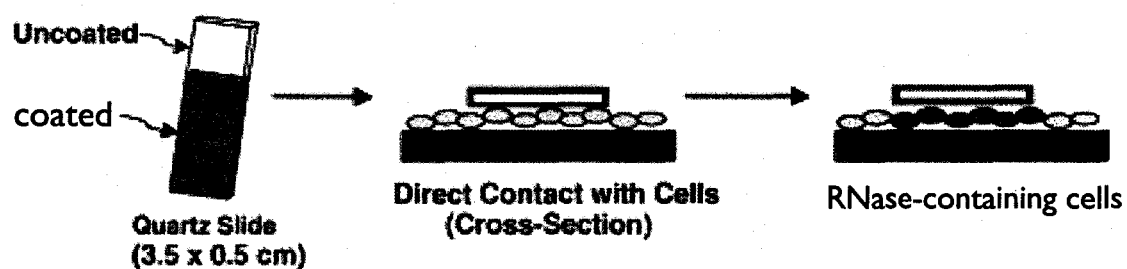
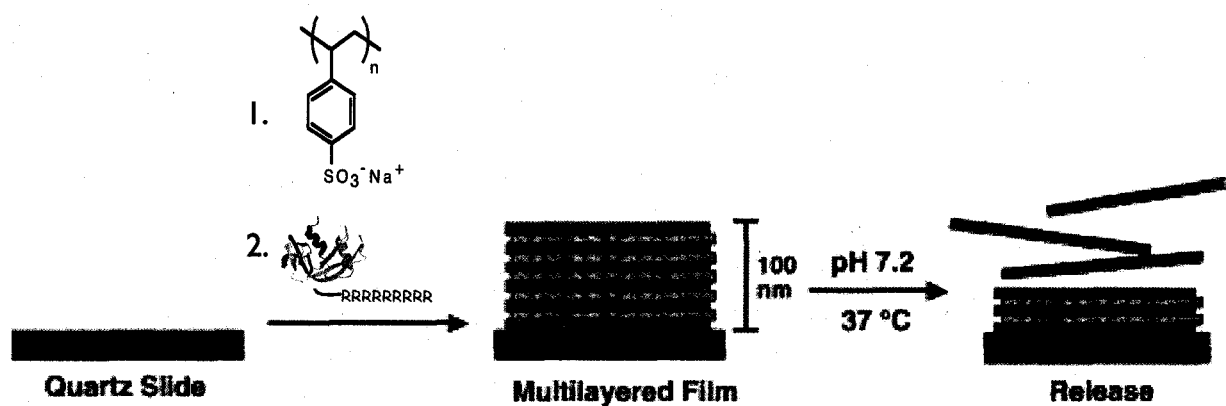


Figure AII-6. Release of RNase A films into COS-7 cells. (Top) Films containing either FI-RNase A or FI-RNase A-R₉ were synthesized and placed on top of COS-7 cells for 4 h at 37 °C. Release of protein from films and subsequent uptake into cells was monitored by microscopy (A, B) Bright field images of COS-7 cells with FI-RNase A (A) or FI-RNase A-R₉ (B) films. (C,D) Corresponding fluorescence images for FI-RNase A and FI-RNase A-R₉ respectively. Images courtesy of Christopher M. Jewell.



References

- Ames, B.N. 1966. Assay of inorganic phosphate, total phosphate, and phosphatases. *Methods Enzymol.* 8:115-118.
- Anghileri, L.J., Heidbreder, M., Mathes, R. 1976. Accumulation of ^{57}Co -poly-L-lysine by tumors: an effect of the tumor electrical charge. *J. Nucl. Biol. Med.* 20(2):79-83.
- Antignani, A., Naddeo, M., Cubellis, M.V., Russo, A., D'Alessio, G. 2001. Antitumor action of seminal ribonuclease, its dimeric structure, and its resistance to the cytosolic ribonuclease inhibitor. *Biochemistry* 40(12):3492-3496.
- Arnold, U., Hinderaker, M.P., Raines, R.T. 2002. Semisynthesis of ribonuclease A using intein-mediated protein ligation. *Sci. World J.* 2:1823-1827.
- Backer, M.V., Aloise, R., Przekop, K., Stoletov, K., Backer, J.M. 2002. Molecular vehicles for targeted drug delivery. *Bioconjug. Chem.* 13(3):462-467.
- Banting, F., Best, C. 1922. The Internal Secretions of the Pancreas. *J. Lab. Clin. Med.* 7(5):1-16.
- Bass, P.S., Drake, A.F., Wang, Y., Thomas, J.H., Davies, D.R. 1990. Cationization of bovine serum albumin alters its conformation as well as its charge. *Lab. Invest.* 62(2):185-188.
- Beerens, A.M., Al Hadithy, A.F., Rots, M.G., Haisma, H.J. 2003. Protein transduction domains and their utility in gene therapy. *Curr. Gene Ther.* 3(5):486-494.
- Belitsky, J.M., Leslie, S.J., Arora, P.S., Beerman, T.A., Dervan, P.B. 2002. Cellular uptake of N-methylpyrrole/N-methylimidazole polyamide-dye conjugates. *Bioorg. Med. Chem.* 10(10):3313-3318.
- Belting, M. 2003. Heparan sulfate proteoglycan as a plasma membrane carrier. *Trends Biochem. Sci.* 28(3):145-151.
- Bianchi, E., Pessi, A. 2002. Inhibiting viral proteases: challenges and opportunities. *Biopolymers* 66(2):101-114.

- Bilozur, M.E., Biswas, C. 1990. Identification and characterization of heparan sulfate-binding proteins from human lung carcinoma cells. *J. Biol. Chem.* 265:19697-19703.
- Bjellqvist, B., Basse, B., Olsen, E., Celis, J.E. 1994. Reference points for comparisons of two-dimensional maps of proteins from different human cell types defined in a pH scale where isoelectric points correlate with polypeptide compositions. *Electrophoresis* 15(3-4):529-539.
- Bjellqvist, B., Hughes, G.J., Pasquali, C., Paquet, N., Ravier, F., Sanchez, J.C., Frutiger, S., Hochstrasser, D. 1993. The focusing positions of polypeptides in immobilized pH gradients can be predicted from their amino acid sequences. *Electrophoresis* 14(10):1023-1031.
- Blasberg, R.G., Tjuvajev, J.G. 2003. Molecular-genetic imaging: current and future perspectives. *J. Clin. Invest.* 111(11):1620-1629.
- Brady, J., Kashanchi, F. 2005. Tat gets the "green" light on transcription initiation. *Retrovirology* 2(1):69.
- Bretscher, L.E., Abel, R.L., Raines, R.T. 2000. A ribonuclease A variant with low catalytic activity but high cytotoxicity. *J. Biol. Chem.* 275:9893-9896.
- Brooks, H., Lebleu, B., Vives, E. 2005. Tat peptide-mediated cellular delivery: back to basics. *Adv. Drug Deliv. Rev.* 57(4):559-577.
- Chandran, S.S., Dickson, K.A., Raines, R.T. 2005. Latent fluorophore based on the trimethyl lock. *J. Am. Chem. Soc.* 127(6):1652-1653.
- Chico, D.E., Given, R.L., Miller, B.T. 2003. Binding of cationic cell-permeable peptides to plastic and glass. *Peptides* 24(1):3-9.
- Chirino, A.J., Ary, M.L., Marshall, S.A. 2004. Minimizing the immunogenicity of protein therapeutics. *Drug Discov. Today* 9(2):82-90.
- Chudakov, D.M., Lukyanov, S., Lukyanov, K.A. 2005. Fluorescent proteins as a toolkit for in vivo imaging. *Trends Biotechnol.* 23(12):605-613.

- Coeytaux, E., Coulaud, D., Le Cam, E., Danos, O., Kichler, A. 2003. The cationic amphipathic α -helix of HIV-1 viral protein R (Vpr) binds to nucleic acids, permeabilizes membranes, and efficiently transfects cells. *J. Biol. Chem.* 278(20):18110-18116.
- Cordingley, M.G., LaFemina, R.L., Callahan, P.L., Condra, J.H., Sardana, V.V., Graham, D.J., Nguyen, T.M., LeGrow, K., Gotlib, L., Schlabach, A.J., et al. 1990. Sequence-specific interaction of Tat protein and Tat peptides with the transactivation-responsive sequence element of human immunodeficiency virus type 1 in vitro. *Proc. Natl. Acad. Sci. U.S.A.* 87(22):8985-8989.
- Cormack, B.P., Valdivia, R.H., Falkow, S. 1996. FACS-optimized mutants of the green fluorescent protein (GFP). *Gene* 173(1 Spec No):33-38.
- Cummings, R.T., McGovern, H.M., Zheng, S., Park, Y.W., Hermes, J.D. 1999. Use of a phosphotyrosine-antibody pair as a general detection method in homogeneous time-resolved fluorescence: application to human immunodeficiency viral protease. *Anal. Biochem.* 269(1):79-93.
- De Coupade, C., Fittipaldi, A., Chagnas, V., Michel, M., Carlier, S., Tasciotti, E., Darmon, A., Ravel, D., Kearsey, J., Giacca, M., Cailler, F. 2005. Novel human-derived cell-penetrating peptides for specific subcellular delivery of therapeutic biomolecules. *Biochem. J.* 390(Pt 2):407-418.
- Decher, G. 1997. Fuzzy Nanoassemblies: Toward Layered Polymeric Multicomposites. *Science* 277:1232-1237.
- delCardayré, S.B., Ribó, M., Yokel, E.M., Quirk, D.J., Rutter, W.J., Raines, R.T. 1995. Engineering ribonuclease A: Production, purification, and characterization of wild-type enzyme and mutants at Gln11. *Protein Eng.* 8:261-273.
- Denicourt, C., Dowdy, S.F. 2003. Protein transduction technology offers novel therapeutic approach for brain ischemia. *Trends Pharmacol. Sci.* 24(5):216-218.
- Derossi, D., Calvet, S., Trembleau, A., Brunissen, A., Chassaing, G., Prochiantz, A. 1996. Cell internalization of the third helix of the Antennapedia homeodomain is receptor-independent. *J. Biol. Chem.* 271(30):18188-18193.

- Derossi, D., Joliot, A.H., Chassaing, G., Prochiantz, A. 1994. The third helix of the Antennapedia homeodomain translocates through biological membranes. *J. Biol. Chem.* 269(14):10444-10450.
- Eguchi, A., Akuta, T., Okuyama, H., Senda, T., Yokoi, H., Inokuchi, H., Fujita, S., Hayakawa, T., Takeda, K., Hasegawa, M., Nakanishi, M. 2001. Protein transduction domain of HIV-1 Tat protein promotes efficient delivery of DNA into mammalian cells. *J. Biol. Chem.* 276(28):26204-26210.
- Elia, G., Silacci, M., Scheurer, S., Scheuermann, J., Neri, D. 2002. Affinity-capture reagents for protein arrays. *Trends Biotechnol.* 20(12 Suppl):S19-22.
- Elmqvist, A., Lindgren, M., Bartfai, T., Langel, U. 2001. VE-cadherin-derived cell-penetrating peptide, pVEC, with carrier functions. *Exp. Cell Res.* 269(2):237-244.
- Esko, J.D., Stewart, T.E., Taylor, W.H. 1985. Animal cell mutants defective in glycosaminoglycan biosynthesis. *Proc. Natl. Acad. Sci. U.S.A.* 82:3197-3201.
- Fawell, S., Seery, J., Daikh, Y., Moore, C., Chen, L.L., Pepinsky, B., Barsoum, J. 1994. Tat-mediated delivery of heterologous proteins into cells. *Proc. Natl. Acad. Sci. U.S.A.* 91(2):664-668.
- Fischer, P.M., Zhelev, N.Z., Wang, S., Melville, J.E., Fahraeus, R., Lane, D.P. 2000. Structure-activity relationship of truncated and substituted analogues of the intracellular delivery vector Penetratin. *J. Pept. Res.* 55(2):163-172.
- Fischer, R., Fotin-Mleczek, M., Hufnagel, H., Brock, R. 2005. Break on through to the other side - Biophysics and cell biology shed light on cell-penetrating peptides. *Chembiochem* 6(12):2126-2142.
- Fischer, R., Waizenegger, T., Kohler, K., Brock, R. 2002. A quantitative validation of fluorophore-labelled cell-permeable peptide conjugates: fluorophore and cargo dependence of import. *Biochim. Biophys. Acta* 1564(2):365-374.
- Fittipaldi, A., Giacca, M. 2005. Transcellular protein transduction using the Tat protein of HIV-1. *Adv. Drug Deliv. Rev.* 57(4):597-608.

- Ford, C.F., Suominen, I., Glatz, C.E. 1991. Fusion tails for the recovery and purification of recombinant proteins. *Protein Express. Purif.* 2:95-107.
- Fotin-Mleczek, M., Fischer, R., Brock, R. 2005. Endocytosis and cationic cell-penetrating peptides--a merger of concepts and methods. *Curr. Pharm. Des.* 11(28):3613-3628.
- Frankel, A.D., Pabo, C.O. 1988. Cellular uptake of the tat protein from human immunodeficiency virus. *Cell* 55(6):1189-1193.
- Fuchs, S.M., Raines, R.T. 2004. Pathway for polyarginine entry into mammalian cell. *Biochemistry* 43(9):2438-2444.
- Fuchs, S.M., Raines, R.T. 2005. Polyarginine as a multifunctional fusion tag. *Protein Sci.* 14(6):1538-1544.
- Futaki, S. 2005. Membrane-permeable arginine-rich peptides and the translocation mechanisms. *Adv. Drug Deliv. Rev.* 57(4):547-558.
- Futaki, S., Nakase, I., Suzuki, T., Youjun, Z., Sugiura, Y. 2002. Translocation of branched-chain arginine peptides through cell membranes: Flexibility in the spatial disposition of positive charges in membrane-permeable peptides. *Biochemistry* 41(25):7925-7930.
- Futami, J., Kitazoe, M., Maeda, T., Nukui, E., Sakaguchi, M., Kosaka, J., Miyazaki, M., Kosaka, M., Tada, H., Seno, M., Sasaki, J., Huh, N.H., Namba, M., Yamada, H. 2005. Intracellular delivery of proteins into mammalian living cells by polyethylenimine-cationization. *J. Biosci. Bioeng.* 99(2):95-103.
- Futami, J., Maeda, T., Kitazoe, M., Nukui, E., Tada, H., Seno, M., Kosaka, M., Yamada, H. 2001. Preparation of potent cytotoxic ribonucleases by cationization: Enhanced cellular uptake and decreased interaction with ribonuclease inhibitor by chemical modification of carboxyl groups. *Biochemistry* 26:7518-7524.
- Futami, J., Nukui, K., Maeda, T., Kosaka, M., Tada, H., Seno, M., Yamada, H. 2002. Optimum modification for the highest cytotoxicity of cationized ribonuclease. *J. Biochem. (Tokyo)* 132:223-228.

- Gleizes, P.E., Noaillac-Depeyre, J., Amalric, F., Gas, N. 1995. Basic fibroblast growth factor (FGF-2) internalization through the heparan sulfate proteoglycans-mediated pathway: an ultrastructural approach. *Eur. J. Cell Biol.* 66(1):47-59.
- Goncalves, E., Kitas, E., Seelig, J. 2005. Binding of oligoarginine to membrane lipids and heparan sulfate: structural and thermodynamic characterization of a cell-penetrating peptide. *Biochemistry* 44(7):2692-2702.
- Green, I., Christison, R., Voyce, C.J., Bundell, K.R., Lindsay, M.A. 2003. Protein transduction domains: Are they delivering? *Trends Pharmacol. Sci.* 24(5):213-215.
- Green, M., Loewenstein, P.M. 1988. Autonomous functional domains of chemically synthesized human immunodeficiency virus tat trans-activator protein. *Cell* 55(6):1179-1788.
- Griesbeck, O. 2004. Fluorescent proteins as sensors for cellular functions. *Curr. Opin. Neurobiol.* 14(5):636-641.
- Gulnik, S., Erickson, J.W., Xie, D. 2000. HIV protease: enzyme function and drug resistance. *Vitam. Horm.* 58:213-256.
- Gupta, B., Levchenko, T.S., Torchilin, V.P. 2005. Intracellular delivery of large molecules and small particles by cell-penetrating proteins and peptides. *Adv. Drug Deliv. Rev.* 57(4):637-651.
- Haas, J., Park, E.C., Seed, B. 1996. Codon usage limitation in the expression of HIV-1 envelope glycoprotein. *Curr. Biol.* 6(3):315-324.
- Hacker, U., Nybakken, K., Perrimon, N. 2005. Heparan sulphate proteoglycans: the sweet side of development. *Nat. Rev. Mol. Cell. Biol.* 6(7):530-541.
- Haigis, M.C., Kurten, E.L., Raines, R.T. 2003. Ribonuclease inhibitor as an intracellular sentry. *Nucleic Acids Res.* 31:1024-1032.
- Haigis, M.C., Raines, R.T. 2003. Secretory ribonucleases are internalized by a dynamin-independent endocytic pathway. *J. Cell Sci.* 116:313-324.

- Hakansson, S., Jacobs, A., Caffrey, M. 2001. Heparin binding by the HIV-1 tat protein transduction domain. *Protein Sci.* 10(10):2138-2139.
- Hallbrink, M., Floren, A., Elmquist, A., Pooga, M., Bartfai, T., Langel, U. 2001. Cargo delivery kinetics of cell-penetrating peptides. *Biochem. Biophys. Acta.* 1515(2):101-109.
- Hanson, G.T., Aggeler, R., Oglesbee, D., Cannon, M., Capaldi, R.A., Tsien, R.Y., Remington, S.J. 2004. Investigating mitochondrial redox potential with redox-sensitive green fluorescent protein indicators. *J. Biol. Chem.* 279(13):13044-13053.
- Hanson, G.T., McAnaney, T.B., Park, E.S., Rendell, M.E., Yarbrough, D.K., Chu, S., Xi, L., Boxer, S.G., Montrose, M.H., Remington, S.J. 2002. Green fluorescent protein variants as ratiometric dual emission pH sensors. 1. Structural characterization and preliminary application. *Biochemistry* 41(52):15477-15488.
- Hart, S.L. 2005. Lipid carriers for gene therapy. *Curr. Drug Deliv.* 2(4):423-428.
- Hashimoto, O., Nakamura, T., Shoji, H., Shimasaki, S., Hayashi, Y., Sugino, H. 1997. A novel role of follistatin, an activin-binding protein, in the inhibition of activin action in rat pituitary cells. Endocytotic degradation of activin and its acceleration by follistatin associated with cell-surface heparan sulfate. *J. Biol. Chem.* 272(21):13835-13842.
- Hearn, M.T., Acosta, D. 2001. Applications of novel affinity cassette methods: use of peptide fusion handles for the purification of recombinant proteins. *J. Mol. Recognit.* 14(6):323-369.
- Hermans, J., Jr., Scheraga, H.A. 1961. Structural studies of ribonuclease. V. Reversible change of configuration. *J. Am. Chem. Soc.* 83:3283-3292.
- Ho, A., Schwarze, S.R., Mermelstein, S.J., Waksman, G., Dowdy, S.F. 2001. Synthetic protein transduction domains: enhanced transduction potential in vitro and in vivo. *Cancer. Res.* 61(2):474-477.
- Hoffman, R.M. 2005. The multiple uses of fluorescent proteins to visualize cancer in vivo. *Nat. Rev. Cancer* 5(10):796-806.

- Hu, K., Clement, J.F., Abrahamyan, L., Strebel, K., Bouvier, M., Kleiman, L., Moulard, A.J. 2005. A human immunodeficiency virus type 1 protease biosensor assay using bioluminescence resonance energy transfer. *J. Virol. Methods* 128(1-2):93-103.
- Huang, Y., Kong, W.P., Nabel, G.J. 2001. Human immunodeficiency virus type 1-specific immunity after genetic immunization is enhanced by modification of Gag and Pol expression. *J. Virol.* 75(10):4947-4951.
- Huang, Y., Wang, J., Shalom, A., Li, Z., Khorchid, A., Wainberg, M.A., Kleiman, L. 1997. Primer tRNA³Lys on the viral genome exists in unextended and two-base extended forms within mature human immunodeficiency virus type 1. *J. Virol.* 71(1):726-728.
- Iozzo, R.V. 2005. Basement membrane proteoglycans: from cellar to ceiling. *Nat. Rev. Mol. Cell. Biol.* 6(8):646-656.
- James, A.M., Ambrose, E.J., Lowick, J.H. 1956. Differences between the electrical charge carried by normal and homologous tumour cells. *Nature* 177(4508):576-577.
- Jewell, C.M., Zhang, J., Fredin, N.J., Lynn, D.M. 2005. Multilayered polyelectrolyte films promote the direct and localized delivery of DNA to cells. *J. Cont. Rel.* 106(1-2):214-223.
- Johannes, L., Lamaze, C. 2002. Clathrin-dependent or not: is it still the question? *Traffic* 3(7):443-451.
- Kabouridis, P.S. 2003. Biological applications of protein transduction technology. *Trends Biotechnol.* 21(11):498-503.
- Kabsch, W. 1988. Evaluation of single-crystal x-ray diffraction data from a position-sensitive detector. *J. Appl. Crystallogr.* 21:916-924.
- Kaplan, I.M., Wadia, J.S., Dowdy, S.F. 2005. Cationic TAT peptide transduction domain enters cells by macropinocytosis. *J. Cont. Rel.* 102(1):247-253.
- Kelemen, B.R., Klink, T.A., Behlke, M.A., Eubanks, S.R., Leland, P.A., Raines, R.T. 1999. Hypersensitive substrate for ribonucleases. *Nucleic Acids Res.* 27:3696-3701.

- Kim, J.-S., Raines, R.T. 1993. Ribonuclease S-peptide as a carrier in fusion proteins. *Protein Sci.* 2:348-356.
- Klugherz, B.D., Jones, P.L., Cui, X., Chen, W., Meneveau, N.F., DeFelice, S., Connolly, J., Wilensky, R.L., Levy, R.J. 2000. Gene delivery from a DNA controlled-release stent in porcine coronary arteries. *Nat. Biotechnol.* 18(11):1181-1184.
- Knowles, J.R. 1987. Tinkering with enzymes: What are we learning? *Science* 236:1252-1258.
- Kobe, B., Deisenhofer, J. 1993. Crystal structure of porcine ribonuclease inhibitor, a protein with leucine-rich repeats. *Nature* 366:751-756.
- Koch, A.M., Reynolds, F., Kircher, M.F., Merkle, H.P., Weissleder, R., Josephson, L. 2003. Uptake and metabolism of a dual fluorochrome Tat-nanoparticle in HeLa cells. *Bioconjug. Chem.* 14(6):1115-1121.
- Kodadek, T. 2001. Protein microarrays: prospects and problems. *Chem. Biol.* 8(2):105-115.
- Kornguth, S.E., Stahmann, M.A., Anderson, J.W. 1961. Effect of polylysine on the cytology of Ehrlich ascites tumor cells. *Exp. Cell Res.* 24:484-494.
- Kothandaraman, S., Hebert, M.C., Raines, R.T., Nibert, M.L. 1998. No role for pepstatin-A-sensitive acidic proteinase in reovirus infections of L or MDCK cells. *Virology* 251:264-272.
- Leamon, C.P., Low, P.S. 1991. Delivery of macromolecules into living cells: A method that exploits folate receptor endocytosis. *Proc. Natl. Acad. Sci. U.S.A.* 88:5572-5576.
- Leamon, C.P., Low, P.S. 1993. Membrane folate-binding proteins are responsible for folate-protein conjugate endocytosis into cultured cells. *Biochem. J.* 291:855-860.
- Leifert, J.A., Lindsay Whitton, J. 2003. "Translocatory proteins" and "protein transduction domains": A critical analysis of their biological effects and underlying mechanisms. *Mol. Ther.* 8:13-20.

- Leifert, J.A., Whitton, J.L. 2003. "Translocatory proteins" and "protein transduction domains": a critical analysis of their biological effects and the underlying mechanisms. *Mol. Ther.* 8(1):13-20.
- Leland, P.A., Raines, R.T. 2001. Cancer chemotherapy—ribonucleases to the rescue. *Chem. Biol.* 8:405-413.
- Leland, P.A., Schultz, L.W., Kim, B.-M., Raines, R.T. 1998. Ribonuclease A variants with potent cytotoxic activity. *Proc. Natl. Acad. Sci. U.S.A.* 98:10407-10412.
- Leland, P.A., Staniszewski, K.E., Kim, B.-M., Raines, R.T. 2001. Endowing human pancreatic ribonuclease with toxicity for cancer cells. *J. Biol. Chem.* 276:43095-43102.
- Levinson, P.D. 2003. Eighty years of insulin therapy: 1922-2002. *Med. Health R. I.* 86(4):101-106.
- Lidholt, K., Weinke, J.L., Kiser, C.S., Lugemwa, F.N., Bame, K.J., Cheifetz, S., Massague, J., Lindahl, U., Esko, J.D. 1992. A single mutation affects both N-acetylglucosaminyltransferase and glucuronosyltransferase activities in a Chinese hamster ovary cell mutant defective in heparan sulfate biosynthesis. *Proc. Natl. Acad. Sci. U.S.A.* 89:2267-2271.
- Lilie, H. 2003. Designer proteins in biotechnology. International Titisee Conference on protein design at the crossroads of biotechnology, chemistry and evolution. *EMBO Rep.* 4(4):346-351.
- Lindsten, K., Uhlikova, T., Konvalinka, J., Masucci, M.G., Dantuma, N.P. 2001. Cell-based fluorescence assay for human immunodeficiency virus type 1 protease activity. *Antimicrob. Agents Chemother.* 45(9):2616-2622.
- Lu, Y., Low, P.S. 2002. Folate-mediated delivery of macromolecular anticancer therapeutic agents. *Adv. Drug Deliv. Rev.* 54(5):675-693.
- Lu, Y., Low, P.S. 2003. Targeted immunotherapy of cancer: development of antibody-induced cellular immunity. *J. Pharm. Pharmacol.* 55(2):163-167.

- Lu, Y., Segal, E., Leamon, C.P., Low, P.S. 2004. Folate receptor-targeted immunotherapy of cancer: mechanism and therapeutic potential. *Adv. Drug Deliv. Rev.* 56(8):1161-1176.
- Lundberg, M., Johansson, M. 2002. Positively charged DNA-binding proteins cause apparent cell membrane translocation. *Biochem. Biophys. Res. Commun.* 29:367-371.
- Lundberg, M., Wikstrom, S., Johansson, M. 2003. Cell surface adherence and endocytosis of protein transduction domains. *Mol. Ther.* 8:143-150.
- Magden, J., Kaariainen, L., Ahola, T. 2005. Inhibitors of virus replication: recent developments and prospects. *Appl. Microbiol. Biotechnol.* 66(6):612-621.
- Magee, W.E., Miller, O.V. 1972. Liposomes containing antiviral antibody can protect cells from virus infection. *Nature* 235(5337):339-341.
- Magzoub, M., Pramanik, A., Graslund, A. 2005. Modeling the endosomal escape of cell-penetrating peptides: transmembrane pH gradient driven translocation across phospholipid bilayers. *Biochemistry* 44(45):14890-14897.
- Mai, J.C., Shen, H., Watkins, S.C., Cheng, T., Robbins, P.D. 2002. Efficiency of protein transduction is cell type-dependent and is enhanced by dextran sulfate. *J. Biol. Chem.* 277(33):30208-30218.
- Maiolo, J.R., Ferrer, M., Ottinger, E.A. 2005. Effects of cargo molecules on the cellular uptake of arginine-rich cell-penetrating peptides. *Biochim. Biophys. Acta* 1712(2):161-172.
- Mandel, R., Fasman, G.D. 1976. Chromatic models. Interactions between DNA and polypeptides containing L-lysine L-valine: circular dichroism and thermal denaturation studies. *Biochemistry* 15(14):3122-3130.
- Marafino, B.J., Jr., Pugsley, M.K. 2003. Commercial development considerations for biotechnology-derived therapeutics. *Cardiovasc. Toxicol.* 3(1):5-12.
- Matousek, J., Gotte, G., Poucková, P., Soucek, J., Slavík, T., Vottariello, F., Libonati, M. 2003a. Antitumor activity and other biological actions of oligomers of ribonuclease A. *J. Biol. Chem.* 278:23817-23822.

- Matousek, J., Soucek, J., Slavík, T., Tománek, M., Lee, J.E., Raines, R.T. 2003b. Comprehensive comparison of the cytotoxic activities of onconase and bovine seminal ribonuclease. *Comp. Biochem. Physiol.*:In Press.
- McKenzie, E., Young, K., Hircock, M., Bennett, J., Bhaman, M., Felix, R., Turner, P., Stamps, A., McMillan, D., Saville, G., Ng, S., Mason, S., Snell, D., Schofield, D., Gong, H., Townsend, R., Gallagher, J., Page, M., Parekh, R., Stubberfield, C. 2003. Biochemical characterization of the active heterodimer form of human heparanase (Hpa1) protein expressed in insect cells. *Biochem. J.* 373:423-435.
- Medina, M.L., Chapman, B.S., Bolender, J.P., Plesniak, L.A. 2002. Transient vesicle leakage initiated by a synthetic apoptotic peptide derived from the death domain of neurotrophin receptor, p75NTR. *J. Pept. Res.* 59(4):149-158.
- Mendelsohn, J.D., Yang, S.Y., Hiller, J., Hochbaum, A.I., Rubner, M.F. 2003. Rational design of cytophilic and cytophobic polyelectrolyte multilayer thin films. *Biomacromolecules* 4(1):96-106.
- Merilainen, O., Hakkarainen, T., Wahlfors, T., Pellinen, R., Wahlfors, J. 2005. HIV-1 TAT protein transduction domain mediates enhancement of enzyme prodrug cancer gene therapy in vitro: a study with TAT-TK-GFP triple fusion construct. *Int. J. Oncol.* 27(1):203-208.
- Mislick, K.A., Baldeschwieler, J.D. 1996. Evidence for the role of proteoglycans in cation-mediated gene transfer. *Proc. Natl. Acad. Sci. U.S.A.* 93(22):12349-12354.
- Mitchell, D.J., Kim, D.T., Steinman, L., Fathman, C.G., Rothbard, J.B. 2000. Polyarginine enters cells more efficiently than other polycationic homopolymers. *J. Pept. Res.* 56(5):318-325.
- Miyawaki, A. 2005. Innovations in the imaging of brain functions using fluorescent proteins. *Neuron* 48(2):189-199.
- Morris, M.C., Depollier, J., Mery, J., Heitz, F., Divita, G. 2001. A peptide carrier for the delivery of biologically active proteins into mammalian cells. *Nat. Biotechnol.* 19(12):1173-1176.

- Nilsson, J., Stahl, S., Lundeberg, J., Uhlen, M., Nygren, P.A. 1997. Affinity fusion strategies for detection, purification, and immobilization of recombinant proteins. *Protein Expr. Purif.* 11(1):1-16.
- Nishihara, M., Perret, F., Takeuchi, T., Futaki, S., Lazar, A.N., Coleman, A.W., Sakai, N., Matile, S. 2005. Arginine magic with new counterions up the sleeve. *Org. Biomol. Chem.* 3(9):1659-1669.
- Nock, S., Spudich, J.A., Wagner, P. 1997. Reversible, site-specific immobilization of polyarginine-tagged fusion proteins on mica surfaces. *FEBS Lett.* 414(2):233-238.
- O'Keefe, D.O., Draper, R.K. 1985. Characterization of a transferrin-diphtheria toxin conjugate. *J. Biol. Chem.* 260(2):932-937.
- Ogawa, Y., Iwama, M., Ohgi, K., Tsuji, T., Irie, M., Itagaki, T., Kobayashi, H., Inokuchi, N. 2002. Effect of replacing the aspartic acid/glutamic acid residues of bullfrog sialic acid binding lectin with asparagine/glutamine and arginine on the inhibition of cell proliferation in murine leukemia P388 cells. *Biol. Pharm. Bull.* 25(6):722-727.
- Ormo, M., Cubitt, A.B., Kallio, K., Gross, L.A., Tsien, R.Y., Remington, S.J. 1996. Crystal structure of the *Aequorea victoria* green fluorescent protein. *Science* 273(5280):1392-1395.
- Pace, C.N. 1986. Determination and analysis of urea and guanidine hydrochloride denaturation curves. *Methods Enzymol.* 131:266-280.
- Pace, C.N., Alston, R.W., Shaw, K.L. 2000. Charge-charge interactions influence the denatured state ensemble and contribute to protein stability. *Protein Sci.* 9(7):1395-1398.
- Pace, C.N., Scholtz, J.M. 1997. Measuring the conformational stability of a protein. In *Protein structure*. Creighton TE, editor. Oxford University Press, New York. 299-321.
- Pardridge, W.M., Triguero, D., Buciak, J.L. 1990. Tissue Uptake of Immunoglobulin-G Is Greatly Enhanced Following Cationization of the Protein. *Clin. Res.* 38(1):A133-A133.

- Park, C.B., Yi, K.S., Matsuzaki, K., Kim, M.S., Kim, S.C. 2000. Structure-activity analysis of buforin II, a histone H2A-derived antimicrobial peptide: the proline hinge is responsible for the cell-penetrating ability of buforin II. *Proc. Natl. Acad. Sci. U.S.A.* 97(15):8245-8250.
- Patick, A.K., Potts, K.E. 1998. Protease inhibitors as antiviral agents. *Clin. Microbiol. Rev.* 11(4):614-627.
- Pokala, N., Handel, T.M. 2001. Review: protein design--where we were, where we are, where we're going. *J. Struct. Biol.* 134(2-3):269-281.
- Pooga, M., Kut, C., Kihlmark, M., Hallbrink, M., Fernaeus, S., Raid, R., Land, T., Hallberg, E., Bartfai, T., Langel, U. 2001. Cellular translocation of proteins by transportan. *FASEB J.* 15(8):1451-1453.
- Potocky, T.B., Menon, A.K., Gellman, S.H. 2003. Cytoplasmic and nuclear delivery of a TAT-derived peptide and a beta-peptide after endocytic uptake into HeLa cells. *J. Biol. Chem.* 278(50):50188-50194.
- Potocky, T.B., Menon, A.K., Gellman, S.H. 2005. Effects of conformational stability and geometry of guanidinium display on cell entry by beta-peptides. *J. Am. Chem. Soc.* 127(11):3686-3687.
- Prochiantz, A. 2000. Messenger proteins: Homeoproteins, TAT and others. *Curr. Opin. Cell Biol.* 12(4):400-406.
- Ragin, A.D., Morgan, R.A., Chmielewski, J. 2002. Cellular import mediated by nuclear localization signal peptide sequences. *Chem. Biol.* 9:943-948.
- Raines, R.T. 1998. Ribonuclease A. *Chem. Rev.* 98:1045-1065.
- Ramos, C.H., Baldwin, R.L. 2002. Sulfate anion stabilization of native ribonuclease A both by anion binding and by the Hofmeister effect. *Protein Sci.* 11(7):1771-1778.

- Richard, J.P., Melikov, K., Brooks, H., Prevot, P., Lebleu, B., Chernomordik, L.V. 2005. Cellular uptake of unconjugated TAT peptide involves clathrin-dependent endocytosis and heparan sulfate receptors. *J. Biol. Chem.* 280(15):15300-15306.
- Richard, J.P., Melikov, K., Vives, E., Ramos, C., Verbeure, B., Gait, M.J., Chernomordik, L.V., Lebleu, B. 2003. Cell-penetrating peptides. A reevaluation of the mechanism of cellular uptake. *J. Biol. Chem.* 278(1):585-590.
- Rijkers, G.T., Justement, L.B., Griffioen, A.W., Cambier, J.C. 1990. Improved method for measuring intracellular Ca^{++} with fluo-3. *Cytometry* 11(8):923-927.
- Rizzo, C.J., Korant, B.D. 1994. Genetic approaches designed to minimize cytotoxicity of retroviral protease. *Methods Enzymol.* 241:16-29.
- Roda, A., Pasini, P., Mirasoli, M., Michelini, E., Guardigli, M. 2004. Biotechnological applications of bioluminescence and chemiluminescence. *Trends Biotechnol.* 22(6):295-303.
- Roghani, M., Moscatelli, D. 1992. Basic fibroblast growth factor is internalized through both receptor-mediated and heparan sulfate-mediated mechanisms. *J. Biol. Chem.* 267(31):22156-22162.
- Rojas, M., Donahue, J.P., Tan, Z., Lin, Y.Z. 1998. Genetic engineering of proteins with cell membrane permeability. *Nat. Biotechnol.* 16(4):370-375.
- Rothbard, J.B., Jessop, T.C., Lewis, R.S., Murray, B.A., Wender, P.A. 2004. Role of membrane potential and hydrogen bonding in the mechanism of translocation of guanidinium-rich peptides into cells. *J. Am. Chem. Soc.* 126(31):9506-9507.
- Rothbard, J.B., Jessop, T.C., Wender, P.A. 2005. Adaptive translocation: the role of hydrogen bonding and membrane potential in the uptake of guanidinium-rich transporters into cells. *Adv. Drug Deliv. Rev.* 57(4):495-504.
- Rothbard, J.B., Kreider, E., VanDeusen, C.L., Wright, L., Wylie, B.L., Wender, P.A. 2002. Arginine-rich molecular transporters for drug delivery: Role of backbone spacing in cellular uptake. *J. Med. Chem.* 45:3612-3618.

- Rousselle, C., Clair, P., Lefauconnier, J.M., Kaczorek, M., Scherrmann, J.M., Temsamani, J. 2000. New advances in the transport of doxorubicin through the blood-brain barrier by a peptide vector-mediated strategy. *Mol. Pharmacol.* 57(4):679-686.
- Rozema, D.B., Ekena, K., Lewis, D.L., Loomis, A.G., Wolff, J.A. 2003. Endosomolysis by masking of a membrane-active agent (EMMA) for cytoplasmic release of macromolecules. *Bioconjug. Chem.* 14(1):51-57.
- Rueping, M., Mahajan, Y., Sauer, M., Seebach, D. 2002. Cellular uptake studies with β -peptides. *Chembiochem* 3:257-259.
- Rutkoski, T.J., Kurten, E.L., Mitchell, J.C., Raines, R.T. 2005. Disruption of Shape-Complementarity Markers to Create Cytotoxic Variants of Ribonuclease A. *J. Mol. Biol.*
- Rybak, S.M., Saxena, S.K., Ackerman, E.J., Youle, R.J. 1991. Cytotoxic potential of ribonuclease and ribonuclease hybrid proteins. *J. Biol. Chem.* 266(31):21202-21207.
- Ryser, H.J. 1967a. A membrane effect of basic polymers dependent on molecular size. *Nature* 215(104):934-936.
- Ryser, H.J. 1967b. Studies on protein uptake by isolated tumor cells. 3. Apparent stimulations due to pH, hypertonicity, polycations, or dehydration and their relation to the enhanced penetration of infectious nucleic acids. *J. Cell Biol.* 32(3):737-750.
- Ryser, H.J. 1968. Uptake of protein by mammalian cells: an underdeveloped area. The penetration of foreign proteins into mammalian cells can be measured and their functions explored. *Science* 159(813):390-396.
- Ryser, H.J., Hancock, R. 1965. Histones and basic polyamino acids stimulate the uptake of albumin by tumor cells in culture. *Science* 150(695):501-503.
- Sadaie, M.R., Hager, G.L. 1994. Induction of developmentally programmed cell death and activation of HIV by sodium butyrate. *Virology* 202(1):513-518.
- Sakai, N., Matile, S. 2003. Anion-mediated transfer of polyarginine across liquid and bilayer membranes. *J. Am. Chem. Soc.* 125(47):14348-14356.

- San Antonio, J.D., Lander, A.D., Karnovsky, M.J., Slayter, H.S. 1994. Mapping the heparin-binding sites on type I collagen monomers and fibrils. *J. Cell Biol.* 125:1179-1188.
- Sasisekharan, R., Myette, J.R. 2003. The sweet science of glycobiology. *Am. Sci.* 91:432-441.
- Sasisekharan, R., Venkataraman, G. 2000. Heparin and heparan sulfate: Biosynthesis, structure and function. *Curr. Opin. Chem. Biol.* 4:626-631.
- Sassenfeld, H.M., Brewer, S.J. 1984. A Polypeptide Fusion Designed for the Purification of Recombinant Proteins. *Bio-Technol* 2(1):76-81.
- Schuler, C., Caruso, F. 2001. Decomposable hollow biopolymer-based capsules. *Biomacromolecules* 2(3):921-926.
- Schwarze, S.R., Dowdy, S.F. 2000. In vivo protein transduction: Intracellular delivery of biologically active proteins, compounds and DNA. *Trends Pharmacol. Sci.* 21(2):45-48.
- Schwarze, S.R., Ho, A., Vocero-Akbani, A., Dowdy, S.F. 1999a. In vivo protein transduction: Delivery of a biologically active protein into a mouse. *Science* 285:1569-1572.
- Schwarze, S.R., Ho, A., Vocero-Akbani, A., Dowdy, S.F. 1999b. In vivo protein transduction: Delivery of a biologically active protein into the mouse. *Science* 285(5433):1569-1572.
- Seyrek, E., Dubin, P.L., Tribet, C., Gamble, E.A. 2003. Ionic strength dependence of protein-polyelectrolyte interactions. *Biomacromolecules* 4(2):273-282.
- Shaw, K.L., Grimsley, G.R., Yakovlev, G.I., Makarov, A.A., Pace, C.N. 2001. The effect of net charge on the solubility, activity, and stability of ribonuclease Sa. *Protein Sci.* 10:1206-1215.
- Shen, W.C., Ryser, H.J. 1979. Poly (L-lysine) and poly (D-lysine) conjugates of methotrexate: different inhibitory effect on drug resistant cells. *Mol. Pharmacol.* 16(2):614-622.
- Shoeman, R.L., Kesselmier, C., Mothes, E., Honer, B., Traub, P. 1991. Non-viral cellular substrates for human immunodeficiency virus type 1 protease. *FEBS Lett.* 278(2):199-203.

- Silhol, M., Tyagi, M., Giacca, M., Lebleu, B., Vives, E. 2002. Different mechanisms for cellular internalization of the HIV-1 Tat-derived cell penetrating peptide and recombinant proteins fused to Tat. *Eur. J. Biochem.* 269(2):494-501.
- Smith, B.D., Soellner, M.B., Raines, R.T. 2003. Potent inhibition of ribonuclease A by oligo(vinylsulfonic acid). *J. Biol. Chem.* 278(23):20934-20938.
- Soellner, M.B., Dickson, K.A., Nilsson, B.L., Raines, R.T. 2003. Site-specific protein immobilization by Staudinger ligation. *J. Am. Chem. Soc.* 125(39):11790-11791.
- Spear, P.G. 2004. Herpes simplex virus: receptors and ligands for cell entry. *Cell. Microbiol.* 6(5):401-410.
- Sperinde, G.V., Nugent, M.A. 2000. Mechanisms of fibroblast growth factor 2 intracellular processing: A kinetic analysis of the role of heparan sulfate proteoglycans. *Biochemistry* 39(13):3788-3796.
- Stanger, O. 2002. Physiology of folic acid in health and disease. *Curr. Drug Metab.* 3(2):211-223.
- Stayton, P.S., El-Sayed, M.E., Murthy, N., Bulmus, V., Lackey, C., Cheung, C., Hoffman, A.S. 2005. 'Smart' delivery systems for biomolecular therapeutics. *Orthod. Craniofac. Res.* 8(3):219-225.
- Stepanenko, O.V., Verkhusha, V.V., Kazakov, V.I., Shavlovsky, M.M., Kuznetsova, I.M., Uversky, V.N., Turoverov, K.K. 2004. Comparative studies on the structure and stability of fluorescent proteins EGFP, zFP506, mRFP1, "dimer2", and DsRed1. *Biochemistry* 43(47):14913-14923.
- Stevens, R.C. 2000. Design of high-throughput methods of protein production for structural biology. *Struct. Fold. Des.* 15:R177-185.
- Sugino, H., Ugiro, K., Hashimoto, O., Shoji, H., Nakamura, T. 1997. Follistatin and its role as an activin-binding protein. *J. Med. Invest.* 44(1-2):1-14.

- Sukhishvili, S.A., Chen, Y., Muller, J.D., Gratton, E., Schweizer, K.S., Granick, S. 2000. Materials science. Diffusion of a polymer 'pancake'. *Nature* 406(6792):146.
- Suzuki, M., Ito, Y., Savage, H.E., Husimi, Y., Douglas, K.T. 2004. Protease-sensitive signalling by chemically engineered intramolecular fluorescent resonance energy transfer mutants of green fluorescent protein. *Biochim. Biophys. Acta* 1679(3):222-229.
- Suzuki, M., Saxena, S.K., Boix, E., Prill, R.J., Vasandani, V.M., Ladner, J.E., Sung, C., Youle, R.J. 1999. Engineering receptor-mediated cytotoxicity into human ribonucleases by steric blockage of inhibitor interaction. *Nat. Biotechnol.* 17:265-270.
- Suzuki, T., Futaki, S., Niwa, M., Tanaka, S., Ueda, K., Sugiura, Y. 2002. Possible existence of common internalization mechanisms among arginine-rich peptides. *J. Biol. Chem.* 277(4):2437-2443.
- Sweeney, R.Y., Kelemen, B.R., Woycechowsky, K.J., Raines, R.T. 2000. A highly active immobilized ribonuclease. *Anal. Biochem.* 286:312-314.
- Tahtaoui, C., Guillier, F., Klotz, P., Galzi, J.L., Hibert, M., Ilien, B. 2005. On the use of nonfluorescent dye labeled ligands in FRET-based receptor binding studies. *J. Med. Chem.* 48(24):7847-7859.
- Tanford, C. 1968. Protein denaturation. *Adv. Protein Chem.* 23:121-282.
- Tang, L., Persky, A.M., Hochhaus, G., Meibohm, B. 2004. Pharmacokinetic aspects of biotechnology products. *J. Pharm. Sci.* 93(9):2184-2204.
- Thierry, A.R., Vives, E., Richard, J.P., Prevot, P., Martinand-Mari, C., Robbins, I., Lebleu, B. 2003. Cellular uptake and intracellular fate of antisense oligonucleotides. *Curr. Opin. Mol. Ther.* 5(2):133-138.
- Thierry, B., Kujawa, P., Tkaczyk, C., Winnik, F.M., Bilodeau, L., Tabrizian, M. 2005. Delivery platform for hydrophobic drugs: prodrug approach combined with self-assembled multilayers. *J. Am. Chem. Soc.* 127(6):1626-1627.

- Thoren, P.E., Persson, D., Isakson, P., Goksor, M., Onfelt, A., Norden, B. 2003. Uptake of analogs of penetratin, Tat(48-60) and oligoarginine in live cells. *Biochem. Biophys. Res. Commun.* 307(1):100-107.
- Thoren, P.E., Persson, D., Karlsson, M., Norden, B. 2000. The Antennapedia peptide penetratin translocates across lipid bilayers—the first direct observation. *FEBS Lett.* 482(3):265-268.
- Triguero, D., Buciak, J., Yang, J., Pardridge, W.M. 1989. Cationization of Immunoglobulin-G (Igg) as a New Strategy for Enhanced Igg Delivery through the Blood-Brain-Barrier. *Clin. Res.* 37(1):A140-A140.
- Tsien, R.Y. 1998. The green fluorescent protein. *Annu. Rev. Biochem.* 67:509-544.
- Tyagi, M., Rusnati, M., Presta, M., Giacca, M. 2001. Internalization of HIV-1 tat requires cell surface heparan sulfate proteoglycans. *J. Biol. Chem.* 276(5):3254-3261.
- Ui, N. 1971. Isoelectric points and conformation of proteins. I. Effect of urea on the behavior of some proteins in isoelectric focusing. *Biochim. Biophys. Acta* 229:567-581.
- Umezawa, N., Gelman, M.A., Haigis, M.C., Raines, R.T., Gellman, S.H. 2002. Translocation of a β -peptide across cell membranes. *J. Am. Chem. Soc.* 124(3):368-369.
- Varki, A., Cummings, R., Esko, J., Freeze, H., Hart, G., Marth, J. 1999. Essentials of Glycobiology. Cold Spring Harbor Laboratory Press, New York.
- Vazquez, E., Dewitt, D.M., Hammond, P.T., Lynn, D.M. 2002. Construction of hydrolytically-degradable thin films via layer-by-layer deposition of degradable polyelectrolytes. *J. Am. Chem. Soc.* 124(47):13992-13993.
- Vendeville, A., Rayne, F., Bonhoure, A., Bettache, N., Montcourrier, P., Beaumelle, B. 2004. HIV-1 Tat enters T cells using coated pits before translocating from acidified endosomes and eliciting biological responses. *Mol. Biol. Cell* 15(5):2347-2360.

- Verkhusha, V.V., Kuznetsova, I.M., Stepanenko, O.V., Zarausky, A.G., Shavlovsky, M.M., Turoverov, K.K., Uversky, V.N. 2003. High stability of Discosoma DsRed as compared to Aequorea EGFP. *Biochemistry* 42(26):7879-7884.
- Vives, E., Brodin, P., Lebleu, B. 1997. A truncated HIV-1 Tat protein basic domain rapidly translocates through the plasma membrane and accumulates in the cell nucleus. *J. Biol. Chem.* 272(25):16010-16017.
- Vives, E., Richard, J.P., Rispal, C., Lebleu, B. 2003. TAT peptide internalization: Seeking the mechanism of entry. *Curr. Protein Pept. Sci.* 4(2):125-132.
- Vocero-Akbani, A., Chellaiah, M.A., Hruska, K.A., Dowdy, S.F. 2001. Protein transduction: delivery of Tat-GTPase fusion proteins into mammalian cells. *Methods Enzymol.* 332:36-49.
- Vocero-Akbani, A., Lissy, N.A., Dowdy, S.F. 2000. Transduction of full-length Tat fusion proteins directly into mammalian cells: analysis of T cell receptor activation-induced cell death. *Methods Enzymol.* 322:508-521.
- Wade, D., Boman, A., Wahlin, B., Drain, C.M., Andreu, D., Boman, H.G., Merrifield, R.B. 1990. All-D amino acid-containing channel-forming antibiotic peptides. *Proc. Natl. Acad. Sci. U.S.A.* 87(12):4761-4765.
- Wadia, J.S., Dowdy, S.F. 2002. Protein transduction technology. *Curr. Opin. Biotechnol.* 13(1):52-56.
- Wadia, J.S., Dowdy, S.F. 2005. Transmembrane delivery of protein and peptide drugs by TAT-mediated transduction in the treatment of cancer. *Adv. Drug Deliv. Rev.* 57(4):579-596.
- Wadia, J.S., Stan, R.V., Dowdy, S.F. 2004. Transducible TAT-HA fusogenic peptide enhances escape of TAT-fusion proteins after lipid raft macropinocytosis. *Nat. Med.* 10(3):310-315.
- Waldo, G.S., Standish, B.M., Berendzen, J., Terwilliger, T.C. 1999. Rapid protein-folding assay using green fluorescent protein. *Nat. Biotechnol.* 17(7):691-695.

- Wender, P.A., Mitchell, D.J., Pattabiraman, K., Pelkey, E.T., Steinman, L., Rothbard, J.B. 2000. The design, synthesis, and evaluation of molecules that enable or enhance cellular uptake: Peptoid molecular transporters. *Proc. Natl. Acad. Sci. U.S.A.* 97(24):13003-13008.
- Wender, P.A., Rothbard, J.B., Jessop, T.C., Kreider, E.L., Wylie, B.L. 2002. Oligocarbamate molecular transporters: Design, synthesis, and biological evaluation of a new class of transporters for drug delivery. *J. Am. Chem. Soc.* 124:13382-13383.
- West, M.L., Fairlie, D.P. 1995. Targeting HIV-1 protease: a test of drug-design methodologies. *Trends Pharmacol. Sci.* 16(2):67-75.
- Westby, M., Nakayama, G.R., Butler, S.L., Blair, W.S. 2005. Cell-based and biochemical screening approaches for the discovery of novel HIV-1 inhibitors. *Antiviral. Res.* 67(3):121-140.
- Whitelock, J.M., Iozzo, R.V. 2005. Heparan sulfate: a complex polymer charged with biological activity. *Chem. Rev.* 105(7):2745-2764.
- Wlodawer, A., Vondrasek, J. 1998. Inhibitors of HIV-1 protease: a major success of structure-assisted drug design. *Annu. Rev. Biophys. Biomol. Struct.* 27:249-284.
- Wood, K.C., Boedicker, J.Q., Lynn, D.M., Hammond, P.T. 2005. Tunable drug release from hydrolytically degradable layer-by-layer thin films. *Langmuir* 21(4):1603-1609.
- Yanagishita, M. 1992. Metabolism of plasma membrane-associated heparan sulfate proteoglycans. *Adv. Exp. Med. Biol.* 313:113-120.
- Yanagishita, M. 1998. Cellular catabolism of heparan sulfate proteoglycans. *Trends Glycosci. Glycobiol.* 10(52):57-63.
- Yanagishita, M., Hascall, V.C. 1992. Cell surface heparan sulfate proteoglycans. *J. Biol. Chem.* 267(14):9451-9454.
- Yanagishita, M., Hascall, V.C. 1984. Metabolism of proteoglycans in rat ovarian granulosa cell culture. *J. Biol. Chem.* 259:10207-10283.

- Yang, F., Moss, L.G., Phillips, G.N., Jr. 1996. The molecular structure of green fluorescent protein. *Nat. Biotechnol.* 14(10):1246-1251.
- Yang, L., Harroun, T.A., Weiss, T.M., Ding, L., Huang, H.W. 2001. Barrel-stave model or toroidal model? A case study on melittin pores. *Biophys. J.* 81(3):1475-1485.
- Yang, Y., Ma, J., Song, Z., Wu, M. 2002. HIV-1 TAT-mediated protein transduction and subcellular localization using novel expression vectors. *FEBS Lett.* 532(1-2):36-44.
- Youle, R.J., D'Alessio, G. 1997. Antitumor RNases. In *Ribonucleases: Structures and Functions*. D'Alessio G, Riordan JF, editors. Academic Press, New York. 491-514.
- Youle, R.J., Newton, D., Wu, Y.-N., Gadina, M., Rybak, S.M. 1993. Cytotoxic ribonucleases and chimeras in cancer therapy. *Crit. Rev. Ther. Drug Car. Syst.* 10:1-28.
- Yuste, R. 2005. Fluorescence microscopy today. *Nat. Meth.* 2(12):902-904.
- Zaccolo, M. 2004. Use of chimeric fluorescent proteins and fluorescence resonance energy transfer to monitor cellular responses. *Circ. Res.* 94(7):866-873.
- Zhang, J., Chua, L.S., Lynn, D.M. 2004. Multilayered thin films that sustain the release of functional DNA under physiological conditions. *Langmuir* 20(19):8015-8021.
- Zhou, H., Casas-Finet, J.R., Heath Coats, R., Kaufman, J.D., Stahl, S.J., Wingfield, P.T., Rubin, J.S., Bottaro, D.P., Andrew Byrd, R. 1999. Identification and dynamics of a heparin-binding site in hepatocyte growth factor. *Biochemistry* 38:14793-14802.
- Zhu, H., Snyder, M. 2003. Protein chip technology. *Curr. Opin. Chem Biol.* 7(1):55-63.
- Ziegler, A., Seelig, J. 2004. Interaction of the protein transduction domain of HIV-1 TAT with heparan sulfate: binding mechanism and thermodynamic parameters. *Biophys. J.* 86(1 Pt 1):254-263.
- Zorko, M., Langel, U. 2005. Cell-penetrating peptides: mechanism and kinetics of cargo delivery. *Adv. Drug Deliv. Rev.* 57(4):529-545.